Multiple-scale Hyperspectral Remote Sensing of Forest Biochemical and Biophysical Properties

THESIS

MULTIPLE-SCALE HYPERSPECTRAL REMOTE SENSING OF FOREST BIOCHEMICAL AND BIOPHYSICAL PROPERTIES

Pingheng LI

Graduate School of

Science and Technology, Education Division

Department of Environment and Energy Systems

Shizuoka University

June 2013

Table of contents

Chapter 1 General introduction

1.1 Background

1.1.1 Remote sensing of biochemical and biophysical parameters

Vegetation is a fundamental element of the earth's surface and has a major influence on the exchange of energy between the atmosphere and the earth's surface (Bacour et al., 2002). Accurate quantitative estimation of vegetation biochemical and biophysical characteristics is necessary for a large variety of agricultural, ecological, and meteorological applications (Asner, 1998; Hansen and Schjoerring, 2003; Houborg et al., 2007). Direct measurement of these characteristics is labor-intensive and costly, and is thus only practical on experimental plots of limited size (Pu et al., 2003), whilst remote sensing, thanks to its global coverage, repetitiveness, non-destructive and relatively cheap characterization of land surfaces, has been recognized as a reliable method and a practical means of estimating various biophysical and biochemical vegetation variables (Cohen et al., 2003; Curran et al., 1994; Weiss and Baret, 1999). However, a major drawback of traditional remote sensing products is that they use bulk spectral information over broad-band widths, resulting in the loss of crucial information available in specific narrow bands (Blackburn, 1998; Thenkabail et al., 2000). In this regard, the advent of hyperspectral remote sensing (section 1.1.2) has offered promising previews with large possibilities to overcome this limitation.

1.1.2 Hyperspectral remote sensing of vegetation parameters

Hyperspectral remote sensing, typically has hundreds of narrow, contiguous spectral bands between 400 and 2500 nm, has the potential to measure specific vegetation variables that are difficult to measure using conventional multi-spectral sensors. There are a bunch of successful applications, for example, Zarco-Tejada et al (2002) assessed vegetation stress from a derivative chlorophyll index using CASI (Compact Airborne Spectrographic Imager) airborne data; Mutanga and Skidmore (2004) overcame the saturation problem in estimating biomass by using narrow-band vegetation indices; Ferwerda et al (2005) demonstrated that across multiple plant species total nitrogen content could be detected by using hyperspectral indices; and Cho (2007) used hyperspectral indices to discriminate species at leaf and canopy scales. Previous studies have shown that hyperspectral data are crucial in providing essential information for quantifying the biochemical (Broge and Leblanc, 2001; Ferwerda et al., 2005; Gamon et al., 1992; Gitelson and Merzlyak, 1997; Mutanga et al., 2005; Peterson et al., 1988) and the biophysical (Blackburn, 1998; Elvidge and Chen , 1995; Gone et al., 1992; Lee et al., 2004; Mutanga and Skidmore, 2004; Schlerf et al., 2005) characteristics of vegetation.

In general, current remote sensing approaches to estimating vegetation biochemical and biophysical parameters include inversion of physically based model or via statistical methods (Skidmore, 2002). The inversion model approaches involve various types of leaf and canopy radiative transfer models, which simulate reflectance

spectra from several biochemical and biophysical parameters and inversely retrieval of parameters from reflectance spectra vice versa (e.g., Feret et al., 2008; Colombo et al., 2008; Riano et al., 2005; Ceccato et al., 2001; Jacquemoud et al., 1996). On the other hand, the most common approaches of applications are spectral indices, which consist in combining several reflected signals measured in narrow or broad spectral bands into mathematical combinations and to correlate them to the target parameters (Blackburn, 1998; Broge and Leblanc, 2001; Filella and Penuelas, 1994; Mutanga and Skidmore, 2004; Thenkabail et al., 2004). Both approaches (radiative transfer models / spectral indices) have been widely applied. In this study, both approaches were investigated in detail for their estimations of typical leaf and canopy properties including leaf chlorophyll content, leaf mass per area, leaf water content, and leaf area index, which are of prime important among many ecological models.

1.2 State of the art

1.2.1 Radiative transfer models

Leaf scale models

During the last fifty years, various types of radiative transfer models have been proposed to explain the leaf optical properties in terms of chlorophyll or water content, leaf internal structure or surface properties. For broadleaves, Ustin et al. (1999) extensively reviewed leaf models from the late sixties to the present, which have greatly improved our understanding of the interaction of light with plant leaves. They can be generally categorized into four classes of models with increasing order of complexity: Plate models, N-flux models, Stochastic models and Ray tracing models. Among the four classes of models, the plate type of models represents a leaf as one or several absorbing plates with rough surfaces giving rise to isotropic diffusion, and is easy to be applied to practice. A well-known example of this type is the PROSPECT model developed by Jacquemoud and Baret (1990), which is in widespread use in the remote sensing community.

Adaption of proposed models to needle-shaped leaves proved to be a difficulty. However, Dawson et al. (1998b) developed a new model named LIBERTY (Leaf Incorporating Biochemistry Exhibiting Reflectance and Transmittance Yields), has the capacity of accurately predicting the spectral response of both dried and fresh stacked pine needles. As a comparison, very few attempts were ever on modeling optical properties for assimilating branches of typical desert plants, which carry out leaf functions, e.g., photosynthesis and transpiration but neither broadleaves nor needle leaves. Despite these desert plants being popularity in arid land, few of the existing studies have ever addressed their reflectance characteristics.

Models are essential for understanding not only how electromagnetic radiation interacts with leaf elements, but also how to directly relate observed optical properties with leaf biochemical and biophysical attributes. In the direct mode, sensitivity analyses, a crucial step in model verification and validation, ensures that the response of the model to the input parameters is the expected one. Recent studies based on statistical methods like the Sobol's method or the Extended Fourier Amplitude

Sensitivity Test (EFAST) extend research further by quantifying the relative effects of each of the input parameters, as well as their interactions (Ceccato et al., 2001). Such information may be helpful in inversion, for instance to detect non-influential optical parameters, like the nitrogen (or protein) content in fresh leaves.

To actually use radiative transfer models for retrieving leaf characteristics from observed reflectance data, they must be inverted (Kims et al., 1998). Different algorithms exist for the inversion of physical models, including numerical optimization methods (e.g., Jacquemoud et al., 2000; Meroni et al., 2004), look-up table (LUT) approaches (e.g., Combal et al., 2002; 2003), and artificial neural network methods (e.g., Fang and Liang, 2005; Schlerf and Atzberger, 2006), each having advantages and disadvantages (Kimes et al., 2000; Liang, 2004). A drawback in using radiative transfer models is the ill-posed nature of model inversion (Atzberger, 2004; Combal et al., 2002), meaning that the inversion solution is not always unique as various combinations of input parameters may yield almost similar spectra (Weiss and Baret, 1999). Several attempts have been made to alleviate the impact of the "ill-posed" problem for model inversion, ranging from restricting the ranges of input parameters (Danson and Bowyer, 2004), to the removal of simulated spectra derived from unlikely combinations of input parameters based on field experience (Yebra and Chuvieco, 2009; Yebra et al., 2008), and the use of prior knowledge about model parameters (Combal et al., 2002), all of which could restrict the operational utility of the inverse modeling approach. Hence, to develop a new model inversion approach to alleviate the so-called "ill-posed" problem is needed, especially for those area that lack *in situ* data.

Canopy scale models

Canopy radiative transfer models describe the spectral variation of canopy reflectance as a function of canopy, leaf and soil background characteristics based on physical laws (Ataberger, 1995; Meroni et al., 2004; Verhoef, 1984). As radiative transfer models are able to explain the transfer and interaction of radiation inside the canopy based on physical laws, they offer an explicit connection between vegetation biophysical and biochemical variables and canopy scale reflectance (Houborg et al., 2007). Various canopy radiative transfer models have been developed and applied to various vegetation canopies (Pinty et al., 2001; 2004; Widlowski et al., 2007), e.g., PROSAIL (Jacquemoud et al., 2009), ACRM (Kuusk, 2001) and FRT (Kuusk and Nilson, 2000, 2009), as three widely used models. PROSAIL combines the leaf optical properties model PROSPECT and the canopy bidirectional reflectance model SAIL and has been used for about 16 years to study plant canopy spectral and directional reflectance in the solar domain. ACRM is a two-layer canopy reflectance (CR) model which describes the vegetation canopy as two layers: a main homogeneous layer of vegetation and a geometrically thin layer of vegetation on the ground surface. This model is an extension of the homogeneous multispectral CR model MSRM (Kuusk, 1994) and the Markov chain CR model MCRM (Kuusk, 1995). The FRT model describes a radiative transfer scheme for a forest canopy composed of two layers: a discontinuous upper canopy of trees in the overstorey, and a continuous, horizontally homogeneous shrub and grass layer in the understorey above the soil surface.

Most of the currently available models have been based on radiative transfer theory

with analytical approximations for the solution, which make the assumption of either a homogeneous one-layer canopy or a structure that is extended to two layers by adding a thin weed layer of understorey vegetation (shrubs and/or grass) under the homogeneous canopy (e.g. Gobron et al., 1997; Liangrocapart and Petrou, 2002; Myneni et al., 1992; Nilson and Kuusk, 1989; Verstraete et al., 1990). However, canopy generally exhibits large heterogeneity of both biophysical and optical properties (Widlowski et al., 2007). Although there are some 3-D simulation models based on true canopy 3-D structures (Cote et al., 2009; Pinty et al., 2004; Widlowski et al., 2007) that explain the effects of canopy heterogeneous structure on canopy reflectance, these models require some geometrical and structural parameters of trees, which are very difficult to measure practically, which reduce their effectiveness. In addition, the canopy also exhibits a large heterogeneity of leaf biochemical and physiological properties such as chlorophyll, water and dry matter contents (Ciganda et al., 2008; Wang and Li, 2012). However, the effects of these heterogeneities on canopy reflectance have not yet been fully addressed, to the best of our knowledge.

Vertical profiles of both biophysical and biochemical properties are one of the main sources of heterogeneity within a vegetation canopy, which has been well recognized and highlighted in many studies (Barton, 2000; Ciganda et al., 2008; Dwyer et al., 1992; Valentinuz and Tollenaar, 2004). Generally, vertical distribution of the target components is a major factor controlling canopy reflectance. Using homogeneous canopy reflectance models for calculating directional reflectance from a vertical heterogeneous canopy by taking average values of biophysical and biochemical properties within the canopy may lead to systematic errors. Hence, accurate modeling of canopy reflectance requires taking this factor into consideration. With this in mind, to develop a computationally efficiently multiple-layer canopy radiative transfer model is needed and will be one main objective of this study.

1.2.2 Spectral indices

The radiative transfer models approach generally involves the famous “ill-posed” inverse problem (Combal et al.,2003), and this approach is computationally demanding and requires a large number of leaf and canopy variables, which may not be available, and hence limits its application (Liang, 2004). An alternative approach is the use of spectral indices, which are based on the principle of combining reflectance measured on several narrow or broad spectral bands into mathematical combinations and correlating them to the target parameter. It is generally accepted that spectral indices offer convenient and non-intrusive tools for rapidly inferring a number of functionally important leaf and canopy properties (Gamon and Surfus, 1999).

The importance of hyperspectral indices for quantifying the biochemical and biophysical characteristics of vegetation have been demonstrated by many studies (Blackburn, 1998; Broge and Leblanc, 2001; Ferwerda et al., 2005; Gamon et al., 1992; Mutanga et al., 2005; Schlerf et al., 2005). As a result, a large number of spectral indices for retrieval different biochemical and biophysical parameters are developed and applied to various vegetation types. At leaf scale, the chlorophyll concentrations, water content, and leaf mass area are specifically focused on as they are three key leaf biochemical properties affecting a number of major ecological processes involved in exchange of matter and energy, like photosynthesis,

evapotranspiration, and respiration (Peterson and Hubbard, 1992). As reviewed by le Maire et al. (2004), Blackburn (2007) and Ustin et al. (2009), dozens of indices ranging from red/NIR ratios, green and red edge types, and derivative types have been designed to estimate leaf scale chlorophyll content, e.g., Modified Normalised Difference (mND705, Sims and Gamon, 2002), Pigment Specific Simple Ratio (PSSR, Blackburn, 1998), Double Difference (DD, le Maire et al., 2004). Similarly, a number of indices have been used to estimate leaf water content (e.g., Roberts et al., 1998; Gao, 1996; Hardisky et al., 1983; Penuelas et al., 1993) and leaf mass area (le Maire et al., 2008; Wang and Li, 2012), e.g.,, Moisture Stress Index (MSI, Hunt and Rock, 1989), Simple Ratio Water Index (SRWI, Zarco-Tejada and Ustin, 2001), Water index (WI, Penuelas et al., 1997). For leaf mass area, Normalised Difference index ($ND_{1710,1340}$, le Maire et al., 2008), Double Difference index ($DDn_{1235,25}$, Wang and Li, 2012) were proposed. At canopy scale, a large number of vegetation indices have been established for retrieval of leaf area index(LAI), a key canopy biophysical variable (Haboudane et al., 2004), e.g. the Normalized difference vegetation index (NDVI, Thenkabail et al., 2000), Ratio vegetation index (RVI, Stenberg et al., 2004), Modified Simple ratio (MSR, Chen, 1996), Modified Chlorophyll absorption ratio index (MCARI, Haboudane et al., 2004), Triangular vegetation index (TVI, Broge and Leblanc, 2001), Modified TVI (MTVI, Haboudane et al., 2004), Modified soil-adjusted vegetation index (MSAVI, Qi et al., 1994), and D_{LAI} (le Maire et al., 2008).

Application of hyperspectral indices to estimate vegetation biochemical and biophysical parameters is simple but apparently has limitations, since it lack robustness and portability. When hyperspectral indices are calibrated to a specific database, the relationships elucidated cannot be generalized to other databases (le Maire et al., 2008). Unfortunately, most experimental databases used for calibration are not broadly representative, especially in the context of ecological concerns. To be useful in ecological studies, the relationships should be sufficiently general for application across locations, species and plant developmental stages (Sims and Gamon, 2002). The ideal way to find efficient and robust indices with broad applicability would be to use a large measurement database, with many species and site conditions. However, it is usually not feasible to obtain such a large database containing thousands of measurements. As an alternative to the use of databases derived from field measurement of specific plant communities or ecosystems, researchers have proposed the use of artificial databases containing reflectance spectra and their corresponding vegetation parameters (le Maire et al., 2004). Such approach of using simulated datasets from radiative transfer models is a popular and advanced way for allocating effective and general vegetation indices developed in recent years (le Marie et al., 2004; 2008; Wang and Li, 2011; 2013b). Since the effect of variation in biophysical and biochemical properties on canopy / leaf reflectance are explicitly through reflectance models (Asner, 1998), such approach has many advantages. They include: most properties can be represented in detail (via thousands of spectra); the influence of a specific property can be decoupled from others; and the effect of a particular property on the spectra is based on physical and physiological processes. As a result, well established indices obtained through such a large simulated database may potentially be applied to a wide range of spectra. Nevertheless, it is worth noting that the accuracy of the approach relies on the capacity of applied radiative models to correctly simulate reflectance under various conditions. Thus, it is essential to validate such indices with experimental measurements.

1.3 Study sites and measurements

This study is mainly conducted at the Naeba Site, which is dominated by a typical temperate deciduous plant--beech (*Fagus crenata*). Field measurements including reflectance in this site can be dated back to 2007 and been continued until now. In addition, in order to test the performance of radiative transfer models and to identify general and robust spectral indices, another site was established in Gurbantünggüt Desert of China in 2009 (hereafter refers to be Desert Site), which is dominated by a typical desert plant -- *H. ammodendron*. The field measurements in the Desert Site were starting from 2009. Detail descriptions of these two sites are given in below.

1.3.1 Naeba Site

The primary study site is in the Naeba Mountain of Japan (36°51' N, 138°40' E, see Fig. 1.1), which has been used since the 1970s by the International Biological Program (Kakubari, 1977). It is also an important site of SpecNet (Gamon et al., 2006). More than 15 plots were delineated along the northern slope of the Naeba Mountain where natural beech forests (*Fagus crenata*) dominated from the elevation of 550–1500 m; these plots were used for the long-term monitoring of stand biomass, leaf area index (LAI), and other stand structural parameters. Furthermore, four towers have been built for four typical stands at 550, 900, and 1500 m; these stands represent the lower, middle, and upper limits of *F. crenata* ecosystems. Two towers were located at 900 m (X1 and X5 with different azimuths) where conditions for growth of *F. crenata* are optimum. The towers served as the platform for meteorological sensors and also provided canopy access for sampling and measurements. The field measurements of this study were mainly conducted in these four tower stands (550-m, 900-m (X1), 900-m (X5), and 1500-m stands).

The 550-m stand is located on the river terrace of a deep valley, 10 m above the current river level. The 900- and 1500-m stands are located on east- and south-facing mountain slopes, respectively (Table 1.1). Bedrock in the study area is predominantly basalt, on which moderately moist brown forest soil has formed. The upper-canopy layer at each elevation consists mainly of *F. crenata* with sporadic occurrence of other species such as *Quercus mongolica* Fisch. ex Ledeb. var. *grosseserrata* (Blume) Rehder & E.H. Wilson, *Magnolia obovata* Thunb. and *Acanthopanax sciadophylloides* (Franch. & Sav.) H. Ohashi at the 550- and 900-m stands, and *Betula grossa* Siebold & Zucc. and *Betula ermanii* Cham. at the 1500-m stand. The prevalence of evergreen bamboo (*Sasa kurilensis* (Rupr.) Makino & Shibata) increases with elevation to more than 90% cover at the 1500-m stand.

This region along the Japan Sea coast is characterized by high precipitation (about 2000 mm $year^{-1}$), much falling as snow, leading to winter snow cover of 3–4 m (Table 1). Mean annual (1999) air temperature was 10.0, 9.3 and 5.6 ℃ at the 550-, 900- and 1500-m stands, respectively. At the 550- and 900-m stands, snowmelt occurs at the beginning of May, whereas at the 1500-m stand, it is delayed until early June. Leaf flush begins in late April or early May at the 550- and 900-m stands and in late May to early June at the 1500-m stand. Autumn leaf coloring begins in early October at all stands.

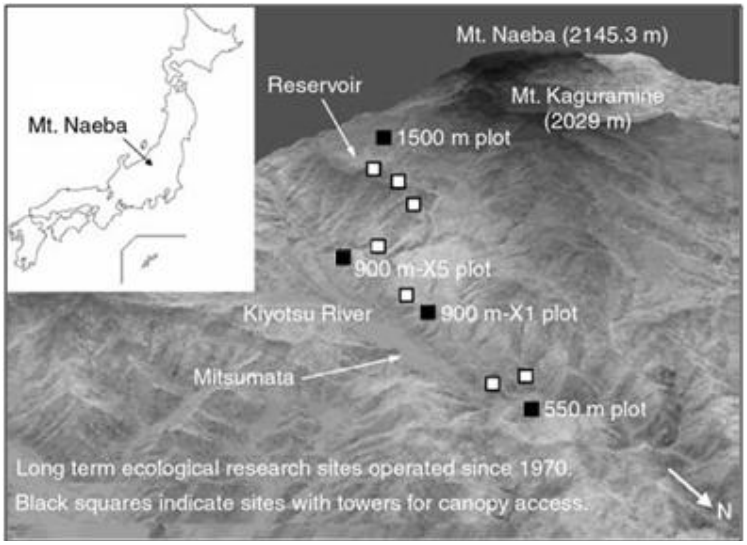

Fig. 1.1 Location of the Naeba site and location of the long-term study stands, black symbols indicate the locations of the four tower stands used in this study.

1.3.2 Desert Site

The second study site is located in the newly set-up Remote Sensing Experimental Site (abbreviated to Desert Site) near Fukang National Field Station of Desert Ecology, Chinese Academy of Sciences, in the hinterland of the Eurasian continent (44 °25' N, 87 °54' E, and 475 m a.s.l.). The Desert Site is located at the southern edge of the Gurbantonggut Desert and 82 km north of the highest peak of the eastern Tianshan Mountains (see Fig. 1.2). The region has a continental arid temperate climate with a hot dry summer and cold winter, where the annual mean temperature is 6.6 °C and annual mean precipitation of 160 mm. High pan evaporation (E) can even reach about 2000 mm (Xu et al. 2007). The soil is highly saline and the groundwater table is more than 5 m. The dominant species is *Haloxylon ammodendron*, with only a few companion species found in these plant communities including some short-life vegetation in spring under the irrigation of snow melting water. Total amount of precipitation of this site during growing season was about 120 mm in 2010, far below the atmospheric water demand and this site experiences severe water shortage.

In Desert Site, a preliminary plot inventory was performed during the plot set-up in 2009. A more detailed inventory was carried out in 2011, with items recorded including tree height, canopy projection area, and stem diameter at base height (Table 1.1). The average *H. ammodendron* canopy coverage was estimated to be 15%.

Table 1.1 General characteristics of the beech stands and climate at the three sites.

Site		Dominant species	Plot size (m^2)	Age (years)	Density (trees ha^{-1})	Mean height (m)	Mean annual temperature (°C)	Mean annual precipitation (mm)	Length of growth season (days)
Naeba Site	550m	beech	2400	260	246	34	11.4	1322	193
	900m	beech	600	70	1033	21	9.6	1343	161
	1500m	beech	1000	300	450	22	6.2	1158	144
Desert Site		*haloxylon*	10^6	>300		1.9	6.6	160	170

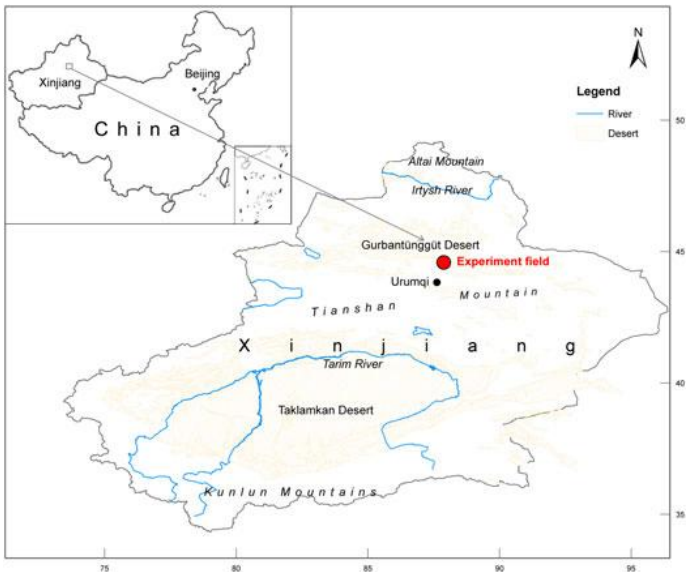

Fig. 1.2 Location of the Desert Site

Fig 1.3 Overshot of the Naeba Site (left) and Desert Site (right).

1.3.3 Field Measurements

Dataset I, II, III from the Naeba site

To evaluate the model performance at different locations and for different species, we have compiled three different data sets from synchronous measurements of both leaf biochemical parameters and leaf and canopy reflectance in a typical cold-temperate mountainous landscape in Japan, on the Naeba Mountain (the Naeba site, see section 1.3.1 for site detail description). Beech (*Fagus crenata*) is the dominant species here and is widely distributed at altitudes from 550 to 1500 m on the northern slope of the mountain. Both leaf properties, e.g., contents of various pigments and nitrogen, maximum carboxylation velocity (*Vc*max), EWT, leaf thickness, LMA, and leaf anatomy, and leaf reflectance have been simultaneously measured using leaf clip since 2006. **Data set I** contains in a total of 222 beech-leaf measurements acquired in 2007 from *Fagus crenata* canopies at three difference layers (bottom, middle, and top) in four tower plots deployed along the northern slope of Naeba Mountain at different altitudes—550, 900 (X1), 900 (X5), and 1500 m—during the growth period, with a frequency of once per two weeks during the leaf flushing and shedding periods and once per month during the summertime. **Data set II** is composed of 83 leaf measurements acquired in the growth period of 2008 at the 900-m X5 site alone, with

the focus on the vertical profile, in which the beech canopy has been grouped into five layers (at 12, 14, 16, 18, and 20 m, respectively). The same variables were measured as in 2007 (i.e., leaf properties and reflectance). In 2008, a field campaign was also launched in August, and similar measurements were acquired for 15 other common species, including *Fraxinus lanuginosa*, *Acer japonicum*, *Magnolia obovata*, *Acanthopanax sciadophylloides*, *Lindera umbellata*, *Hamamelis japonica*, *Acer tschonoskii*, *Quercus crispula*, *Viburnum furcatum*, *Acer shirasawanum* Koidz, *Clethra alnifolia*, *Prunus grayana* Maxim, *Sasa spp.*, *Magnolia salicifolia*, and *Acer rufinerve* in this region around the 900-m plots. These are the measurements on which **Data set III** is based (45 leaves from 15 species in total). The three data sets together include data on hundreds of leaves (350 leaves in total), representing various species, canopy heights, growing conditions, and growth stages. In all data sets, canopy directional–hemispherical reflectance spectra were measured by use of a field spectroradiometer (ASD FR, USA) covering wavelengths from 400 to 2500 nm with a 5 ° field of view, view nadir angle and view azimuth angle were both 0 °, and sun zenith angle was calculated by the measured time. Leaf reflectance spectra were measured in the optical range with the field spectroradiometer equipped with a leaf clip. For all data sets, we selected four biochemical parameters expressed in the same units in each case: chlorophyll a (Chl*a*), chlorophyll b (Chl*b*), water depth (*Cw* or EWT), and dry matter content (*Cm* or LMA). For sampling, leaf disks for various biochemical measurements were collected using a cork borer immediately after taking spectral measurements. The remaining leaf parts were scanned to determine the leaf areas, and their fresh weights were measured before placing them in a drying oven at 85℃ for 48 h and then reweighing them to determine their water content (expressed as a percentage), EWT (in centimeters or in grams per square centimeter), and LMA (in grams per square centimeter). Pigments were extracted using organic solvents by grinding fresh or frozen leaf disks in a chilled mortar with a small amount of quartz sand and $MgCO_3$ to prevent acidification (Arnon, 1949). Following centrifugation, the absorbance of the supernatant was measured using dual beam scanning UV-Vis spectrophotometers (Ultrospec 3300 pro, Biosciences, U.S.). The leaves' contents of chlorophylls a and b, expressed in micrograms per square centimeter, were then determined by multi-wavelength analysis (Arnon, 1949). All measurements were taken three to five times. Table 1.2 summarizes the main characteristics of these three data sets. In addition, Leaf area index (LAI) during the growing season was estimated through litter traps. The LAI vertical variation within canopy was obtained *in situ* in a similar way as described in Iio et al. (2011).

Dataset IV from the desert site

To evaluate the models performance on assimilating branches of desert vegetation, another data set (data set IV) from synchronous measurements of both leaf biochemical parameters and reflectance in a typical desert vegetation (*Haloxylon ammodendron*) on the desert site (see section 1.3.2 for site detail description). *Haloxylon ammodendron* is the only native dominant vegetation in the area. **Data set IV** contains in a total of 120 assimilating branch measurements from *H. ammodendron* crowns at three difference layers (bottom, middle, and top) in the desert site. The methods of assimilating branch reflectance (both leaf and canopy) and biochemical parameters (CHL, EWT and LMA) are the same with datasets I~III. Mean, maximum, minimum and standard deviation of chlorophyll concentrations observed for *H. ammodendron* measurements are reported in Table 1.2.

Table 1.2 Main characteristics of the datasets compiled from field measurements

Dataset	I	II	III	IV
Year	2007	2008	2008	2009~2012
Sample sites	550m, X1, X5, 1500m	900 m X5	Near X1 and X5	Desert site
No. of samples	222	83	45	120
Sample species	1	1	15	1
Sample position	top, middle, bottom	5 canopy layers	top	top, middle, bottom
Chlorophyll ($\mu g/cm^2$)				
Min	7.15+2.09	8.25+3.17	17.40+5.46	4.70
Max	74.82+24.49	49.18+18.34	45.69+16.64	29.18
Mean	42.59 +15.15	29.07+10.63	30.25+11.49	14.54
EWT (g/cm^2)				
Min	0.0026	0.0033	0.0057	0.0019
Max	0.0158	0.0127	0.0145	0.0147
Mean	0.0066	0.0067	0.0086	0.0074
LMA (g/cm^2)				
Min	0.0028	0.0026	0.0034	0.0030
Max	0.0113	0.0109	0.0119	0.0124
Mean	0.0063	0.0057	0.0062	0.0087

1.4 Research Objectives

This study aims to investigate the potential of hyperspectral remote sensing for estimating biochemical and biophysical vegetation properties at leaf and canopy scale using both radiative transfer model inversion and hyperspectral indices approaches. The main objectives of this study are to: (1) investigate the potential of leaf scale radiative transfer models for inversely estimating biochemical properties (e.g., leaf chlorophyll, water and mass content) for both broadleaves of typical temperate deciduous species and assimilating branches of typical desert species, and develop a new model inversion approach to alleviate the so-called "ill-posed" problem when doing the model inversion; (2) identify several efficient and robust hyperspectral indices for estimating leaf biochemical parameters (e.g., leaf chlorophyll, water and mass content) by combining model simulated and field measured data sets, which insensitive to species, phenological stages, locations, and leaf anatomies; (3) develop a multiple-layer canopy radiative transfer model which considers the vertical heterogeneity of biochemical and biophysical parameters within the canopy, and present scenarios to reveal the effect of vertical variation of each parameter on canopy reflectance; (4) identify a potentially general and robust spectral index that insensitive to within canopy vertical variations of LAI and biochemical components for estimating LAI based on simulated datasets generated from the multiple-layer canopy radiative transfer model.

1.5 Thesis outline

This thesis comprises four main chapters, corresponding to two different scales of investigation.

1.5.1 Leaf scale

Chapter 2 and 3 investigate the potential of estimating leaf biochemical properties using hyperspectral measurements. In brief, chapter 2 investigates two widely used leaf scale radiative transfer models (PROSPECT and LIBERTY) for estimating leaf biochemical characteristics through model inversion. The investigation involves plant species from typical temperate deciduous forests in humid area to typical desert forest in arid area. In this chapter, the "ill-posed" model inversion problem has been emphasized and a new model inversion approach is developed to alleviate the ill-posed problem.

Chapter 3 investigates several types of hyperspectral indices to estimate leaf biochemical parameters. The investigation combines various model simulated and field measured data sets to identify general and robust spectral indices for each parameter. The simulated data sets are generated from the calibrated PROSPECT model as in chapter 2, and field measured data sets include various plant species from typical temperate deciduous forests in humid area (Naeba Site, see section 1.3.1) to typical desert forest in arid area (Desert Site, see section 1.3.2).

1.5.2 Canopy scale

Chapter 4 and 5 investigate the potential of estimating canopy properties using hyperspectral remote sensing. In chapter 4, a multiple-layer canopy radiative transfer model and its inversion algorithm were developed for studying the vertical heterogeneity of both biochemical and biophysical properties within the canopy. Chapter 5 investigates several types of hyperspectral indices to estimate canopy LAI. The investigation combines various model simulated data sets (based on the canopy model developed on Chapter 4) and field measurements to identify the general and robust spectral indices for estimating canopy LAI that insensitive to vertical heterogeneity of LAI and biochemical properties.

Finally, in chapter 6, the findings of this study are summarized and the contribution of the thesis within the context of vegetation biophysical and biochemical parameter estimation from hyperspectral remote sensing is discussed, especially the performance of the radiative transfer model inversion approach versus the spectral indices approach on different forests (typical temperate deciduous forest in humid area and typical desert forest in arid area) has been evaluated.

Chapter 2 Leaf scale applications: inverse retrieval of leaf biochemical properties

Abstract

This chapter evaluated inversion of leaf scale radiative transfer models (PROSPECT and LIBERTY) for estimating leaf biochemical parameters (leaf chlorophyll, leaf water and leaf mass content) in typical temperate deciduous and desert forests. Retrieval of leaf biochemical parameters using model inversion generally faces "ill-posed" problems, which dramatically decreases the estimation accuracy of an inverse model. In this chapter, a new approach was proposed and the results indicate that the new approach greatly improves the performance of inversion models. Before applying these models to the two typical vegetations, these models were calibrated using field-measured reflectance data to make them more accuracy for simulating the leaf reflectance curve. This process was especially needed for the desert vegetation, as the original LIBERTY and PROSPECT exhibited tangible error for simulating leaf reflectance of the desert vegetation. However, their calibrated versions were capable of accurately retrieval of biochemical parameters inversely from reflectance spectra. As for field-measured datasets of typical temperate deciduous forests, the inversed PROSECT estimates of biochemical parameters recorded an RMSE of 8.11 $\mu g/cm^2$, 0.0012 g/cm^2 and 0.0008 g/cm^2 for leaf chlorophyll (CHL), leaf water (EWT) and leaf mass content (LMA). For typical desert vegetation, the inversed LIBERTY estimates of CHL, EWT and LMA recorded RMSE of 3.43 $\mu g/cm^2$, 0.0012 g/cm^2 and 0.0008 g/cm^2, and the RMSE of 34.76 mg/m^2, 0.0012 g/cm^2 and 0.0010 g/cm^2 for the inversed PROSPECT. The results indicated that both LIBERTY and PROSPECT are applicable for estimation leaf biochemical parameters inversely for both typical temperate deciduous and desert plants after careful calibration, which is a necessary when prior coupling with canopy models to make further canopy and stand level biochemical properties estimations.

2.1 Introduction

A number of attempts have been made to apply this approach by inverting various types of physically based models (Ceccato et al., 2001; Colombo et al., 2008; Danson and Bowyer, 2004; Dawson et al., 1998; Feret et al., 2008; Ganapol et al., 1998; Jacquemoud and Baret, 1990; Jacquemoud et al., 1996; Riaño et al., 2005; Vittorio, 2009; Yebra et al., 2008; Yebra and Chuvieco, 2009). As a prerequisite, such physically based models should be able to simulate reflectance spectra accurately while being sufficiently simple for easy inversion. The development of radiative transfer models has brought a better understanding of the interactions between light and plant leaves (Verdebout et al., 1994).

Currently, the common widely used and validated leaf-level radiative transfer models include PROSPECT (Jacquemoud and Baret 1990) and LIBERTY (Dawson et al., 1998; Moorthy et al. 2004). PROSPECT has been used for broad leaves, and describes leaf optical properties as a function of four parameters: a structure parameter N, chlorophyll concentration, leaf mass, and water content. On the other

hand, LIBERTY is suitable for conifer needles, where Melamed's radiative transfer theory for suspended powders are used (Melamed 1963) and assumes that the needle structure is composed of roughly spherical cells. Many studies have inversed either PROSPECT or LIBERTY to estimate leaf/needle biochemical parameters including chlorophyll content and reported high estimation accuracy after being validated and calibrated with real measurements of leaf/needle reflectance (Jacquemoud and Baret 1990; Jacquemoud et al. 1996; Dawson et al., 1998; Ganapol et al. 1998; Sims and Gamon 2002; le Maire et al. 2004; Coops and Stone 2005; Blackburn 2007; Feret et al. 2008; Moorthy et al. 2008; Vittorio 2009; Li and Wang 2011). However, to the best of our knowledge, there are limited studies that have ever applied inversed radiative transfer models on desert vegetation in arid land, such as *Haloxylon ammodendron*.

Haloxylon ammodendron is a stem-succulent shrub and a typical desert plant dominant in most areas of Asian deserts (Wu 1995), possesses distinct structural features of xeromorphism. Generally, their leaves are extremely degenerated or exist as basal leaves. The young green twigs carry out photosynthesis, and these young green twigs are universally referred to as 'assimilating branches' in biology (Pyankov et al. 1999). Despite its popularity in arid land, few of the existing studies have ever attempted to test any radiative transfer model to such assimilating branches and to retrieve the biochemical properties of these assimilating branches through the model inversion.

To actually use radiative transfer models for retrieving leaf biochemical properties from observed reflectance data, they must be inverted by assigning to each observed spectrum the biochemical content value of the most similar simulated spectrum (Kims et al., 1998). However, the estimation of biochemical parameters via models inversion is challenging for several reasons, which make its operational application very difficult, mainly arising from the uncertainty of the inversion procedure. When searching for the most similar simulated spectrum to an observed spectrum, a wide range of values can be retrieved, since very similar reflectance spectra can be obtained from very different combinations of input parameters, leading to the well-known "ill-posed" inverse problem (Combal et al., 2002; Wang et al., 2007; Yebra and Chuvieco, 2009). Hence, it is essential to provide simulation conditions as close as possible to those expected, to avoid potential errors caused by unrealistic combinations of input parameters and thus reduce the "ill-posedness" of the problem. Several attempts have been made to alleviate the impact of the "ill-posed" problem for model inversion, ranging from restricting the ranges of input parameters (Danson and Bowyer, 2004) to the removal of simulated spectra derived from unlikely combinations of input parameters based on field experience (Yebra et al., 2008; Yebra and Chuvieco, 2009), all of which could restrict the operational utility of the inverse modeling approach.

Here, in this chapter, we firstly propose a new approach to alleviate the so-called "ill-posed" problem when inverting radiative transfer models to estimate the main biochemical parameters, and then we calibrate the radiative transfer models to typical temperate deciduous and desert vegetations for estimating leaf biochemical parameters.

2.2 Material and methods

2.2.1 Study sites and field measurements

The field measured dataset has been compiled from synchronous measurements of leaf biochemical parameters and reflectance in the Naeba Site. The detail descriptions of the Naeba site and methods of each measurement can see chapter 1.3.3.

2.2.2 Radiative transfer models

Models description

The first model explored in this study is PROSPECT (Jacquemoud and Baret 1990; Feret et al. 2008), which is a general radiative transfer plate model that assumes the leaf to be composed of one or a series of transparent plates with rough Lambertian reflecting surfaces. Leaf optical properties from 400 to 2500 nm are defined in PROSPECT as a function of four parameters: a structure parameter *N*, chlorophyll concentration, dry matter content, and water content (Table 2.1). PROSPECT linearly sums the specific absorption coefficients k_i of constituents *i*, scaled by their respective concentrations C_i, to calculate a global spectral absorption coefficient K_λ. Although the PROSPECT model is preliminary designed for broad leaf species, we nevertheless decided to test its potential on assimilating branches for the following reasons: (a) it has been widely validated with various species (Jacquemoud et al. 1995; Demarez 1999; Feret et al. 2008); (b) it has simple inversion capabilities with few input parameters (Jacquemoud et al. 1996, 2000; Zhang et al. 2007; Li andWang 2011); and (c) it has also a high adaptation to non-flat targets such as conifer needles (Zarco-Tejada et al. 2004). The version of the PROSPECT model used in this study is PROSPECT-4 developed by Feret et al. (2008).

Table 2.1 LIBERTY and PROSPECT input parameters.

Model	Parameters	Units	Range	Calibrated value
PROSPECT	Leaf structure parameter (N)	/	1~3	1.87
	Chlorophyll a+b content (C_{ab})	mg/m^2	0~600	need inverse
	Equivalent water thickness (C_w)	g/cm^2	0.004~0.04	0.01
	Dry matter content (C_m)	g/cm^2	0.0019~0.0165	0.004
LIBERTY	Average cell diameter (D)	mm	30~100	24
	Intercellular air space (x_u)	/	0.01~0.10	0.077
	Needle thickness (h)	/	1~10	1.6
	Baseline absorption ($C_{baseline}$)	/	0.004~0.010	0.0006
	Albino absorption (C_{albino})	/	1~10	2
	Chlorophyll content (C_{chl})	mg/m^2	0~600	need inverse
	Water content (C_w)	g/m^2	0~500	100
	Lignin and cellulose content (C_{lig})	g/m^2	10~80	40
	Nitrogen content (C_n)	g/m^2	0.3~2.0	1

The second model explored in this study is LIBERTY (Dawson et al., 1998), which employs nine biophysical/chemical properties to simulate the needle reflected

spectrum between 400 and 2500 nm (Table 2.1). Similarly to PROSPECT, this model linearly sums specific absorption coefficients that were measured during the BOREAS campaigns, scaled by their respective concentrations, to calculate a global absorption coefficient K_λ. This global absorption coefficient, in conjunction with the structural parameters of average cell diameter, intercellular air gap, and needle thickness are used to calculate needle reflectance and transmittance between 400 and 2500 nm (Moorthy et al. 2004; Moorthy et al. 2008). Since the outward appearance of *H. ammodendron* assimilating branches is similar to conifer needles, a good performance of LIBERTY in estimating *H. ammodendron* assimilating branch chlorophyll content was hence anticipated.

Models sensitivity analysis

Sensitivity analysis (SA) estimates the fractional contribution of a given input variable X_i to the variance of Y. In order to calculate the sensitivity indices for a set of independent X_i's, the total variance $V(Y)$ of the model output is decomposed as

$$V = \sum_i V_i + \sum_{i<j} V_{ij} + \sum_{i<j<m} V_{ijm} + \ldots + V_{12..k}, \quad (2\text{-}1)$$

where

$$V_i = V(E(Y|X_i)), \quad (2\text{-}2)$$

$$V_{ij} = V(E(Y|X_i, X_j)) - V_i - V_j, \quad (2\text{-}3)$$

and so on. The generic sensitivity index of order s is defined as:

$$S_{i_1,i_2,\ldots i_s} = V_{i_1,i_2,\ldots i_s} / V, \quad (2\text{-}4)$$

where i_1, i_2, etc., refer to the input factors. For example, S_i for the factor X_i is defined as V_i/V , and S_{ij} is the pure interaction effect between X_i and X_j , i.e., that part of the variation in Y due to X_i and X_j which cannot be explained by the sum of the individual effects of X_i and X_j , and so on.

A number of estimation procedures for S_i are available at present, e.g., the method of Sobol (Sobol, 1993) and methods listed up in Saltelli *et al.*(2000), Bowyer and Danson (2004). Sobol's method provides two sets of sensitivity indices, namely, the first-order indices and interaction indices. The first-order sensitivity indices give the independent effect of the corresponding parameters, while the interaction sensitivity indices consider the interaction effects of each parameter with the others.

In this study, we performed the SA using the method of Sobol for the two radiative transfer models, which examines the sensitivity of each parameter by suitably selecting combinations of parameter values within defined ranges.

Models' calibrations

Radiative transfer models need to be calibrated before they can accurately simulate vegetation spectra at the local scale and inversed to estimate input parameters (Kobayashi et al. 2001; Feret et al. 2008; Li and Wang 2011), particularly for the assimilating branches of *H. ammodendron*, which are apparently different to normal broad leaf and conifer needle.

For typical temperate forests (Datasets I~III), to avoid potential systematic bias and error propagation in the inversion process, we have calibrated the PROSPECT model

to ensure as much accuracy as possible at the very beginning of the process, according to the calibration algorithm of Feret et al. (2008). The data used for calibration were selected from Dataset I, as it is the largest one of the three and the only one to include leaves with a wide biochemical properties range, from very low to high. Ten percent of the total data in the dataset were randomly selected for calibration.

For the desert plant (Dataset IV), we calibrated PROSPECT and LIBERTY models also according to the calibration algorithm of Feret et al. (2008), using a randomly selected 10% of the total spectra from field measurements (12 out of the total 120 samples), and the other 90% was used for model validation. For LIBERTY, there are nine parameters that contribute to the variation in reflectance between 400 and 2500 nm. The result of sensitivity analysis (Figure 2.3) indicated that the spectra variation in 400–2500 nm is highly sensitive to variations in the five parameters (*D*, *x*u, CHL, EWT and LMA) in LIBERTY. The other four parameters were therefore kept constant, with default values, due to their low impacts on the model simulation and inversion.

Models simulation

After the model being calibrated, we then applied the calibrated model to generate the simulated data set using the defined range of input parameters. We used the minimum and maximum values of each parameter over the three data sets for the defined ranges of C_{ab} (CHL), C_w (EWT), and C_m (LMA), and we assigned a reasonable range of one to four for N. Logarithmic distributions were assumed for all four parameters, within the ranges defined earlier, leading to a total of 10 000 combinations. To ensure generalizable results, a uniform distribution was chosen for each varied parameter, so that a reflectance spectrum obtained with extreme parameter values has the same weight as other spectra on the indices' calibration procedure. In order to reproduce in the simulations the observed radiometric noise of real measured reflectance, a random noise has been added to each spectrum of this database. This step is important to eliminate noise sensitive indices and indices with artificially close wavelengths (le Maire et al., 2004). An additive random Gaussian noise with a standard deviation of 3% of reflectance amplitude has been applied on each wavelength of each reflectance spectrum of the artificial data set.

2.2.3 Model inversion Approaches

Common Model Inversion Method

The standard application of the inverse PROSPECT model for estimating biochemical parameters uses the whole optical domain from 400 to 2500 nm during the inversion. This determines the water and dry matter contents at the same time as that of chlorophyll. In practice, the inversion consists of finding the parameter set, symbolized by the vector θ, which minimizes the merit function [(2-5)], using a typical optimization algorithm such as the constrained Powell's search method with the merit function

$$J(\theta) = \sum_{\lambda_{min}}^{\lambda_{max}} (R^*(\lambda) - R_{mod}(\lambda, \theta))^2 , \qquad (2\text{-}5)$$

where R^* is the measured reflectance and R_{mod} is the modeled one.

New Approach

The standard approach to model inversion, by minimizing the merit function to determine the Chl content, EWT, and LMA simultaneously from the whole optical domain of 400 to 2500 nm, may be not efficient enough and is faced with a serious ill-posed inverse problem if used without any *a priori* information. We present here a new algorithm for model inversion that aims to reduce the "ill-posed" of the problem. The general flow of this algorithm is shown in Fig. 2.1, and a detailed description is as follows.

Step 1) *Wavelength selection*. Identify the specifically sensitive wavelength domains for each of the four parameters (*N*, CHL, EWT, and LMA) in the PROSPECT model based on the SA results. Each specific wavelength domain should be sensitive to the specific parameter only, while being as insensitive to other parameters as possible.

Step 2) *N* determination. Determine the parameter *N* by minimizing its merit function at its specific wavelength band λ_N, for fixed values of CHL, EWT, and LMA. The optimization algorithm applied in this study is the genetic algorithm (Conn et al., 1997) since it can greatly reduce computational time and also handle complex constraints. This optimization algorithm was also used for Steps 3) and 4).

Step 3) CHL and EWT determination. Determine the parameters CHL and EWT by minimizing their merit functions at their specific wavelength bands identified in the SA, using the inversely computed value of *N* and a fixed value of LMA.

Step 4) LMA determination. Determine LMA by minimizing its merit function at the specific wavelength domain identified in Step 1), using the inversely computed values for *N*, CHL, and EWT.

Step 5) Parameter stabilization. Repeat Steps 2) to 4) using the computed values of *N*, CHL, EWT, and LMA until the merit function has been minimized. This strategy helps to improve the stability and reliability of the retrieved results.

Compared with the standard approach, the proposed new approach retrieves each of the four parameters inversely from different runs based on specific merit functions for each. Merit functions are based on the SA and utilize only identified sensitive wavelengths for each parameter rather than the whole wavelength domain.

2.2.4 Model Performance and Residual Analysis

To quantify the performance of PROSPECT and LIBERTY models inversion and empirical methods, the estimated values (*Y'*) and independent reference measurements (*Y*) were calculated for each parameter, and the following statistics were calculated (Ceccato et al., 2001; Colombo et al., 2008; Feret et al., 2008; Ganapol et al., 1998; Riaño et al., 2005): the root-mean-square error (RMSE) and bias (BIAS), which indicate the absolute estimation errors, and the coefficient of determination (R^2), which indicates the goodness of fit of the estimated values to the observed values. Since absorption is very sensitive to variations in small amounts of leaf absorbers, the

parameters' retrieval may be more accurate for leaves with rich contents of absorbers. The magnitude of the error will consequently be proportional to their contents. In such cases, Williams (1987) recommends comparing the Standard Error of Prediction Corrected for bias (SEPC) with the mean value of the retrieved parameter to evaluate the significance of the error, which is termed as the coefficient of variability (CV).

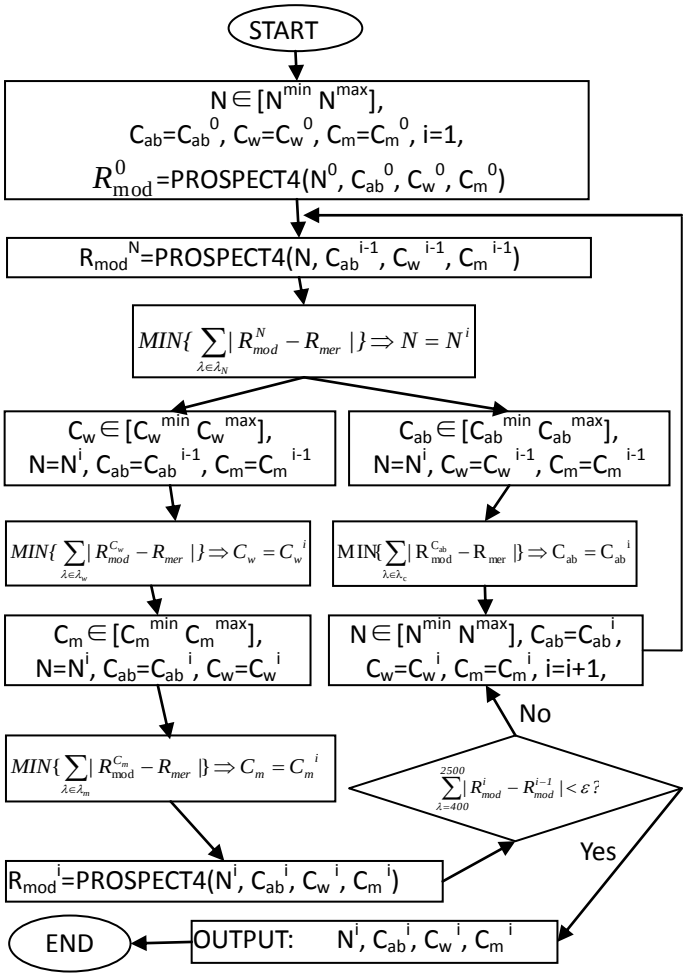

Figure 2.1 General flowchart of the newly proposed algorithm for model inversion. N, Cab, Cw and Cm represent values for parameters of N, CHL, EWT, and LMA, respectively. Rmer denotes the measured reflectance, Rmod denotes the modeled reflectance, i represents the ith run, ε represents the threshold value for ending the program.

In detail, the calculations are as follows. Let y_j and y'_j be the measured and predicted values, respectively, $\bar{y}$ be the average of the observed values, and n be the number of observations, then

$$R^2 = 1 - \sum_{j=1}^{n} (y'_j - y_j)^2 / \sum_{j=1}^{n} (y'_j - \bar{y})^2 , \quad (2\text{-}6)$$

$$RMSE = \sqrt{\sum_{j=1}^{n} (y'_j - y_j)^2 / n} , \quad (2\text{-}7)$$

and

$$CV = 100 \times (SEPC / \bar{y}), \quad (2\text{-}8)$$

where

$$SEPC = \sqrt{\sum_{j=1}^{n} (y_j' - y_j - BIAS)^2 / n}, \quad (2\text{-}9)$$

and

$$BIAS = \sum_{j=1}^{n} (y_j' - y_j) / n. \quad (2\text{-}10)$$

In order to evaluate the generality of the proposed approach and also to know the extent of the "ill-posed" problem that it can reduce, we have designed a new statistical index P_{ill}. The P_{ill} is the probability of retrieving an "ill-posed" value (defined here as one with a relative error > 30%) for each parameter

$$P_{ill} = P\left\{ x \left| \frac{|x^* - x|}{x} > 30\% \right. \right\} / n, \quad (2\text{-}11)$$

where x is the value of the parameter (CHL, EWT, or LMA) in the simulation data set, x^* is its retrieved value, and n is the number of values in the data set.

2.3 Results

2.3.1 Seasonal, vertical, and inter-species variations of leaf biochemical parameters and corresponding reflectance spectra

The three field-based data sets contained reflectance spectra and biochemical measurements from leaves that differed in phenology (season collected), position in canopy, and plant species. Table 1.2 summarizes the main characteristics of the three data sets compiled from measurement of field-collected leaves. The ranges of CHL, EWT, and LMA for all three data sets were 9.24–99.31 μg cm^{-2}, 0.0026–0.0158 g cm^{-2}, and 0.0028–0.0119 g cm^{-2}, respectively. Among the three data sets, data set I is the most comprehensive in that it contained the broadest ranges of CHL, EWT, and LMA.

Apparent seasonal variations were noted for leaf biochemical parameters. For the top, sunlit leaves in the 900-m X5 plot (in data set I), for example, CHL, LMA, and EWT all showed clear phenological patterns (Fig. 2.2a). CHL was highest in September and lowest in October of 2007. Both EWT and LMA were lowest in August before increasing in the next 2 months. Correspondingly, the spectra in October had the largest reflectance in the green band and the lowest in the near-infrared wavelengths because the lowest CHL values occurred in October of that year (Fig. 2.2b). Spectra within water absorption bands, as expected, exhibited clear troughs throughout the growing season. Moreover, the spectral troughs were shallowest and EWT was lowest in August.

Data set II, which was focused on vertical effects, contained bio-chemical parameters and reflectance spectra from leaves collected at 2-m intervals along the vertical axis

of trees in the 900-m X5 plot in 2008. Vertical changes in leaf biochemical parameters were evident (Fig. 2.2c). Values for CHL, LMA, and EWT were large for the sunlit leaves high in the canopy (>18 m), but values decreased sharply in the middle layers (14–16 m). The bottom leaves had the lowest values for CHL, LMA, and EWT, but these values did not differ very much from those of the middle layers. As a result, the leaf spectra of the bottom and middle, shaded layers had high reflectance in the green and near-infrared bands, and shallow troughs within water absorption bands (Fig. 2.2d). In contrast, the spectra of top, sunlit leaves had low values in the green and near-infrared bands and had the deepest troughs within the water-absorption bands.

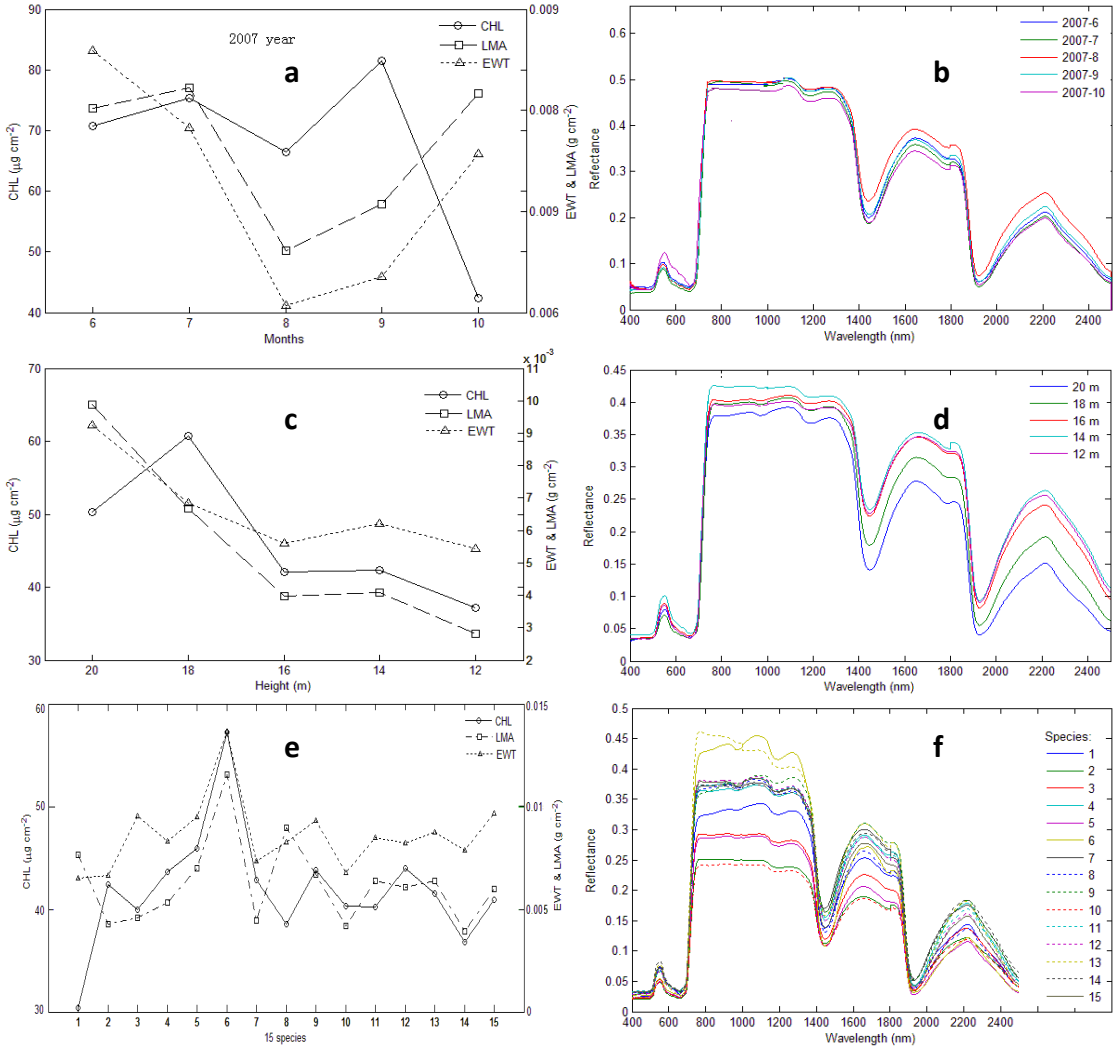

Fig. 2.2 Seasonal, vertical, and inter-species variations of leaf biochemical parameters and corresponding spectra contained in data sets compiled from measurements of field-collected leaves. Panels a and b, c and d, and e and f are from data sets I, II, and III, respectively.

Based on data set III, leaf biochemical parameters were dramat-ically different among different species even in the same region (Fig. 2.2e). H. japonica had the largest values of all three leaf bio-chemical parameters among the 15 species. The lowest CHL values were in *Fraxinus lanuginosa*, while the lowest LMA and EWT values were in *A. shirasawanum* Koidz. Spectra from the different species differed substantially, especially within the near-infrared domains (Fig. 2.2f). For the near-infrared domains, A. *shirasawanum* Koidz had the lower limit of reflectance and

H. japonica had the upper limit. Other clear differences in spectra were found in the domains of 1600–1800 nm and 2100–2300 nm. The differences of spectra in water absorption bands, however, were not as large as those in the wavelength domains noted above.

2.3.2 Models sensitivity analysis

PROSPECT

Sensitivity analysis showed that the sum of the first-order sensitivity indices (C_{ab}, C_w, C_m, and N) averaged 96.1% from 400 to 2500 nm, indicating a minor contribution from interactions in the whole domain. This suggests that the uncertainty in the PROSPECT output is not driven by interactions among the parameters, but rather by the four parameters independently. The remaining uncertainty of 4% can be explained by interactions among the parameters. For the reflectance within the domain 400 to 760 nm, C_{ab} had the greatest influence (90%), followed by N, and their interaction also contributed to the uncertainty of the outputs. As for the wavelengths from 760 to 1300 nm, N was found to have the greatest influence (94%) and C_m accounted for the remaining 6% in the uncertainty; no interaction effect between N and C_m was found to contribute in this domain. For longer wavelengths, C_w had great influence, accounting for 50 to 70% of contributions in the absorption peaks. However, unlike at the shorter wavelengths, the other two parameters, N and C_m, also significantly affected the behavior. Despite this, we could still identify three specific wavelength domains (1400-1600 nm, 1880-2100 nm, and 2300-2500 nm) at which C_w had a predominant or important influence and two at which C_m (1600-1800 nm and 2100-2400 nm) had an important influence (Fig. 2.3). The identified specific wavelength domains for a given parameter were then used to inversely retrieve it in the next step.

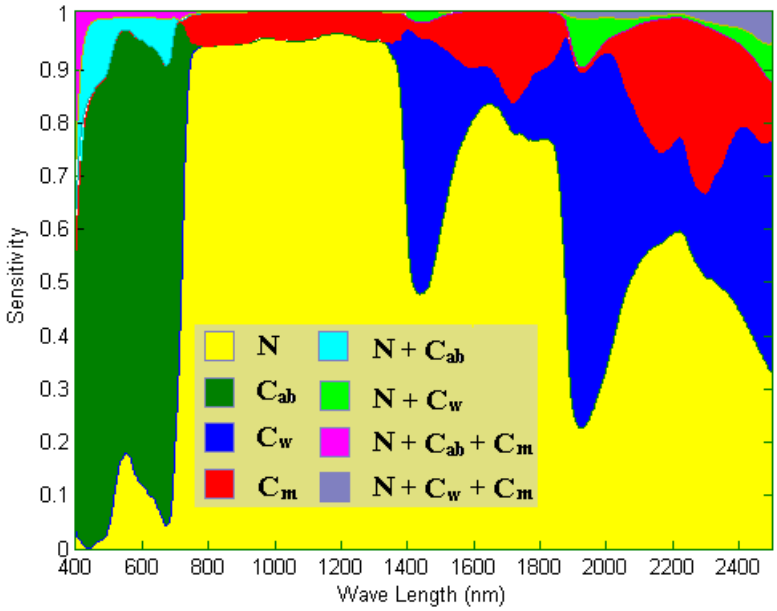

Figure 2.3 Sensitivity analyses of the input parameters for PROSPECT to spectra

LIBERTY

Sensitivity analysis (SA) of LIBERTY showed that the sum of the first-order sensitivity indices (D, xu, thickness, baseline, albino absorption, CHL) averaged 85% from 400 to 800 nm, indicating there was only a minor contribution from interactions for the whole domain. This suggests that the uncertainty in LIBERTY output is not driven by interactions among the parameters, but rather by the six parameters independently. Less than 20% of the remaining uncertainty can be explained by interactions among the parameters. For the reflectance within 400 to 750 nm domain, CHL had the greatest influence (50%), followed by xu and D, and their interaction may have also contributed to the uncertainty of the outputs. As for the wavelengths from 750 to 800 nm, xu were found to have the greatest influence (50%) and D accounted for 20% in the uncertainty., Three parameters (thickness, baseline, albino absorption) had little influence in the whole 400 to 800 nm wavelengths, accounting for 3 to 14% of contributions in uncertainty (Fig. 2.4).

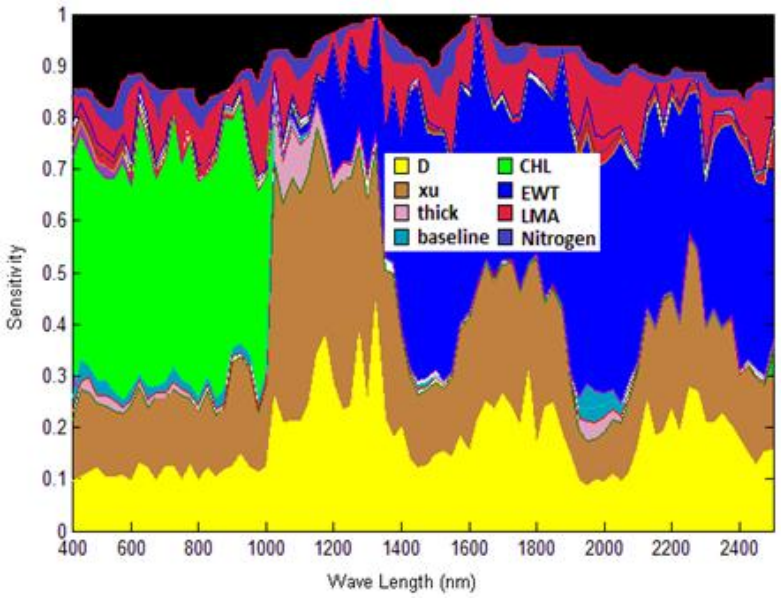

Figure 2.4 Sensitivity analyses of the input parameters for LIBERTY to spectra

2.3.3 Models simulation and calibration

PROSPECT for temperate deciduous vegetations

The PROSPECT model needs to be calibrated before its inversion to estimate leaf biochemical parameters, especially the refractive index n(λ) (Feret et al., 2008). In this study, we used the algorithm in Feret et al. (2008) to calibrate n(λ). Ten percent of the total data in the dataset I were randomly selected for calibration. Fig. 2.2 shows the calibrated refractive index using Dataset I and the original provided by PROSPECT-4. The calibrated refractive indices are clearly higher than the original values for most of the wavelengths, especially in the red edge and 1900-2500 nm domains. While the remaining 90% of dataset I is used to check the calibration accuracy. The calibration accuracy is high, as the RMSE of the modeled reflectance is very low for all wavelengths, indicating that the PROSPECT model can simulate the

reflectance very accurately using the calibrated refractive index (see Fig. 2.5).

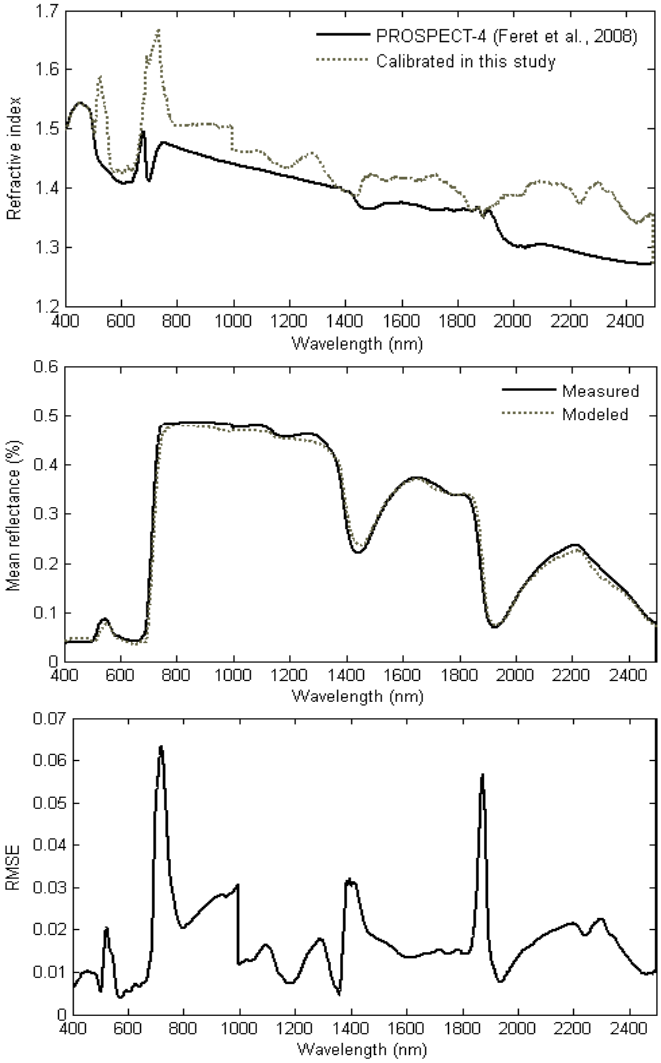

Figure 2.5 Calibrated refractive indices and the performance of PROSPECT based on the calibrated refractive indices

PROSPECT and LIBERTY for desert vegetation

Fig. 2.6a shows the chlorophyll absorption coefficients that originally provided by PROSPECT and calibrated using measured dataset. The calibrated chlorophyll absorption coefficients exhibited a little lower than the original values for most of the wavelengths, especially in the 400-500 and 650-700 nm domains. Reflectance simulations have been carried out using both original and calibrated PROSPECT (Fig. 2.6b). The simulation accuracy is apparently high after model calibration, as the RMSE of the modeled reflectance is very low for the whole 400-800 wavelengths, indicating that the PROSPECT model can simulate the reflectance very accurately after being calibrated. In comparison, the reflectance simulated by the original model had very big errors within the 400-800 nm range.

Similar procedures have been applied for LIBERTY. Fig. 2.6c shows the calibrated chlorophyll absorption coefficient using measured dataset and the original one provided by the LIEBERTY. The calibrated chlorophyll absorption coefficients are a

little lower than the original values for most of the wavelengths, especially in the 650-700 nm domains. The calibration accuracy is also high, as the RMSE of the modeled reflectance is very low for all 400-800 wavelengths, indicating accurate simulation of reflectance through LIBERTY model using the calibrated parameters. For comparison, the origin LIBERTY was found to be able to simulate accurately at most of the wavelengths except 650-700 nm and 750-800 nm range (Fig. 2.6d).

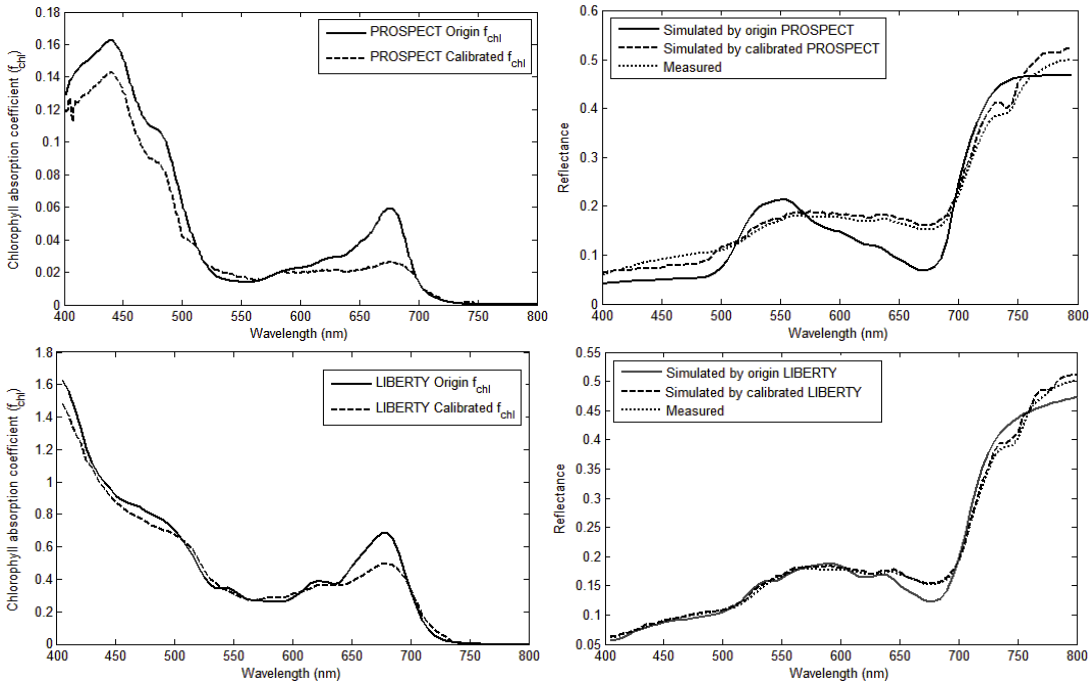

Figure 2.6 Calibrated chlorophyll absorption coefficients (f_{chl}) and the performance of reflectance simulation for the origin and calibrated models.

2.3.4 Performance of the models inversion

For data set I~III (temperate deciduous vegetations)

Leaf biochemical parameters (N, CHL, EWT, and LMA) were retrieved based on the proposed algorithm illustrated in Fig. 2.1. The performance of inverse PROSPECT using the new designed algorithm (Fig. 2.1) was then validated with the three datasets composed of *in situ* field measurements. Fig. 2.7 shows the predicted versus measured values of CHL, EWT and LMA. The values are clustered around the 1:1 line in all three cases, which indicates very good overall performance of the approach. Table 2.2 further summarizes the results of the inversion model in terms of the RMSE, R^2, CV and BIAS for each parameter. The RMSEs for CHL for all three datasets are low (RMSE < 9 μg/cm^2), with an overall RMSE of 8.11 μg/cm^2 when all three datasets are pooled. However, the coefficient of determination (R^2) for CHL for Datasets II and III is not high (R^2 = 0.40 and 0.37 for Datasets II and III, respectively), possibly due to the limited ranges of CHL contained in these two datasets. Similarly, low RMSEs of EWT were obtained for all three datasets (RMSE ≤ 0.0013 g/cm^2), and high R^2 values, from 0.56 to 0.67, were also obtained for the three datasets. Encouraging results for LMA, with RMSE ≤ 0.0013 g/cm^2 and high R^2 values from 0.75 to 0.94 across all three datasets, were obtained from the inversion model using the proposed algorithm.

When pooling all three datasets together, high performance of the inversion model based on the newly proposed algorithm on estimating all three parameters is evident. Among the three parameters, CHL is estimated better than EWT and LMA, using the CV as the criterion for judgment, although the RMSE and R^2 of CHL are lower than those of EWT and LMA. CHL estimation had a small negative bias for Dateset I but had positive biases for both Datasets II and III. On the contrary, the inversion model produced a positive bias for Dataset I while negative biases for Datasets II and III for EWT retrieval. And it generally had negative biases for LMA retrieval.

Table 2.2 Performance of PROSPECT inversion for retrieving CHL, EWT, and LMA using the proposed algorithm and the standard approach

		Data set	**I**	**II**	**III**	**All**
new algorithm	CHL	RMSE	8.69	7.41	5.85	8.11
		CV(%)	14.99	17.65	13.81	15.43
		R^2	0.73	0.40	0.37	0.56
		BIAS	-6.85	3.29	4.89	-3.18
		P_{ill}	0.10	0.14	0.18	0.12
	EWT	RMSE	0.0013	0.0011	0.0012	0.0012
		CV(%)	20.30	19.88	19.27	20.10
		R^2	0.67	0.71	0.56	0.63
		BIAS	0.0008	-0.0006	-0.0010	0.0005
		P_{ill}	0.16	0.20	0.17	0.17
	LMA	RMSE	0.0006	0.0013	0.0010	0.0008
		CV(%)	9.20	22.12	16.19	13.75
		R^2	0.94	0.75	0.75	0.84
		BIAS	-0.0004	-0.0012	-0.0015	-0.0007
		P_{ill}	0.014	0.31	0.35	0.13
standard method	CHL	RMSE	11.17	13.48	11.90	11.84
		CV(%)	15.21	31.09	25.32	22.43
		R^2	0.67	0.28	0.31	0.54
		BIAS	-7.15	8.62	10.87	-6.18
		P_{ill}	0.15	0.34	0.38	0.21
	EWT	RMSE	0.0021	0.0019	0.0018	0.0020
		CV(%)	19.53	25.13	20.31	15.83
		R^2	0.59	0.61	0.60	0.60
		BIAS	0.0007	-0.0007	-0.0013	0.0011
		P_{ill}	0.19	0.27	0.18	0.21
	LMA	RMSE	0.0028	0.0024	0.0029	0.0027
		CV(%)	35.62	33.32	25.32	38.61
		R^2	0.54	0.64	0.52	0.44
		BIAS	0.0015	-0.0018	-0.0019	-0.0015
		P_{ill}	0.30	0.45	0.42	0.34

For comparison, we performed the model inversion using the standard approach and the results are also presented in Table 2.2. The RMSEs of CHL, EWT and LMA (11.17-13.48 $\mu g/cm^2$, 0.0018-0.0021 g/cm^2, 0.0024-0.0029 g/cm^2, respectively, over the three datasets) are much higher than those obtained using the approach proposed in this study. The most dramatic improvement was noted for LMA retrieval, for which the RMSE is reduced from 0.0027 g/cm^2 using the standard approach to less than one third of this value (0.0008 g/cm^2) using the proposed algorithm, when pooling all datasets for validation. Correspondingly, the R^2 nearly doubles, increased from 0.44 to 0.84, with the BIAS reduced from -0.0015 to -0.0007 g/cm^2 and the P_{ill} decreased from 0.34 to 0.13 as well.

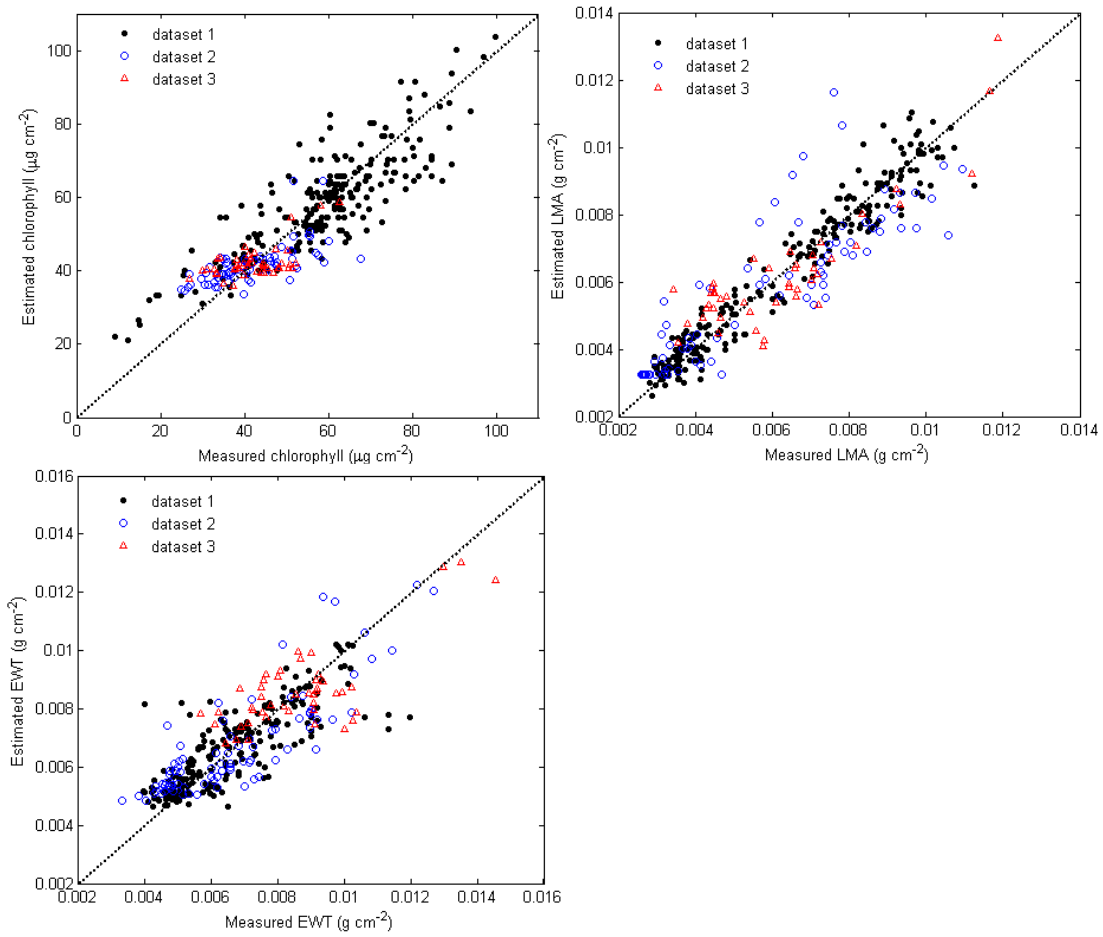

Figure 2.7 Scatter diagrams of measured and estimated CHL, LMA and EWT obtained by model inversion using the proposed approach

For data set IV(desert vegetation)

Three biochemical parameters (CHL, EWT and LMA) of assimilating branches were retrieved based on the two inversion models. Performances of inversion were then validated with *in situ* field measurements, and the results are listed in Table 2.3. For estimating CHL, the RMSE is 34.33 mg/m^2, the coefficient of determination (R^2) is 0.55, the bias is 7.16 mg/m^2 and the CV is 23.09% for the calibrated LIBERTY model inversion. For calibrated PROSPECT, the results indicated a little dropped R^2 (0.53) and a little increased RMSE and nearly identical CV with that of calibrated LIBERTY. However, the bias shifted from the positive of calibrated LIBERTY to negative (-10.03 mg/m^2). For estimating EWT, the RMSE is 0.0012 g/cm^2, R^2 is 0.63, the bias is 0.0009 g/cm^2 and the CV is 20.10% for the calibrated LIBERTY model inversion. For calibrated PROSPECT, the RMSE is 0.0012 g/cm^2, R^2 is 0.67, the bias is -0.0008 g/cm^2 and the CV is 19.27%. For estimating LMA, the RMSE is 0.0008 g/cm^2, R^2 is 0.76, the bias is -0.0012 g/cm^2 and the CV is 13.75% for the calibrated LIBERTY model inversion. For calibrated PROSPECT, the RMSE is 0.0010 g/cm^2, R^2 is 0.73, the bias is -0.0015 g/cm^2 and the CV is 16.19%. Fig. 2.8 shows the diagrams of predicted versus measured values of CHL, EWT and LMA. For both models, the values are clustered around the 1:1 line, indicating overall good performance of both model inversions.

Table 2.3 Results of the CHL, EWT and LMA inversion by the original and calibrated models.

Biochemicals	Models		R^2	RMSE	Bias	CV (%)
CHL	PROSPECT	origin	0.19*	9.13	-4.79	78.23
		calibrated	0.53***	3.47	-1.00	23.28
	LIBERTY	origin	0.32**	6.54	2.86	59.45
		calibrated	0.55***	3.43	0.71	23.09
EWT	PROSPECT	origin	0.27**	0.0018	-0.0013	20.31
		calibrated	0.67***	0.0012	-0.0008	19.27
	LIBERTY	origin	0.21**	0.0020	0.0011	21.15
		calibrated	0.63***	0.0012	0.0009	20.10
LMA	PROSPECT	origin	0.44**	0.0029	-0.0019	28.61
		calibrated	0.73***	0.0010	-0.0015	16.19
	LIBERTY	origin	0.52***	0.0027	-0.0016	25.32
		calibrated	0.76***	0.0008	-0.0012	13.75

*Notes: *: p<0.05; **: p<0.01; ***: p<0.001*

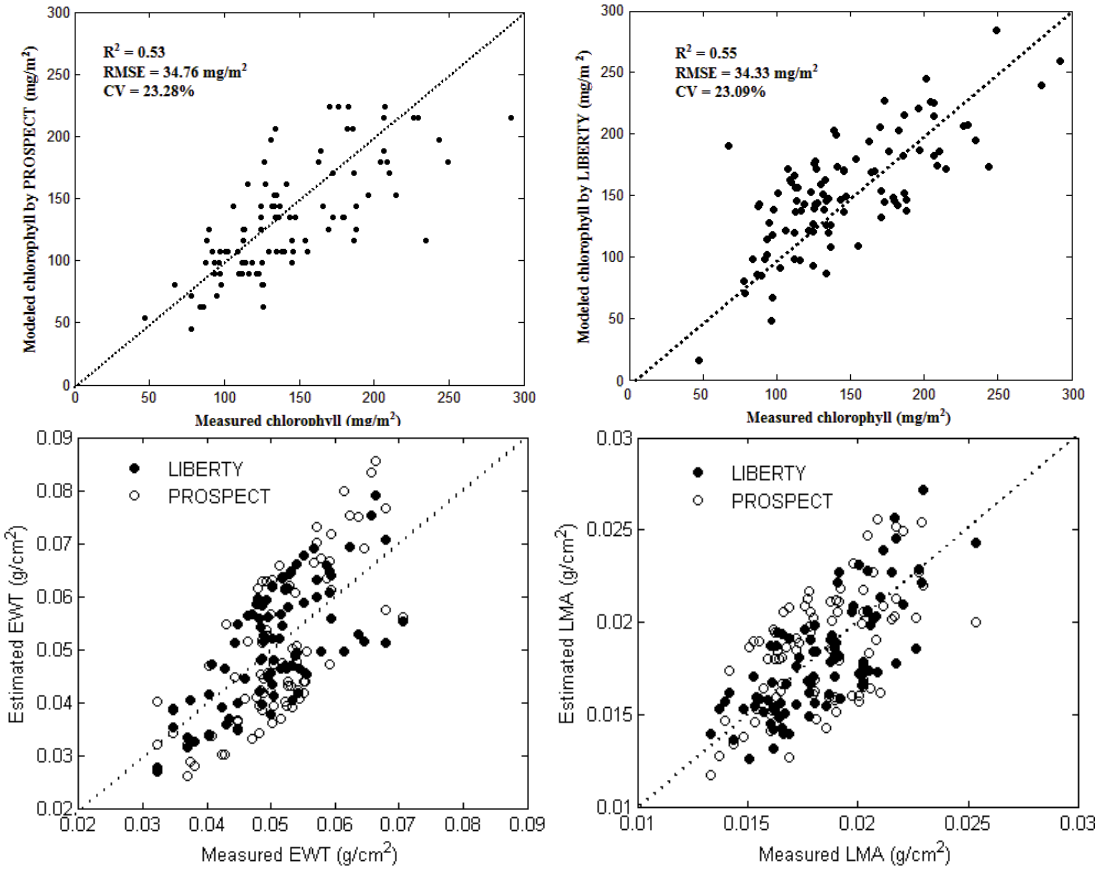

Fig. 2.8 Scatter diagrams of measured and estimated CHL, EWT and LMA obtained by recalibrated PROSPECT and LIBERTY model inversion

Comparative performance of the two original models was also list in Table 2.3. The results shows that both the LIBERTY and PROSPECT original models perform not satisfied in the CHL inversion (R^2 is 0.32 and 0.19, RMSE is 6.54 and 9.13 μg/cm^2, CV is 59.45% and 78.23% for LIBERTY and PROSPECT, respectively), EWT

inversion (R^2 is 0.21 and 0.27, RMSE is 0.0018 and 0.0020 g/cm^2, CV is 20.31% and 21.15% for LIBERTY and PROSPECT, respectively) and LMA inversion (R^2 is 0.44 and 0.52, RMSE is 0.0029 and 0.0027 g/cm^2, CV is 28.61% and 25.32% for LIBERTY and PROSPECT, respectively). For comparison the two radiative transfer models, the LIBERTY performs a little better than the PROSPECT (both for origin and calibrated versions).

In order to further validate the reliability of the two calibrated models, independent data sets collected in July 2010 and 2011 (total 60 samples, using the same measurements, process and inversion approach) were used for validation of the two calibrated models. The results expressed similar high CHL estimation accuracy with an R^2 of 0.52 and RMSE of 3.49 μg cm^{-2} for LIBERTY calibrated, and with an R^2 of 0.51 and RMSE of 3.51 μg cm^{-2} for PROSPECT-4 calibrated. For estimating EWT and LMA, the results also expressed similar high estimation accuracy. This implies that the calibrated models are reliable and robust for estimating chlorophyll content for assimilating branches of the local desert plant.

2.4 Discussion

2.4.1 Highlights of the new model inversion approach

It is evident that the performance of the inverse model has been improved by using the proposed approach and the "ill-posed" problem has been greatly reduced compared with using the standard approach. This is primarily due to the separate application of merit functions to parameter-specific wavebands. Rather than inversely estimating all biochemical parameters simultaneously using one merit function as in the standard approach, the proposed approach retrieves different biochemical parameters in steps, at each of which a merit function is assigned for a specific parameter. This greatly eliminates unexpected combinations of parameters and thus alleviates the "ill-posed" problem. In order to know the extent of the "ill-posed" problem that it can reduce, we examined the new approach with the simulated dataset (see section 2.2.2). CHL, EWT and LMA were retrieved from the simulated reflectance dataset using both the proposed approach and the standard approach. Table 2.4 summarizes the result of these inversions in terms of RMSE, CV, R^2, BIAS and P_{ill} obtained for each parameter. As shown in Table 2.4, the RMSEs of CHL, EWT and LMA when using the newly proposed approach are 7.12 μg/cm^2, 0.0012 g/cm^2 and 0.0019 μg/cm^2, respectively, much lower than those obtained with the standard approach (11.36 μg/cm^2, 0.0032 g/cm^2, and 0.0040 g/cm^2 for CHL, EWT and LMA, respectively). When considering the CV, R^2, and BIAS, the results obtained using the new approach are also much better than those obtained using the standard approach. The P_{ill} of CHL, EWT and LMA when using the new inversion algorithm are 13%, 15% and 9%, respectively, compared with 19%, 25% and 33% when using the standard approach, an average reduction of about 10% in the frequency of ill-posed inversion values overall.

It is worthy of notice that the alleviations by using the newly proposed approach are apparently different with distinctive parameter retrieving. Validation results from the datasets composed of field measurements, as well as the artificial dataset from the

PROSPECT-simulated spectra, indicate that the improvement for LMA retrieval is larger than for the other two, with the smallest improvement for CHL retrieval. This may be primarily due to the fact that CHL only has predominant control in the shortwave domain and does not affect the spectra in the near infrared or longer domains, and thus has fewer unexpected combinations with other parameters (Fig. 2.3). In contrast, LMA does not predominantly influence any specific wavelength domains, instead its effects on spectra are largely mixed with those of other parameters, leading to more possibilities for "ill-posedness". EWT is intermediate in terms of its contributions to specific wavelength domains, compared to CHL and LMA, and the improvement observed with the new approach is also intermediate.

Table 2.4 Validation of the retrieval results from PROSPECT inversion using the proposed approach and the standard approach based on the artificial dataset

		RMSE	CV	R^2	BIAS	P_{ill}
new	CHL	7.12	11.26	0.76	-3.45	0.13
approach	EWT	0.0012	10.61	0.80	0.0006	0.15
	LMA	0.0019	12.79	0.91	-0.0008	0.09
standard	CHL	11.36	16.32	0.66	-7.02	0.19
approach	EWT	0.0032	27.92	0.60	0.0012	0.25
	LMA	0.0040	40.71	0.47	-0.0019	0.33

2.4.2 Evaluation of the radiative transfer model inversion approach

To date, many authors have applied the inverse PROSPECT model using the standard approach to retrieve broadleaves biochemical contents, e.g. Baret and Fourty (1997), Colombo et al. (2008), Feret et al. (2008), Jacquemoud et al. (2000), Newnham and Burt (2001), Riaño et al. (2005). We have collated their results in Table 2.5. Their studies show that the RMSEs of CHL, EWT and LMA are in the ranges of 5.17-32.35 $\mu g/cm^2$, 0.0017-0.0057 g/cm^2, and 0.0016-0.0049 g/cm^2, respectively. The retrieval accuracies of these studies are lower than the results obtained in datasets I~III of this chapter (typical temperate deciduous forests) using the proposed new inversion approach. Again the greatest improvement was found for LMA retrieval, for which the R^2 was in the range 0.75 to 0.94, compared with R^2 values of 0.009 to 0.65 from the earlier studies. This may be primarily due to the fact that the effects of EWT and LMA are not decoupled in the standard approach, a shortcoming that has been specifically addressed in the new approach. Hence, we believe the approach applied in this study is promising for solving the "ill-posed" problems that model inversion generally faces and can provide an efficient method for quantifying biochemical parameters from leaf reflectance spectra.

Datasets I~III were obtained from the Naeba site, dataset I contained data from four different stands with the same species (*Fagus crenata*), Dataset II contained data from one stand and also one species (*Fagus crenata*) with leaf samples from different canopy vertical layers, and Dataset III contained data from the same area with 15 different species (they are all temperate deciduous forests). The results of estimating biochemical parameters using PROSPECT model inversion for these three datasets were similar but had slight difference. For estimating CHL, the performance based on RMSE is Dataset III > Dataset II > Dataset I, for estimating EWT, the performance is Dataset II > Dataset III > Dataset I, and for estimating LMA, the performance is

Dataset I > Dataset III > Dataset II (Table 2.2). One potential reason is that the No. of samples were different between the three datasets (No. of samples is Dataset I > Dataset II > Dataset III), and another potential reason is that some factors such as the different stands, vertical positions and different species will affect the samples reflectance and cause the slight difference of the model inversion accuracies between the three datasets, although the model inversion is a physical-based approach.

Table 2.5 Leaf biochemical parameters retrieved by the models inversion in previous studies

Models	Source	Parameter	RMSE	R^2	CV	BIAS
PROSPECT	Baret and Fourty (1997)	EWT	0.0025	×	×	×
		LMA	0.0016	×	×	×
	Jacquemoud et al. (2000)	CHL	9.1	0.67	×	×
		EWT	0.0018	0.95	×	×
		LMA	0.0022	0.65	×	×
	Newnham and Burt (2001)	CHL	×	0.78	×	×
		EWT	×	0.93	×	×
	Riaño et al. (2005)	EWT	×	0.94	×	×
		LMA	×	0.38	×	×
	Colombo et al. (2008)	EWT	×	0.65	×	×
		LMA	×	0.009	×	×
	Feret et al. (2008)	CHL	5.17~32.35	×	14.7~60.1	-1.42~30.07
		EWT	0.0017~0.0057	×	15.1~19.8	-0.0001~-0.0015
		LMA	0.0026~0.0049	×	27.5~51.1	-0.0035~0.0021
LIBERTY	Moorthy et al. (2004)	CHL	22.9	0.08	×	×

Comparing the widely used of PROSPECT to a wide range of species and locations in many studies, the LIBERTY model had only been used to conifer forests in several studies (Kobayashi et al., 2001; Moorthy et al., 2004), as LIBERTY was developed specifically to needles, and its structure was more complex and its input parameters were more than that of PROSPECT. Moorthy et al. (2004) compared LIBERTY and PROSPECT to retrieval CHL for Pine needles and results indicated the PROSPECT obtained much more accuracy of estimating CHL than LIBERTY (the RMSE is 12.7 μg/cm^2 for PROSPECT and 22.9 μg/cm^2 for LIBERTY).

In this chapter, we used both PROSPECT and LIBERTY to a typical desert plant *Haloxylon ammodendron* assimilating branches, as the assimilating branches of such desert plant are not broadleaves or needles. This was among the few that ever attempted to retrieve biochemical parameters of assimilating branches of typical desert plant from common leaf scale radiative transfer models. The results showed that both LIBERTY and PROSPECT models after calibrated by local measured dataset can simulate *Haloxylon ammodendron* assimilating branches reflectance and retrieve their biochemical parameters successfully and have similar fairly good retrieval accuracy. As for comparison, the original versions of $LIBERTY_{origin}$ and $PROSPECT_{origin}$ produced rather bad performances, with a much bigger RMSE error and a much lower R^2 (see Table 2.3). There were several potential reasons for original models' inability to properly invert the measured assimilating branch spectral measurements. Firstly, the *Haloxylon ammodendron* assimilating branches are not real needles or leaves (Pyankov et al., 1999), while the original PROSPECT and LIBERTY model were either oriented for broadleaf or conifer needles. Therefore, these models had some inconsistency when applied for describing the spectra of

assimilating branches. These were proved from the results where the simulated spectra by the two original models did not match the field measured spectra accurately (Fig. 2.6), and this will inevitably have great impact on the accuracy of inversion. The secondly potential reason for poor original models estimation is that the high-sensitive parameters (such as D and xu in LIBERTY, and N in PROSPECT) for the spectrally measured assimilating branches were unknown. Consequently, the inversion process can generate significant errors without such prior information, as previously studied with simulated spectra (Combal et al., 2002; Moorthy et al., 2008; Li and Wang, 2011). In addition, another possible limitation includes the discrepancies between original models specific chlorophyll, water and dry mass absorption coefficients and the coefficients embedded in calibrated models (Fig. 2.6). Upon examination of the different matters absorption coefficients in conjunction with measured spectra, it can be deduced that the calibrated models coefficients are more representative of measured assimilating branch spectra. These inconsistencies inhibited inversion capabilities of the original models to accurately estimate assimilating branch biochemical parameters from measured spectra.

In order to further validate the reliability of the two calibrated models, independent datasets collected in 2010 and 2011, were used for the two calibrated models, using the same inversion approach. The results expressed similar high CHL, EWT and LMA estimation accuracy for both $LIBERTY_{calibrated}$ and $PROSPECT_{calibrated}$. This implies that the calibrated models are reliable and robust for use in estimating biochemical parameters from assimilating braches of the local desert plant.

It is worthy of notice that LIBETY model was slightly accurate in comparison with PORSPECT model. Compared to broadleaves, the outward appearance of *Haloxylon ammodendron* assimilating branches is more similar to conifer needles; hence LIBERTY model was expected to be more suitable than PROSPECT model. This was confirmed from both simulation and biochemical parameters inversion results of the origin LIBERTY model which were more accurate than results from origin PROSPECT model (Table 2.4). Astonishingly, we also obtained very similar performance from PROSPECT, which was originally oriented for broadleaves. These results proved that we can calibrate the models input parameters to extend the models' application range, which was in agreement with some previous studies, e.g. (Malenovsky et al., 2006) where PROSPECT was applied to Norway spruce needles. Direct comparison of the measured and simulated reflectance revealed the requirement to calibrate the PROSPECT chlorophyll specific absorption coefficients, and the subsequent validation of the calibrated PROSPECT, hence showed close agreement with the spectral measurements. Zarco-Tejada et al. (2004) showed that the PROSPECT plate model in principle could be adapted to non-flat targets such as conifer needles. Moorthy et al. (2004) had compared the PROSPECT and LIBERTY model on needle chlorophyll content estimation, and the results showed that even the calibrated PROSPECT model had higher accuracy of needle chlorophyll content estimation than the LIBERTY model. Zhang et al. (2008) used the modified PROSPECT model to simulate and inversely retrieve for the conifer needles of black spruce forest in Canada, and the results showed that the retrieval of needle chlorophyll content with the modified PROSPECT was improved with an accuracy of $R^2 = 0.59$ compared with the original PROSPECT model only of $R^2 = 0.31$.

2.5 Conclusion

The chapter examined two radiative transfer models (PROSPECT and LIBERTY) to inversely retrieve biochemical parameters (CHL, EWT and LMA) of typical temperate deciduous and desert forests. As retrieval of leaf biochemical parameters using model inversion generally faces “ill-posed” problems, which dramatically decreases the estimation accuracy of an inverse model. This chapter proposed a new model inversion approach and the results indicate that the new approach greatly improves the performance of inversion models. After calibrated with field measurements, the models inversely using the new approach performed well and were in good agreement between estimates and measurements for both temperate deciduous and desert forests, thus we believe that this proposed approach could be widely applicable as a faster, efficient, robust and non-destructive method for retrieving biochemical properties from broadleaves of temperate deciduous forests to assimilating braches of desert forests through reflectance spectra. This avails a potential opportunity of coupling them with canopy models to estimate foliar biochemical parameters of different vegetations from airborne and satellite data.

Chapter 3 Leaf scale applications: hyperspectral indices

Abstract

This chapter aims at identifying efficient hyperspectral indices for estimating three leaf biochemical parameters: chlorophyll content (CHL, μg cm^{-2}), leaf water thickness (EWT, g cm^{-2}), and leaf mass per area (LMA, g cm^{-2}) in typical temperate forests. These parameters are required by most biogeochemical models to describe ecosystem functions. We have identified the most efficient hyperspectral indices (both the index types and the wavelength domains) based on both a simulated data set (produced with the calibrated leaf reflectance model PROSPECT) and with data sets (I, II, and III) from measurement of field-collected leaves. Results indicated that CHL, EWT, and LMA can be estimated with high precision using a two-waveband vegetation index (Double Deference index, DDn) for all parameters, with an over-all root mean square error (RMSE) of 6.87 μg cm^{-2} for CHL, 0.0011 g cm^{-2} for EWT, and 0.0015 g cm^{-2} for LMA. The best overall indices for temperate deciduous forests were DDn(715, 185) for CHL, DDn(1530, 525) for EWT, and DDn(1235, 25) for LMA, although these indices were not necessarily the best for every specific data set (especially for the simulated data set). Moreover, discrepancies were obvious when the identified indices were applied to different data sets. Even if the wavelengths of calibrated indices have been accurately determined through the simulated data set, the regressions between the indices and the biochemical parameters must be calibrated with field-based measurements. The indices identified in this study are applicable to various species (data set III), various phenological stages and locations (data set I), and various leaf anatomies (data set II) and may therefore be widely applicable for temperate deciduous forests and possibly for other plant communities.

3.1 Introduction

Leaf biochemical properties (e.g., chlorophyll concentrations, water content, and leaf mass area) affect a number of major ecological processes involved in exchange of matter and energy, like photosynthesis, evapotranspiration, and respiration (Peterson and Hubbard, 1992). Chlorophyll concentrations affect photosynthesis, which can be considered the major driving force for life on Earth (Nelson and Yocum, 2006). Leaf biochemical properties especially foliar lignin and cellulose concentrations (represented by leaf mass area) affect litter decomposition, which is fundamental to the cycling of carbon, nitrogen, and other important elements (Melillo et al., 1982). Foliar water content and associated water potential is a primary limiting factor for plant transpiration and carbon gain (Stimson et al., 2005) and is particularly important in dryland ecosystems where water is usually limiting (Ludwig et al., 1997). Hence, leaf biochemical properties substantially affect the growth and decomposition processes of ecosystems and are closely linked with carbon and nitrogen cycling (Aber and Federer, 1992).

Traditional methods of leaf biochemistry analysis (e.g., measurement of pigments by extraction and spectrophotometric or HPLC analysis, measurement of water status by weight loss with drying or with pressure chamber methods) are all destructive, time consuming, and expensive. In contrast, measurement of spectral reflectance is

nondestructive and rapid (Gamon and Qiu, 1999). In fact, remote estimation of leaf biochemical properties from various platforms has been the subject of many studies aimed at increasing our understanding of terrestrial ecosystem functioning.

One widespread approach to retrieve leaf biochemical information from reflectance measurements is the use of indices, which are based on the principle of combining reflectance measured on several narrow or broad spectral bands into mathematical combinations and correlating them to a particular biochemical property of the observed leaf. It is becoming clear that reflectance indices offer convenient and non-intrusive tools for rapidly inferring a number of functionally important leaf and canopy properties (Gamon and Surfus, 1999). Although both narrowband (based on hyperspectral information) and broadband indices have been applied to estimate leaf biochemical properties, the hyperspectral-based narrowband indices have several advantages over broadband indices. The most important advantage is that hyperspectral-based narrowband indices utilize wavelengths in the whole 400–2500 nm domain (le Maire et al., 2008), and it is these narrow-spectrum wavelengths that are most useful for assessing vegetation biochemical properties (Broge and Mortensen, 2002), as narrowband information located in specific portions of the spectrum can dramatically improve discrimination capabilities and classification accuracies compared with their broadband counterparts (Thenkabail et al., 2004). Consequently, hyperspectral indices are now preferred over broadband indices for estimating foliar biochemistry.

Application of hyperspectral indices to estimate leaf biochemistry is simple but apparently has limitations. When hyperspectral indices are calibrated to a specific database, the relationships elucidated cannot be generalized to other databases (le Maire et al., 2008). Unfortunately, most of the experimental databases used for calibration are not broadly representative, especially in the context of ecological concerns. To be useful in ecological studies, the relationships should be sufficiently general for application across species and leaf developmental stages (Sims and Gamon, 2002). Currently, most relationships have been developed and tested for only one or at most a few closely related species (e.g., le Maire et al., 2004; Gamon and Surfus, 1999; Datt, 1999; Blackburn, 1998), and few investigations of hyperspectral indices and leaf biochemistry have considered structural differences between leaves. Some currently available databases, e.g., LOPEX (Hosgood et al., 1994) and ANGERS (Feret et al., 2008), have composed spectra from various species but have ignored developmental stages. Sims and Gamon (2002) used a relatively large experimental database of nearly 400 leaves composed of a vast range of functional types, leaf structures, and development stages. For developmental stage, however, they used mainly three large categories: young, mature, and senescent leaves. Moreover, leaf anatomy and function differ depending on vertical position in the canopy; for example, leaf position within the canopy affects parameters like leaf mass area and leaf thickness (Ourcival et al., 1999). These changes are related to important photosynthetic and/or stomatal conductance modifications (Ashton and Berlyn, 1994). To date, no study has examined the relationship between hyperspectral indices and biochemical properties of leaves that differ in both developmental stage and location in the canopy.

Furthermore, indices are sensitive to spatial resolution and may be sensitive to more than one biochemical parameter (le Maire et al., 2008). It follows that indices are

usually calibrated for each database. The best way to find efficient indices with broad applicability would be to use a large measurement database, with many species and site conditions. Unfortunately, it is usually not feasible to obtain such a large database containing thousands of measurements.

As an alternative to the use of databases derived from field measurement of specific plant communities or ecosystems, researchers have proposed the use of artificial databases containing reflectance spectra and their corresponding leaf biochemistries (le Maire et al., 2004). Such databases have important advantages such as: many leaf biochemicals are represented (thousands of spectra); the influence of each biochemical can be totally decoupled from that of others; and the effect of a particular biochemical on the spectra is based on physical processes that are modeled at a small scale. Therefore, well-established indices obtained on such a large simulated database may potentially be applied to a wide range of spectra. However, the use of a model relies on its capacity to correctly simulate the reflectance of a wide range of leaves, which generally requires specific calibrations based on local measurements. Thus, it is essential to test these indices with field measurements.

In this chapter, we have identified the best hyperspectral indices for estimating three typical leaf biochemical parameters – chlorophyll (CHL), equivalent water thickness (EWT), and leaf mass area (LMA) – based on data from field-collected leaves (field-based data sets hereafter) and from a simulated data set generated with the PROSPECT model. The field-based data sets contained extensive spectra from different leaf developmental stages and different positions within canopies (a total of 348 spectra), as well as from 16 species in typical temperate forest stands. The simulated data set was generated using an improved and newly calibrated version of the PROSPECT model (Feret et al., 2008) and contained over 10,000 spectra. The best hyperspectral indices were determined through regression analysis via the trade-off between the simulated and field-based data sets.

3.2 Material and methods

3.2.1 Simulated data set

An improved (1-nm resolution) and recalibrated version of the leaf reflectance model PROSPECT was used in this study (Feret et al., 2008). The PROSPECT model (Jacquemoud et al., 2000, 1996; Jacquemoud and Baret, 1990) considers the leaf as a succession of absorbing layers. The new version calculates the leaf hemispherical reflectance and transmittance between 400 and 2500 nm with a 1-nm step as a function of leaf structure index (N), leaf chlorophyll content (CHL, μg cm^{-2}), leaf water content (EWT, g cm^{-2}), and leaf mass area (LMA, g cm^{-2}). We calibrated the PROSPECT model according to the calibration algorithm of Feret et al. (2008), using randomly selected spectra from field-based data set I in the following (about 10% of the total spectra in data set I). We then used the newly calibrated PROSPECT model to generate the reflectance data set using a range of input parameters, which had been computed for every combination of these parameters (Table 3.1). To ensure generalizable results, a uniform distribution was chosen for each varied parameter, so that a reflectance spectrum obtained with an extreme parameter value had the same

weight as other spectra on the indices' selecting procedure. To reproduce in the simulations the observed radiometric noise of real, measured reflectance, random noise was added to each spectrum of this data set. This step is important because it eliminates noise-sensitive indices and indices with artificially close wavelengths (le Maire et al., 2004). An additive random Gaussian noise with a standard deviation of 3% of reflectance amplitude was applied to each wavelength of each reflectance spectrum of the PROSPECT data set

Table 3.1 Parameters and parameter values used to build the 10000 spectra of PROSPECT dataset.

Parameter	Minimum	Step	Maximum
CHL (μg cm^{-2})	5	1	120
EWT (g cm^{-2})	0.001	0.0001	0.025
LMA (g cm^{-2})	0.001	0.0001	0.025
N	1	0.1	3

3.2.2 Measured data sets

To evaluate the indices for different sites and different species, we composited three datasets from the synchronous measurements on leaf biochemical parameters and reflectance in Naeba site. Detail description of the three datasets can see chapter 1.3.3.

3.2.3 Determination of best indices

This study used seven types of indices, ranging from the very simple (reflectance, R) to sophisticated (Double Difference index, DDn) (see Table 3.3 in Section 3). These types of indices are currently the most commonly used, as reviewed by le Maire et al. (2008). The DDn index was designed by le Maire et al. (2008) based on the finding of a double-peak of derivatives near the red-edge. Although le Maire et al. (2008) used DDn only for CHL estimation, the current study used the DDn index for estimations of CHL, EWT, and LMA.

Determination and evaluation of indices in this study followed two steps. First, we determined the best combination for a given type of index by regressing the index on the given biochemical parameter to determine how well the index described the biochemical parameter in the whole wavelength domain. Second, we compared the performance of different types of index. In comparing indices for each biochemical parameter, we considered the regression of the index on both simulated and measured data sets. A weight of 50% was assigned to the simulated data set and to the field-based data set; this implies that evaluation of the index was based on the average of the root mean square error (see next paragraph) for the regression with the simulated and the field-based data sets.

Regression analysis was performed for all possible combinations of wavelengths for a given index type with a wavelength step of 5 nm. For each combination, index values were calculated from each spectrum contained in the data set, and polynomial regressions (linear to the second order) were fit between index values and the biochemical parameter to be predicted (CHL, EWT, or LMA). Higher order polynomials were also tested but did not result in significant improvement. The root

mean square error (RMSE) is the common criterion used to compare different indices and was used in this study (Eq. (1)). For a given type of index of all possible combinations of wavelengths, the best index should have the lowest RMSE:

$$RMSE = \sqrt{\frac{\sum_{j=1}^{n}(y'_j - y_j)^2}{n}} \quad (1)$$

with y_j indicating the predicted value, y'_j indicating the observation for the ith spectrum, and n indicating the number of spectra.

3.3 Results

3.3.1 CHL indices

Seven types of indices for deriving leaf CHL were examined (Tables 3.2 and 3.3). For each type of index, the one giving the least RMSE for the simulated and field-based data sets (Table 3.2) and for the simulated data set alone (Table 3.3) is listed. The best indices all had the central wavelengths (λ_1) within the red edge domain. Judging from RMSEs (Table 3.2), the best index for estimating CHL was DDn(715, 185).

The double difference (DD) type of index was designed to solve the "peak jump" of the first derivative of the reflectance in deriving CHL (le Maire et al., 2004). The identified DDn(715,185) index had an RMSE of 6.78 μg cm^{-2} and was not the best index if performance was determined solely with the simulated data set (Table 3.3). DDn(715,185) was inferior to SR(780,830) and ND(780,830), both of which had RMSEs of 4.09 μg cm^{-2} based on the simulated data set (Table 3.3). However, it performed best for all three field-based data sets (RMSE of 6.55, 8.30, and 6.82 μg cm^{-2} for data sets I, II, and III, respectively). In fact, it was the most robust index for CHL prediction and was the only one efficient for both the simulated data set and the field-based data sets. The normalized difference (ND) type and simple ratio (SR) type of index, both with the central wavelengths of 735 nm and 755 nm, performed similarly based on both the simulated and field-based data sets (Table 3.2).

The modified normalized difference (mND) and modified normalized difference (mSR) type of index also performed similarly, although they had an additional waveband at 405 nm. The best difference (D) type of index used two wavelengths near or within the red edge domain and its RMSE was nearly 30% larger (8.82 μg cm^{-2}) than that of the best DDn type of index. The reflectance (R) type of index uses a single wavelength and is the simplest type among those examined. The best R type of index, R705, performed poorly compared to the other types of index examined; the RMSE of the R type of index was nearly twice as large as that of the best DDn type of index.

Table 3.2 Evaluation of the general types of indices for estimating CHL, EWT, and LMA based on both the PROSPECT simulated data set and field-based data sets. RMSE values are the means of RMSE values from the simulated data set (50% weight) and the field-based data sets (50% weight).

Parameter	Index type	Formulation	λ_1 (nm)	λ_2 / Δ (nm)	λ_3 (nm)	RMSE
CHL	R	$R_{\lambda1}$	705			13.70
($\mu g\ cm^{-2}$)	D	$R_{\lambda1}-R_{\lambda2}$	745	750		8.82
	SR	$R_{\lambda1}/R_{\lambda2}$	735	755		7.63
	ND	$(R_{\lambda1}-R_{\lambda2})/(R_{\lambda1}+R_{\lambda2})$	735	755		7.62
	mND	$(R_{\lambda1}-R_{\lambda2})/(R_{\lambda1}+R_{\lambda2}-2R_{\lambda3})$	735	755	405	7.66
	mSR	$(R_{\lambda1}-R_{\lambda3})/(R_{\lambda2}-R_{\lambda3})$	735	755	405	7.65
	DDn	$2R_{\lambda}-R_{\lambda-\Delta}-R_{\lambda+\Delta}$	715	185		6.87
EWT	R	$R_{\lambda1}$	1890			0.0028
($g\ cm^{-2}$)	D	$R_{\lambda1}-R_{\lambda2}$	1065	1310		0.0015
	SR	$R_{\lambda1}/R_{\lambda2}$	1020	1025		0.0013
	ND	$(R_{\lambda1}-R_{\lambda2})/(R_{\lambda1}+R_{\lambda2})$	1020	1025		0.0013
	mND	$(R_{\lambda1}-R_{\lambda2})/(R_{\lambda1}+R_{\lambda2}-2R_{\lambda3})$	1020	1025	405	0.0013
	mSR	$(R_{\lambda1}-R_{\lambda3})/(R_{\lambda2}-R_{\lambda3})$	1020	1025	405	0.0013
	DDn	$2R_{\lambda}-R_{\lambda-\Delta}-R_{\lambda+\Delta}$	1530	525		0.0011
LMA	R	$R_{\lambda1}$	2295			0.0035
($g\ cm^{-2}$)	D	$R_{\lambda1}-R_{\lambda2}$	1185	1300		0.0017
	SR	$R_{\lambda1}/R_{\lambda2}$	2190	2210		0.0016
	ND	$(R_{\lambda1}-R_{\lambda2})/(R_{\lambda1}+R_{\lambda2})$	2190	2210		0.0016
	mND	$(R_{\lambda1}-R_{\lambda2})/(R_{\lambda1}+R_{\lambda2}-2R_{\lambda3})$	2190	2210	405	0.0016
	mSR	$(R_{\lambda1}-R_{\lambda3})/(R_{\lambda2}-R_{\lambda3})$	2190	2210	405	0.0016
	DDn	$2R_{\lambda}-R_{\lambda-\Delta}-R_{\lambda+\Delta}$	1235	25		0.0015

Note: R: reflectance at a given wavelength; D: reflectance difference; SR: simple ratios; ND: normalized differences; mND: modified normalized differences; mSR: modified simple ratios; DDn: double difference.

Table 3.3 Evaluation of the general types of indices for estimating CHL, EWT, and LMA based solely based on the PROSPECT simulated data set.

Parameter	Index type	Formulation	λ_1 (nm)	λ_2 / Δ (nm)	λ_3 (nm)	RMSE
CHL	R	$R_{\lambda1}$	705			18.37
($\mu g\ cm^{-2}$)	D	$R_{\lambda1}-R_{\lambda2}$	780	835		7.63
	SR	$R_{\lambda1}/R_{\lambda2}$	780	830		4.09
	ND	$(R_{\lambda1}-R_{\lambda2})/(R_{\lambda1}+R_{\lambda2})$	780	830		4.09
	mND	$(R_{\lambda1}-R_{\lambda2})/(R_{\lambda1}+R_{\lambda2}-2R_{\lambda3})$	780	830	405	4.38
	mSR	$(R_{\lambda1}-R_{\lambda3})/(R_{\lambda2}-R_{\lambda3})$	780	830	405	4.38
	DDn	$2R_{\lambda}-R_{\lambda-\Delta}-R_{\lambda+\Delta}$	715	185		6.78
EWT	R	$R_{\lambda1}$	1890			0.0043
($g\ cm^{-2}$)	D	$R_{\lambda1}-R_{\lambda2}$	945	1275		0.0016
	SR	$R_{\lambda1}/R_{\lambda2}$	980	990		0.0010
	ND	$(R_{\lambda1}-R_{\lambda2})/(R_{\lambda1}+R_{\lambda2})$	980	990		0.0010
	mND	$(R_{\lambda1}-R_{\lambda2})/(R_{\lambda1}+R_{\lambda2}-2R_{\lambda3})$	980	990	405	0.0010
	mSR	$(R_{\lambda1}-R_{\lambda3})/(R_{\lambda2}-R_{\lambda3})$	980	990	405	0.0010
	DDn	$2R_{\lambda}-R_{\lambda-\Delta}-R_{\lambda+\Delta}$	1525	600		0.0010
LMA	R	$R_{\lambda1}$	2285			0.0059
($g\ cm^{-2}$)	D	$R_{\lambda1}-R_{\lambda2}$	1155	1270		0.0017
	SR	$R_{\lambda1}/R_{\lambda2}$	1525	1865		0.0019
	ND	$(R_{\lambda1}-R_{\lambda2})/(R_{\lambda1}+R_{\lambda2})$	1525	1865		0.0019
	mND	$(R_{\lambda1}-R_{\lambda2})/(R_{\lambda1}+R_{\lambda2}-2R_{\lambda3})$	1525	1865	405	0.0024
	mSR	$(R_{\lambda1}-R_{\lambda3})/(R_{\lambda2}-R_{\lambda3})$	1525	1865	405	0.0023
	DDn	$2R_{\lambda}-R_{\lambda-\Delta}-R_{\lambda+\Delta}$	1240	10		0.0019

Measured and simulated CHL values were regressed against the DDn(715,185) index from all data sets (simulated and field-based) (Fig. 3.1a). Although most points were located near the regression line, the regression coefficients apparently differed among the data sets because the values from any one data set were usually located on only one side of the regression line. A scatter diagram of estimated CHL values (from the linear regression) and measured CHL values in the field-based data sets indicated that the regression based on the DDn index performed well such that the data were distributed along the 1:1 line (Fig. 3.1b).

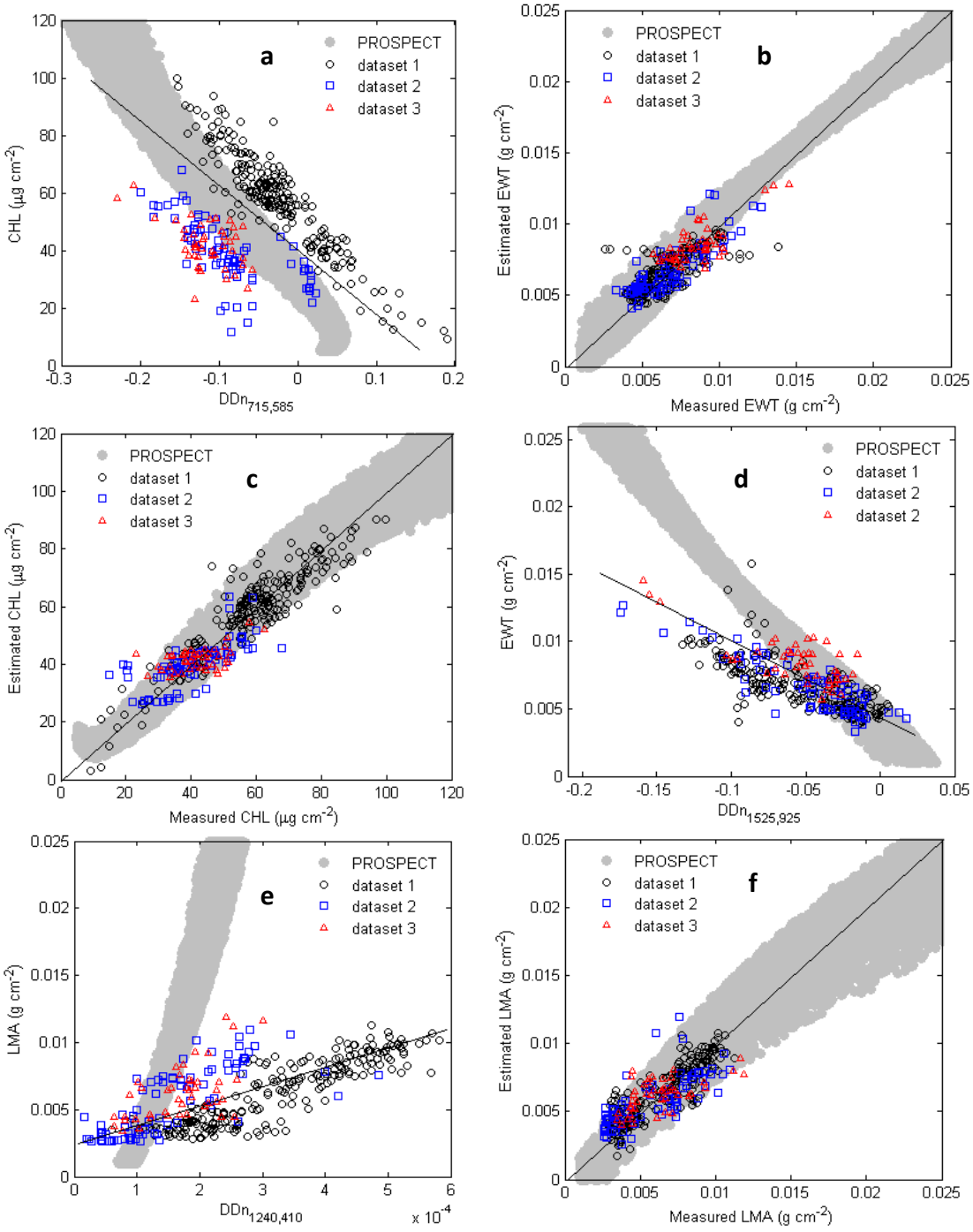

Fig. 3.1 Regressions of estimated parameter values on spectral values (a, c, e) based on the best DDn index for estimating the parameters CHL, EWT, and LMA, and plots of estimated parameter values on measured parameter values (b, d, and f).

3.3.2 EWT indices

The seven types of index were also investigated for estimating EWT (Tables 3.2 and 3.3). As was the case for CHL, the DDn type of index was the best because it produced the lowest RMSE (0.0011 g cm^{-2}) for the simulated and field-based data sets (Table 3.2). Furthermore, the best DDn type of index, DDn(1530, 525), performed best among all indices for the simulated data set (RMSE of 0.0010 g cm^{-2}) and the field-based data sets (RMSE of 0.0014, 0.0013, and 0.0013 g cm^{-2} for data sets I, II, and III, respectively).

Performance was similar for the SR, ND, mSR, and mND types of index, all of which had an RMSE of 0.0013 g cm^{-2} for the simulated and field-based data sets (Table 3.2). Moreover, the best indices for all these types were confined to two nearby wavebands of 1020 nm and 1025 nm, with an additional wavelength of 405 nm for the mSR and mND types. The simple R type of index performed poorly (Tables 3.2 and 3.3). Performance of the best D type of index, which utilized two wavelengths (1065 and 1310 nm), was similar to that of SR, ND, mSR, and mND types of index (Table 3.2).

Measured and simulated EWT values were regressed against the DDn1530,525 index for all data sets (Fig. 3.1c). Although some differences among the slopes were noted for the simulated data set and field-based data sets, the regression parameters for field-based data sets were generally consistent. A scatter diagram of EWT values estimated by the linear regression and measured values from the field-based data sets indicated that the regression performed well in that most values were located along the 1:1 line, except for several that were mainly from data set I (Fig. 3.1d).

3.3.3 LMA indices

The seven types of index were examined for their potential to estimate leaf LMA (Tables 3.2 and 3.3). As was the case for CHL and EWT, the DDn type of index was the best because it produced the lowest RMSE for the simulated and field-based data sets (Table 3.2). The best DDn type of index for LMA, which used the central wave-length of 1235 nm and a narrow distance Δ of 25 nm, had an overall RMSE of 0.0015 g cm^{-2} (Table 3.2). The SR, ND, mSR, and mND types of index, which used the central wavelengths of 2190 and 2210 nm, all had a larger RMSE of 0.0016 g cm^{-2} (Table 3.2). The D type of index, $R_{1185} - R_{1300}$, had an RMSE of 0.0017 g cm^{-2}, which was less than half of the RMSE of the best index of the R type (0.0035 g cm^{-2}). Further analysis revealed that DDn type of index performed consistently for the simulated data set and the field-based data sets (data not shown).

Measured and simulated LMA values were regressed against the DDn(1235,25) index for all data sets, and the regression fit the measured values much better than it fit the simulated values (Fig. 3.1e). In addition, the fitted coefficients also differed among the field-based data sets. However, the scatter diagram indicated excellent agreement between estimated and measured LMA values (Fig. 3.1f).

3.4 Discussion

3.4.1 Hyperspectral indices for estimating leaf biochemical parameters

Researchers have commonly used the empirical relationships between hyperspectral indices and leaf biochemical parameters to estimate leaf biochemical properties at the leaf scale. As reviewed by le Maire et al. (2004), Blackburn (2007) and Ustin et al. (2009), dozens of indices ranging from red/NIR ratios, green and red edge types, and derivative types have been designed to estimate leaf-scale CHL content. Similarly, a number of indices have been used to estimate EWT (e.g., Roberts et al., 1998; Gao, 1996; Hardisky et al., 1983; Penuelas et al., 1993). Relatively few indices, however, have been used to estimate LMA. Most of indices types can be grouped into four general categories, as indicated by le Maire et al. (2004): (1) indices that use a single reflectance or a difference between two wavelengths; (2) indices that use a simple ratio (SR); (3) indices that use normalized ratios of differences (ND); and (4) indices based on reflectance derivatives. The seven types examined in this study covered all four categories and therefore provided a relatively comprehensive comparison of commonly applied indices.

As noted, the selected wavelengths were similar for the normalized indices (ND, mND) or their simple counterparts (SR, mSR), and their performances based on RMSE values were comparable. The normalized indices were introduced to avoid the effects of differences in background constant terms for normalized reflectance-based indices (e.g., different atmosphere conditions or soil moisture in the case of canopy measurements). No improvement for any biochemical parameter estimation was observed with these normalized indices because all reflectance spectra were measured with a leaf clip. When calibrated and used with canopy-level data, the normalized indices should perform better than their simple counterparts.

On the other hand, the "modified" indices mSR and mND did not perform better than their simple counterparts (SR and ND) even at the leaf level in this study (see Table 3.2). The modified indices use a "base wavelength" (here 405 nm), originally introduced to avoid the effects of differences in leaf surface reflectance (specular effect as opposed to effects from internal component) (Sims and Gamon, 2002). This modification might have failed to improve the results at the leaf level as the inclusion of a supplementary wavelength might increase the sensitivity to noise in the reflectance spectra and thereby increase subsequent scattering.

The best indices for CHL estimation identified in this study, all used wavelengths within the red edge domain, indicating the close relationship between the red edge reflectance information and CHL content, as reported by numerous former studies (e.g., Sims et al., 2006; le Maire et al., 2004; Gitelson and Merzlyak, 1996). The performances of the best indices for each index type in this study lie in the middle of all CHL estimation indices reviewed by le Maire et al. (2004). However, it should be noted that our results were validated with both simulated and field-based data sets, rather than with only a simulated data set, as in le Maire et al. (2004). For a comparison, the best indices for CHL estimation in the current study based only on the simulated data set, SR780,830 and ND780,830, both had an RMSE of 4.09 μg

cm^{-2} (Table 3.3), which was only slightly higher than the RMSEs of $(R_{734} - R_{747})/(R_{715} + R_{720})$ and $(R_{734} - R_{747})/(R_{715} + R_{726})$ from Vogelman et al. (1993) and of BR_{754}/BR_{704} from Datt (1999) among all CHL indices examined by le Maire et al. (2004).

Numerous indices have been designed to detect water status because of the critical role of water in ecosystem functions. These include the water index (WI, R_{895}/R_{972}) (Penuelas et al., 1993); the Normalized Difference Water Index (NDWI, $(R_{860} - R_{1240})/(R_{860} + R_{1240})$ (Gao, 1996); the Moisture Stress Index (R_{1599}/R_{819}) (Hunt and Rock, 1989); the Normalized Difference Infrared Index (NDII, $(R_{819} - R_{1649})/(R_{819} + R_{1649})$ (Hardisky et al., 1983); and the integrated reflectance from R_{867} through R_{1068} (Roberts et al., 1998). Although a number of parameters have been used to indicate water status (Seelig et al., 2008), EWT is commonly used (Colombo et al., 2008), which can be traced back to Allen et al. (1971). The popularly of EWT is increasing with increasing application of the leaf PROSPECT model (Jacquemoud et al., 1996) because EWT can be inversely derived from the model. Our results, how-ever, demonstrated that the above indices perform less well than the newly identified indices with our data sets. The best indices identified in this study, except the R and D type of indices, all had a normalized RMSE lower than 10%; the results were comparable with those of Colombo et al. (2008), even though the EWT range was much greater in the current study.

Leaf spectral information has been used relatively infrequently to predict LMA. Ourcival et al. (1999) reported that spectral information can be used to accurately predict LMA in Quercus ilex leaves. Their research, however, was based on partial least squares (PLS) analysis, which used the whole wavelength domains from 400 to 2500 nm, rather than index approaches emphasized here. le Maire et al. (2008) provided various indices to estimate LMA at the leaf scale; based on field-observed data, they obtained an RMSE of 0.00164 g cm^{-2} for the best ND type of index, a value very similar to that in the current study. However, the central wavelengths determined for the best ND type of index were longer in the current study than in le Maire et al. (2008) (2190 and 2210 nm vs. 1710 and 1340 nm). The DDn type of index, which was not been included in le Maire et al. (2008), performed best (RMSE = 0.0015 g cm^{-2}) among all indices examined in the current study.

3.4.2 DDn type of index

The DDn type of index was designed by le Maire et al. (2008) and is a simplification of the DD index of le Maire et al. (2004) but follows the same underlying principle in that it is based on the double-peak of derivatives near the red edge for estimating CHL. This type of index was the most robust and best one among all seven types of indices examined to estimate CHL in the current study, which tested the indices with both simulated and field-based data sets. The RMSEs for CHL estimation were nearly identical for all data sets, whether simulated or field-based. This suggests the DDn type of index might be universally applicable. However, it was also obvious that the fitted parameters, especially the intercept for the best DDn index for CHL estimation, DDn(715, 185), varied among the data sets (Fig. 3.1a). Hence, a much larger calibration data set is needed before a general regression to calculate CHL from the identified DDn index can be determined. The identified DDn index in this study

performed similarly to that given by le Maire et al. (2008); the RMSE for a simulated data set was 6.78 μg cm^{-2} in the current study and 6.53 μg cm^{-2} in le Maire et al. (2008). In addition, we found that simple linear regression, instead of the higher order polynomial regressions like those used in le Maire et al. (2008), is sufficient for estimating CHL, as indicated by the scatter diagram (Fig. 3.1b).

In addition to using the DDn type of index to estimate CHL, we have applied this concept to estimate EWT and LMA, although the underlying principle of the index has not been clarified for these two parameters. The DDn type of index was unexpectedly among the best indices for estimating EWT and LMA. Moreover, DDn pro-vided nearly identical RMSEs for both simulated and field-based data sets (Tables 3.2 and 3.3), suggesting that the identified indices may have broad application. This is further illustrated in Fig. 3.1c for EWT estimation, in which the regression parameters nearly kept fixed for all field based data sets. Compared with EWT, the regression coefficients (especially the slope) of the identified DDn type index with LMA varied among the field-based data sets (Fig. 3.1e), suggesting that a larger calibration data set is needed before a general relationship can be described.

As expected, the identified DDn index for estimating CHL had the central wavelength of 715 nm, the red edge point of our data sets. However, the distance (185 nm in our case) was much larger than that reported by le Maire et al. (2008). We obtained the central wavelengths of 1530 nm for EWT and 1235 nm for LMA, respectively. The distances were 525 nm for EWT and a very narrow 25 nm for LMA.

To further illustrate the performance of different combinations of central wavelengths and distances of the DDn type of index for estimating leaf biochemical properties, we constructed 2D matrix representations of RMSEs for the DDn indices (Fig. 3.2). The RMSE for each DDn index from the different combinations of central wavelengths and distances is visualized based on a color legend so that wavelength combinations producing small and large RMSE values can rapidly be determined. Fig. 3.2a clearly shows that the brown to red colors (low RMSEs) were centered at λ = 715 nm for CHL estimation, with the distance (Δ) varied from 0 to ca. 300 nm. Another area of low RMSEs occurred along the line of $\lambda = 780 + \Delta$ ($\Delta < 300$ nm). In other regions of the plot, RMSEs were large (usually > 20 μg cm^{-2}).

RMSE matrices using DDn indices to estimate EWT are shown in Fig. 3.2b. Apparently more DDn indices can be applied to estimate EWT accurately than to estimate CHL accurately because the brown to red colors (low RMSEs) occupied large areas. The low-est RMSEs occurred in the region below the line of $\lambda = 800 + \Delta$ (800 nm < λ <1200 nm, $\Delta < 300$ nm) and in the region with a central wavelength λ from 1400 to 1600 nm and the distance Δ within [400 nm, 800 nm].

The RMSE matrices using the DDn indices to estimate LMA produced only small and scattered areas with low RMSEs (Fig. 3.2c). The lowest RMSE area occurred with the central wavelength λ of 1235 nm and the distance $\Delta < 50$ nm. Another low RMSE area occurred with a central wavelength around 2100 nm and the distance around 380 nm. Hence, only a few DDn indices can be applied to estimate LMA accurately.

Overall, the DDn type of index was identified as the best indices for estimating CHL, EWT and LMA. However, as a derivative hyper-spectral index, the DDn type index is

inherently sensitive to noise and requires profound smoothing before analysis. Hence, as the result obtained by le Maire et al. (2004), its performance may somehow depend on the applied smoothing methods. Sophomoric smoothing methods may enhance its performance, although algorithms based on least-square fits are most commonly selected. However, this deserves further investigations in the future.

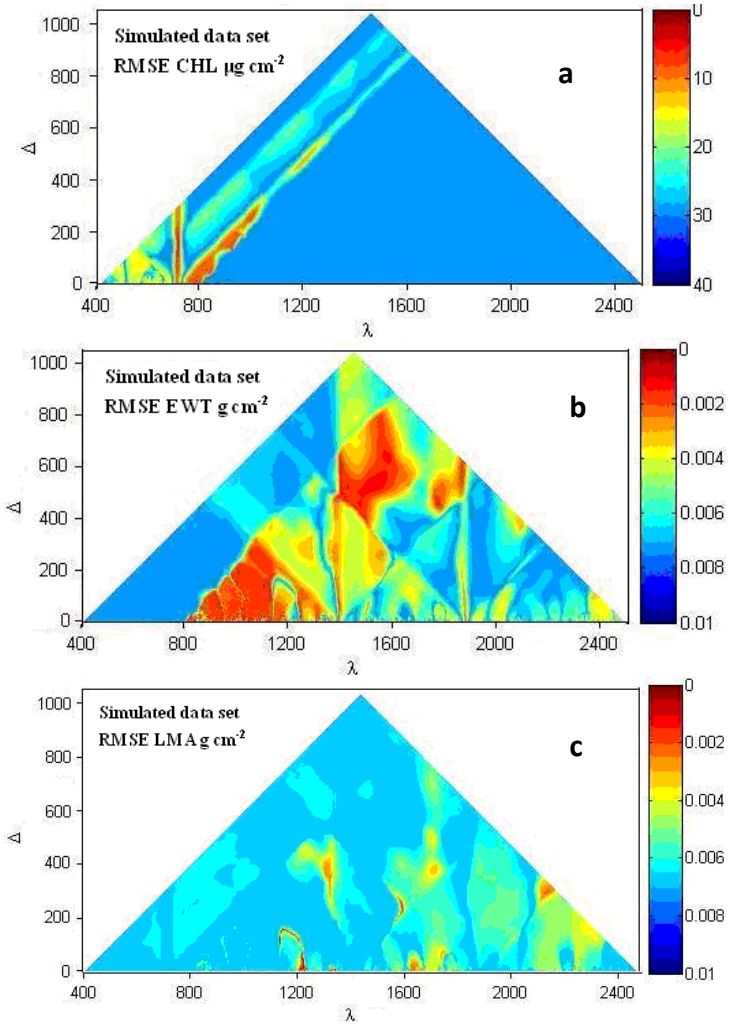

Fig. 3.2 RMSE matrices of CHL, EWT, and LMA estimations using DDn indices with different combinations of the central wavelength (λ) and the distance (Δ) based on the simulated data set. The legends on the right indicate RMSE values (blue indicates large values and red indicates small values).

3.4.3 Simulated data set vs. field-based data sets

A large data set for calibration is essential for obtaining general indices. Because of cost limitations, field-measured and field-based data sets are always confined to a given species, region, and growth stages, making it nearly impossible to provide a comprehensive measured data set for calibration. This limitation explains the cur-rent situation in which researchers have identified many diverse indices that are only applicable to specific conditions.

On the other hand, a simulated data set generated from a mechanistic reflectance

model like PROSPECT can represent a vast range of leaf reflectance spectra, which may provide an alternative resource for identifying general indices. Furthermore, as claimed by le Maire et al. (2008), the use of a simulated data set can reduce problems of covariance that often occur with field-measured data sets where some of the measured characteristics may have significant covariance. As a consequence, an index calibrated for a particular biophysical characteristic could in reality be linked to another characteristic if the index is based only on field-measured or field-based data sets, such as EWT and LMA at different phenological stages. This decreases the generic application of such empirically based indices. Using a simulated data set will prevent such problems because each simulated characteristic can be varied independently of other characteristics.

In using a simulated data set, however, the researcher assumes that the reflectance model can accurately simulate the actual reflectance spectra. In most cases, depending on the reflectance wavelengths used, the agreement between simulated and actual reflectance spectra is often imperfect, as illustrated in Fig. 3.3, which presents an overview of how well simulated and field-based reflectance spectra match. The lower and upper bounds of the simulated reflectance spectra are superimposed on the 348 field-based spectra. Some discrepancies can be easily identified in several wavelength domains, e.g., in the 400–520, 600–700, and 720–1320 nm domains. Hence, the underlying assumption, that the reflectance model accurately matches the actual reflectance spectra, could often be incorrect, and using a simulated data set alone may lead to incorrect answers.

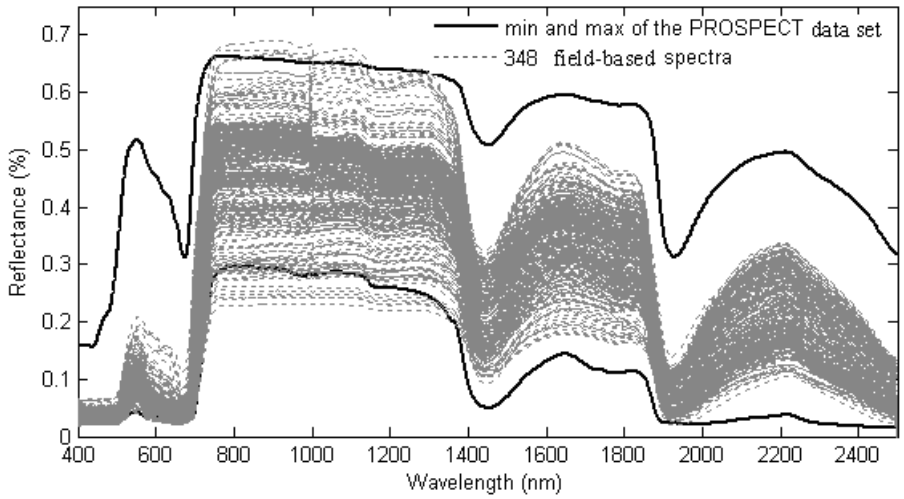

Fig. 3.3 Reflectance spectra of the simulated data set and 348 spectra from field-based data sets I, II, and III.

The current study demonstrates the problems of basing a study entirely on a simulated data set. We have also attempted to deter-mine the best indices by first examining all types of indices based on the PROSPECT simulated data set for CHL, EWT, and LMA and then by applying these indices to individual field-based data sets. However, based only on the simulated data set, the best D, SR, ND, mND, and mSR indices all had the smallest RMSE values at the wavelengths of 780 and 830 nm (835 nm for the D type), i.e., the wavelengths were all within near-infrared domains. Not unexpectedly, these indices all performed poorly with field-based data sets (data not shown) because such wavelengths are not sup-ported by physiological or physical mechanisms.

Interestingly, both approaches determined exactly the same DDn type of index (DDn (715, 185)) for CHL estimation. This could be due to the fact that only a limited number of wavelengths provide useful estimations for this type of index (see Fig. 3.2a). It may be difficult to identify an index with general applicability when many combinations of wave-bands for a given type of index produce similar RMSEs, as was the case with the DDn type of index for EWT estimation (Fig. 3.2b). Thus, a simulated data set may augment actual data sets but will not be sufficient by itself for identifying an index with general applicability. For comprehensive calibration and validation, both simulated and measured data sets should be used.

3.5 Conclusion

To obtain generic and widely applicable hyperspectral indices for leaf biochemical properties, we tested seven types of indices using every possible combination of wavelength based on both simulated and field-based data sets. The results indicated that certain indices can be generally used to estimate leaf biochemical parameters. The best indices identified in this study are DDn(715, 185) for leaf CHL, DDn(1530, 525) for EWT, and DDn(1235, 25) for LMA. These indices performed well, with an overall RMSE of 6.87 μg cm^{-2} for CHL, 0.0011 g cm^{-2} for EWT, and 0.0015 g cm^{-2} for LMA. Moreover, they performed consistently well with different field-based data sets. Because the field-based data sets included in this study encompass measurements under various conditions (i.e., different locations, different stands, different species, different canopy levels, and different phenological stages), we infer that the newly identified indices will have general applicability, at least for temperate deciduous forests. The regressions (biochemical parameter values regressed against spectral values), however, differed somewhat among the data sets, indicating the need for a further calibration before the indices can be applied to other sites. A synthetic data set can be of great help in searching for indices with general applicability but can provide misleading results if used alone. Simulated data should be used with measured data to identify indices that are supported by physiological or physical mechanisms and that have wide application.

Chapter 4 Canopy scale applications: developing of MRTM

Abstract

A multiple-layer canopy radiative transfer model (MRTM) has been developed in this chapter. The model is based on radiative transfer theory which has specifically treated the vertical heterogeneity of biophysical and biochemical parameters within the canopy. This model was validated with field measurements from a deciduous forest canopy. The results presented that the model could reproduce the measured reflectance quite well. In addition, the performance of MRTM was found to be superior in comparison to other canopy models such as PROSAIL, ACRM and FRT. The significant effect of vertical heterogeneity on the canopy reflectance was clearly identified by different scenarios, which indicates that the influence of vertical variation in leaf area density and leaf chlorophyll, water, and dry matter contents cannot be neglected, especially when the total LAI is large. If such influences are ignored, significant biases in the estimated canopy reflectance can be expected. Since this multiple-layer model is a hybrid one that offers efficient calculation, it could serve as a primary model to develop more accurate reflectance models for inhomogeneous forests at plot and regional scales in future studies.

4.1 Introduction

Remotely sensed data in the reflective optical domain function as a unique cost-effective source for providing spatially and temporally distributed information on key biophysical and biochemical parameters of land surface vegetation. Remote sensing techniques for estimating vegetation characteristics from reflective optical measurements have been based either on the empirical–statistical approach that links vegetation indices (VI) and vegetation properties using experimental data, or on the inversion of a physical canopy reflectance (CR) model. Empirical approach is simple and computationally efficient, and the potential of empirical VI relationships for the determination of plant properties has been demonstrated in numerous studies (e.g. Broge and Mortensen, 2002; Colombo et al., 2003; Gitelson et al., 2005). However, a fundamental problem with the VI approach is its lack of generality. The shape and form of canopy reflectance spectra depend on a complex interaction of several internal (e.g. vegetation structure, leaf biochemical composition, soil background) and external (e.g. view-sun-target geometry, atmospheric state) factors (Baret, 1991; Houborg et al., 2009) that may vary significantly in time and space, and from one canopy type to another. As a consequence, there is no unique relationship between a sought vegetation parameter and a VI of choice, but rather a family of relationships, each a function of canopy characteristics, soil background effects and external conditions (Baret and Guyot, 1991; Colombo et al., 2003; Gobron et al., 1997; Haboudane et al., 2004; Houborg et al., 2007; Zarco-Tejada et al., 2003).

Physically-based models have proven to be a promising alternative as they describe the transfer and interaction of radiation inside the canopy based on physical laws and hence provide an explicit connection between the biophysical variables and the canopy reflectance. Various CR models have been developed and applied to various vegetation canopies (Pinty et al., 2001; 2004; Widlowski et al., 2007). Most of current

available models have been based on radiative transfer theory with analytical approximations for the solution, which either make the assumption of homogeneous one layer canopy or two layers by adding a thin weed layer of understory vegetation (shrubs and/or grass) under the homogeneous canopy (e.g., Gobron, et al., 1997; Liangrocapart and Petrou, 2002; Myneni, et al., 1992; Nilson and Kuusk, 1989; Verstraete et al., 1990). However, canopy generally exhibits large heterogeneity on both biophysical and optical properties (Widlowski et al., 2007). Although there are some 3-D simulation models based on true canopy 3D structures (Cote et al., 2009; Pinty et al., 2004; Widlowski et al., 2007) that explain the effects of canopy heterogeneous structure on canopy reflectance, these models requires some geometrical and structural parameters of trees, which are very difficult to be measured practically, and hence there is likely to be a reduction in their effectiveness. In addition, the canopy also exhibits large heterogeneity on leaf biochemical and physiological properties such as chlorophyll, water, and dry matter content (Ciganda et al., 2008; Wang and Li, 2011). However, the effects of these heterogeneities on canopy reflectance have not been fully addressed, to the best of our knowledge.

Vertical profiles of both biophysical and biochemical properties are one of the main heterogeneities within a vegetation canopy, which has been well recognized and highlighted in many studies (Barton, 2000; Ciganda et al., 2008; Dwyer et al., 1992; Valentinuz and Tollenaar, 2004). Generally, vertical distribution of the target components is a major factor controlling canopy reflectance. If using homogeneous canopy reflectance models for calculating directional reflectance from a vertical heterogeneous canopy using average values of biophysical and biochemical properties within the canopy may lead to systematic errors. Hence, accurate modeling of canopy reflectance requires taking this factor into consideration.

With this in mind, a computationally efficient radiative transfer model, multiple-layer canopy reflectance model (hereafter called MRTM), has been developed with focus on canopy vertical heterogeneity to canopy reflectance. Similarly to the approaches of ACRM (Kuusk, 2001), FRT (Kuusk and Nilson, 2000) and PROSAIL (Jacquemoud et al., 1995; 2009), it is a hybrid-type model, including the properties of both geometrical and radiative transfer equation-based models. However, the uniqueness of this model lies in the fact that it has grouped a canopy into discrete multiple layers from bottom to the top over a horizontal bottom soil surface. The bidirectional reflectance distribution function (BRDF) of each layer in the canopy are realistically simulated through the consideration of leaf area density, leaf inclination angle, major leaf biochemical parameters such as chlorophyll, water and dry matter. Moreover, this model aims at allowing one to use multi-angular, multispectral and hyperspectral remote sensing data.

In this chapter, we have first given the mathematical description of the model, which was validated with field-measured data sets, then presented a preliminary comparison between this model and other canopy models such as ACRM, FRT and PROSAIL. Finally, we have presented scenario simulations to reveal the effect of vertical variation of each parameter on canopy reflectance.

4.2 Material and methods

4.2.1 Description of the MRTM

Vegetation canopy is treated as a constituent of discrete multiple layers from canopy above a horizontal bottom soil surface. All layers are characterized by the following set of phytometric parameters: leaf area density (LAD), leaf angle distribution (LA) parameter, and leaf size (LS); and biochemical parameters, which control the optical properties of leaves: the amount of chlorophyll (CHL), water (EWT), and dry matter (represented by dry leaf mass per area, LMA). A leaf optics model, PROSPECT (Jacquemoud and Baret 1990; Jacquemoud et al., 1996) or LIBERTY (Dawson, et al., 1998) is applied for calculation of leaf reflectance and transmittance, while weights of Price's functions are used for the calculation of the soil reflectance spectrum (Price, 1990).

In this model, other canopy models such as SAIL, ACRM and FRT are referenced for calculating directional and diffuse radiations, single-scattering and diffuse fluxes for each single layer, and for calculating non-Lambertian soil reflectance, the specular reflection of direct sun rays on leaves, the hot spot effect, and a two-parameter leaf angle distribution (LA). The main mathematical formulations of this model are shown below:

The canopy hemispherical–directional reflectance ρ is calculated as a sum of directional and diffuse components,

$$\rho = (S_\lambda^{'} / Q_\lambda)\rho_1 + \rho_d \qquad (4\text{-}1)$$

Where ρ_1 is the single-scattering component of the bidirectional reflectance factor, ρ_d is the share of diffuse fluxes in hemispherical–directional reflectance factor, and $S_\lambda^{'}$ and Q_λ are the direct solar and total spectral irradiances in a horizontal plane above the plant canopy.

Single scattering of radiation

Single scattering of direct radiation from an N-layer (NL) canopy can be represented as the sum of NL+1 components:

$$\rho_1 = \rho_1^{c1} + \rho_1^{c2} + \Lambda + \rho_1^{cn} + \rho_1^{soil} \qquad (4\text{-}2)$$

Here ρ_1^{c1}, ρ_1^{c2}, … ρ_1^{cn} are the N single scattering contributions from bottom to top of the NL canopy layers, respectively, while ρ_1^{soil} is the component of single scattering from the soil layer. The single scattering of the top of the *n* layer (the top layer) is calculated as for the one-layer canopy in ACRM (Kuusk, 1991),

$$\rho_1^{cn} = \frac{\Gamma^{(n)}(r_1, r_2)u_L^{(n)}}{\mu_1\mu_2} \int_0^{H(n)} Q^{(n)}(r_1, r_2, z)dz \qquad (4\text{-}3)$$

where $\Gamma^{(n)}(r_1, r_2)$ is the phase function, r_1 and r_2 are unit vectors in the sun and view directions, respectively, $u_L^{(n)}$ is the leaf area density (m^2/m^3) in the top layer,

$\mu_i = cos(\theta_i)$, i = 1, 2 are the polar angles of vectors r_1 and r_2, $Q^{(n)}(r_1, r_2, z)$ is the bidirectional gap probability in the layer *n* at level z, and H(*n*) is the depth of layer *n*.

Similarly, the single scattering from the *n*-1, *n*-2 … 1 layer is calculated as:

$$\rho_1^{cn\text{-}1} = \frac{\Gamma^{(n\text{-}1)}(r_1, r_2) u_L^{(n-1)}}{\mu_1 \mu_2} Q^{(n)}(r_1, r_2, H(n)) \int_0^{H(n\text{-}1)} Q^{(n\text{-}1)}(r_1, r_2, z) dz \quad (4\text{-}4)$$

$$\rho_1^{cn\text{-}2} = \frac{\Gamma^{(n\text{-}2)}(r_1, r_2) u_L^{(n-2)}}{\mu_1 \mu_2} Q^{(n)}(r_1, r_2, H(n)) Q^{(n-1)}(r_1, r_2, H(n-1)) \int_0^{H(n\text{-}2)} Q^{(n\text{-}2)}(r_1, r_2, z) dz \quad (4\text{-}5)$$

$$\rho_1^{c1} = \frac{\Gamma^{(1)}(r_1, r_2) u_L^{(1)}}{\mu_1 \mu_2} Q^{(n)}(r_1, r_2, H(n)) \Lambda\ Q^{(2)}(r_1, r_2, H(2) \int_0^{H(1)} Q^{(1)}(r_1, r_2, z) dz \quad (4\text{-}6)$$

The single scattering from soil is obtained by:

$$\rho_1^{soil} = \rho_{soil}(r_1, r_2) Q^{(0)}(r_1, r_2, H) \quad (4\text{-}7)$$

Where $\rho_{soil}(r_1, r_2)$ is the soil bidirectional reflectance factor, $Q^{(0)} = Q^{(1)}(r_1, r_2) Q^{(2)}(r_1, r_2) \Lambda\ Q^{(n)}(r_1, r_2)$, $Q^{(j)}(r_1, r_2) = p_1^{(j)} p_2^{(j)} C_{HS}^{(j)}(\gamma)$, and $H^{(j)}$ is the depth of the layer j. Here $p_i^{(j)}$ is the gap probability in the layer j in direction r_i. Calculation of $p_i^{(j)}$ can be found in Kuusk (1991).

Expressions for the single scattering in all layers are similar, except the bidirectional reflectance of the j layer is multiplied by the bidirectional gap probability in the upper layers j+1, j+2 … NL.

Diffuse fluxes

Calculation of diffuse fluxes for a given layer is similar to that in the SAIL model (Verhoef, 1984; 2002). In the SAIL model, diffuse fluxes of multiple scattering and of the sky are considered together in a four-stream approximation (Verhoef, 1984, 2002; Verhoef and Bach, 2007). Detail description of the SAIL model can be seen in Verhoef (1984), Verhoef (2002) and Verhoef and Bach (2007).

A series of reflection and transmission coefficients (operators) is introduced for the calculation of the diffuse component ρ_d for a single layer,

$$\rho_d = \rho_d^{plants} + \rho_d^{sol} \quad (4\text{-}8)$$

Where

$$\rho_d^{plants} = SQr_{so} + (1 - SQ) r_{do} + [SQp_1 r_{sd}^{soil} t_{do} + SQt_{sd} r_{dd}^{soil} t_{do}] / (1 - r_{dd} r_{dd}^{soil}) \quad (4\text{-}9)$$

and

$$\rho_d^{soil} = (SQt_{sd} + (1 - SQ) r_{dd}) r_{ds}^{soil} p_2 \quad (4\text{-}10)$$

Here $SQ = S_\lambda^{'} / Q_\lambda$ is the share of direct flux in the total irradiance, $p_i = p(r_i)$ is the gap probability in direction r_i, r_{sd}^{soil} is the soil directional–hemispherical reflectance, r_{ds}^{soil} is the soil hemispherical–directional reflectance, and r_{dd}^{soil} is the soil hemispherical–hemispherical reflectance. The defining of r_{so}, r_{do}, t_{do}, t_{sd}, and t_{dd} can be seen in Kuusk (2001).

In a multiple-layer canopy the diffuse components ρ_d^{plants} and ρ_d^{soil} are also computed with Eqs. (4-9) and (4-10), where the scattering operators for the composite leaf layers are calculated using the adding method (Liu and Weng, 2006; Sobolev, 1956; Verhoef, 1985). The strategy of adding method is to reduce the reflectance and transmittance of the combined layer by calculating the successive reflectances and transmittances between these two layers. Consider two layers with reflection R_i and R_{i+1} and transmission T_i and T_{i+1}; then the combined reflectance $R_{i,i+1}$ and transmittance $T_{i,i+1}$ can be calculated as (Fig. 4.1):

$$\begin{aligned} R_{i,i+1} &= R_i + T_i R_{i+1} T_i + T_i R_{i+1} R_i R_{i+1} T_i + T_i R_{i+1} R_i R_{i+1} R_i R_{i+1} T_i + \Lambda = \\ & R_i + T_i R_{i+1} T_i [1 + R_i R_{i+1} + (R_i R_{i+1})^2 + \Lambda\ ] = R_i + T_i R_{i+1} T_i / (1 - R_i R_{i+1}) \end{aligned} \tag{4-11}$$

$$\begin{aligned} T_{i,i+1} &= T_i + T_i R_{i+1} R_i T_{i+1} + T_i R_{i+1} R_i R_{i+1} R_i T_{i+1} + \Lambda \\ &= T_i T_{i+1} [1 + R_i R_{i+1} + (R_i R_{i+1})^2 + \Lambda\ ] \\ &= T_i T_{i+1} / (1 - R_i R_{i+1}) \end{aligned} \tag{4-12}$$

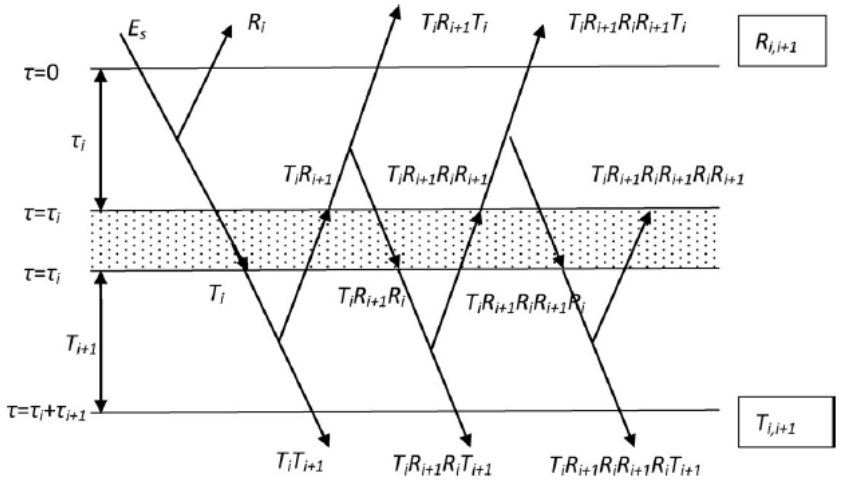

Fig. 4.1 Diagram of radiative transfers between layer i and layer i+1.

The numerical procedure of the adding method can be described as follows: at the starting point, one may calculate the reflectance and transmittance functions of the layer i using the single-scattering approximation. Then Eqs. (4-11) and (4-12) are used to compute the reflectance and transmittance functions of the layer i+1. The desired optical layer is achieved by repeating Eqs. (4-11) and (4-12) for each newly added layer.

The scattering operators of the layer i, r_{dd}^i, r_{so}^i, r_{do}^i, t_{dd}^i, t_{sd}^i and t_{do}^i can be updated by the loop program (i = 2 to NL) as below:

$$
\begin{aligned}
r_{dd}^{i} &= r_{dd}^{i} + t_{dd}^{i} \bullet r_{dd}^{i-1} \bullet t_{dd}^{i} / (1 - r_{dd}^{i-1} \bullet r_{dd}^{i}) \\
r_{so}^{i} &= r_{so}^{i} + (p_1^{i} \bullet r_{so}^{i-1} \bullet p_2^{i} + p_1^{i} \bullet r_{sd}^{i-1} \bullet t_{do}^{i} + t_{sd}^{i} \bullet r_{dd}^{i-1} \bullet t_{do}^{i} + t_{sd}^{i} \bullet r_{do}^{i-1} \bullet p_2^{i}) / (1 - r_{dd}^{i-1} \bullet r_{dd}^{i}) \\
r_{do}^{i} &= r_{do}^{i} + (t_{dd}^{i} \bullet r_{do}^{i-1} \bullet p_2^{i} + t_{dd}^{i} \bullet r_{dd}^{i-1} \bullet t_{do}^{i}) / (1 - r_{dd}^{i-1} \bullet r_{dd}^{i}) \\
t_{dd}^{i} &= t_{dd}^{i-1} \bullet t_{dd}^{i} / (1 - r_{dd}^{i-1} \bullet r_{dd}^{i}) \\
t_{sd}^{i} &= (t_{sd}^{i-1} \bullet p_1^{i} + t_{sd}^{i} \bullet t_{dd}^{i-1}) / (1 - r_{dd}^{i-1} \bullet r_{dd}^{i}) \\
t_{do}^{i} &= (t_{dd}^{i-1} \bullet t_{do}^{i} + t_{do}^{i-1} \bullet p_2^{i}) / (1 - r_{dd}^{i-1} \bullet r_{dd}^{i})
\end{aligned}
\qquad (4\text{-}13)
$$

4.2.2 Field measurements and dataset

Field measured dataset for model validation

To evaluate the model's performance, we have compiled a field measured data set from synchronous measurements of both leaf biophysical and biochemical parameters and reflectance in Naeba site. The Dataset was compiled from the data acquired in the growth period of August 2008 at the 900 m site, with special focus on vertical profiles of properties, for which the beech canopy has been grouped into five layers (boundaries at 12, 14, 16, 18, and 20 m). Both leaf and canopy properties, for example, contents of various pigments, leaf water, leaf dry matter, leaf thickness, leaf angle, leaf size and leaf area density of each layer, and leaf and canopy reflectance have been measured simultaneously. Detail methods of each measurements can see chapter 1.3.3. The mean values of all measurements are given in Table 4.1.

Table 4.1 Values of model parameters in scenario simulations and the measured dataset.

Parameter	Abbr. in model	Unit	Synthetic dataset	Measured dataset
Sun zenith angle		degree	50	30.54
view nadir angle		degree	30	0
view azimuth angle		degree	0	0
Canopy layers	NL	-	1~7	5
Leaf area index	LAI	m^2/m^2	1,3,6	5.88
Leaf size parameter	SL	cm^2	40	25.14
Mean leaf angle	thm	degree	90	60
Chlorophyll content	C_{ab}	$\mu g/cm^2$	64	45.74
Leaf water thickness	C_w	g/cm^2	0.024	0.0063
Leaf dry matter	C_m	g/cm^2	0.016	0.0051
Leaf structure parameter	N	-	1.12	1.88
Ratio of refraction indices of leaf wax and air	c_n	-	0.9	0.9
Soil parameters	s1	-	0.22	0.01

Synthetic dataset for sensitively analysis

As the field measured dataset has limited ranges for the parameters, a synthetic dataset was generated from different combinations of the main biophysical parameter LAI and main biochemical parameters (CHL, EWT, and LMA) with their vertical profile scenarios. This dataset was used for studying the effect of different vertical profiles of each parameter on the canopy reflectance. Detailed configuration of the synthetic dataset is described in Table 4.2. Except those vertically varied parameters,

most of the model parameters were fixed for generating the synthetic dataset. A full list of model parameters, the values of fixed parameters and the "standard" values of varied parameters is also given in Table 4.1.

4.2.3 Model validation

The MRTM has been validated with the field-measured dataset. Before validation of the canopy reflectance, the leaf reflectance had been validated using the measured leaf biochemical parameters and the leaf structure parameter N fitted by using the measured leaf reflectance. As field measurements had grouped the canopy into five layers, the model was operated in two modes, the first having one homogeneous layer and the second having five vertical layers. Averaged values of measured parameters (LAD, LA, LS, CHL, EWT, and LMA) of all the five layers were used for the model simulation in the one-layer mode.

Table 4.2 Vertical profile of biophysical and biochemical parameters for the synthetic dataset, LAI=3 and canopy layers NL=7, layer depth = 1 m.

	1	2	3
Vertical profile curves for model parameters		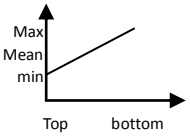	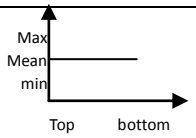
	Max	Min	Mean
LAD of each layer (m^2/m^3)	6/7	0	3/7
Leaf Size (cm^2)	70	10	40
CHL ($\mu g/cm^2$)	100	20	60
EWT (g/cm^2)	0.04	0.01	0.025
LMA (g/cm^2)	0.04	0.01	0.025

To quantify the performance of the model simulations, the estimated values (Y') and independent reference measurements (Y) were calculated for each parameter and the following statistics were calculated (Eqs. (4-14) - (4-16)): the root mean square error (RMSE) and bias (BIAS), which indicate the absolute estimation errors, and the relative error (RE), which indicates the relative estimation errors. In detail, the calculations are as follows:

$$RMSE = \sqrt{\sum_{j=1}^{n} (y_j' - y_j)^2 / n} \quad (4\text{-}14)$$

$$BIAS = \sum_{j=1}^{n} (y_j' - y_j) / n \quad (4\text{-}15)$$

$$RE = 100 \times RMSE / \bar{y} \quad (4\text{-}16)$$

where y_j and y_j' are the measured and predicted reflectance, respectively, $\bar{y}$ is the average of the measured values, and n is the number of wavelengths.

In addition, MRTM has been compared with three widely used canopy models PROSAIL (Jacquemoud et al., 2009), ACRM (Kuusk, 2001) and FRT (Kuusk and

Nilson, 2000; 2009). The PROSAIL combined the leaf optical properties model PROSPECT and the canopy bidirectional reflectance model SAIL and has been used for about 16 years to study plant canopy spectral and directional reflectance in the solar domain. ACRM is a two-layer canopy reflectance (CR) model which describes the vegetation canopy as two layers: a main homogeneous layer of vegetation and a geometrically thin layer of vegetation on the ground surface. This model is an extension of the homogeneous multispectral CR model MSRM (Kuusk, 1994) and the Markov chain CR model MCRM (Kuusk, 1995). The FRT model describes a radiative transfer scheme for a forest canopy composed of two layers: a discontinuous upper canopy of trees in the overstory, and a continuous, horizontally homogeneous shrub and grass layer in the understory above the soil surface.

All three models were parameterized and validated using the same field measured dataset in this study. The values of main model parameters for PROSAIL, ACRM and FRT are list in Table 4.3. The performance for the three canopy reflectance models was evaluated using *in situ* hyperspectral canopy reflectance measurements.

Table 4.3 Values of main model parameters of PROSAIL, ACRM and FRT in the measured dataset

Models	**Parameter**	**Unit**	**Value**
Common parameters	Chlorophyll content	μg/cm^2	45.74
	Leaf water thickness	g/cm^2	0.0063
	Leaf dry matter	g/cm^2	0.0051
	Leaf structure parameter	-	1.88
	Sun zenith angle	degree	30.54
	view nadir angle	degree	0
	view azimuth angle	degree	0
	Leaf area index	m^2/m^2	5.88
PROSAIL	Hot spot parameter	-	0.2
	Soil coefficient	-	0.01
	Ratio of diffuse to total incident radiation	-	0.1
	average leaf angle	-	60
FRT	Tree height	m	23
	Crown length	m	10
	Crown radius	m	5
	Cylindrical part of crown	m	1
	Stem DBH	cm	22
	Branch area/leaf area	-	0.1
	Tree distribution parameter	-	1.49
	Shoot shading coefficient	-	0.7
	Refraction index ratio	-	0.9
	Shoot length	m	0.1
	Soil parameters (Price's functions)	-	0.01
	The Markov parameter	-	1
ACRM	Leaf size parameter	-	25.14
	Mean leaf angle	degree	60
	Refraction index ratio	-	0.9
	soil parameters (Price's functions)	-	0.01

4.2.4 Scenario simulation

Validated MRTM has been applied to simulate canopy reflectance scenarios with different vertical layers (from one to seven layers) of three different total LAI levels

(LAI=1, 3, 6). A full list of model parameters, values for those fixed parameters, and the "standard" values of varying parameters were given in Table 1. If not otherwise stated, the parameter values were kept the same in different layers. Some scenarios were included in the synthetic dataset described above to study the influences of the main biophysical and biochemical parameters (LAD, CHL, EWT and LMA) on canopy reflectance and angular distribution in the different vertical profiles. Among them, three simple artificial vertical profiles were applied, in which the LAI vertical profile decreased linearly from top to bottom, increased linearly from top to bottom, or was kept constant through the canopy (Table 4.2). For instance, the total canopy LAI was kept at 3 in some scenarios and the canopy layers NL at 7 in all simulations.

4.3 Results

4.3.1 Canopy vertical profiles of vegetation properties

Vertical changes in the biophysical and biochemical parameters LAD, LA, LS, LT, and leaf CHL, LMA, and EWT contents were apparent in the beech canopy (Fig. 4.2). In order to address them, all the parameters and leaf and canopy reflectance spectra were collected from five vertical layers (at intervals of 2 m along the canopy depth) at the Naeba site in August 2008. As shown in Fig. 4.2(a)–(c), the LAI was smallest in the top layer but increased sharply toward the 18 m and 16 m layers before dropping in the 14 m layer. However, the LAI in the bottom layer (12 m) increased again compared to the 14 m layer. LA, LT, CHL, EWT and LMA had similar vertical distributions, where large values were found for the top sunlit leaves (the top two layers), but decreased sharply toward the middle layers (14–16 m) and the bottom leaves, which had the lowest values. On the other hand, leaf size was smallest in the top sunlit leaves (the top two layers) but increased sharply in the 16 m layer before decreasing toward the bottom two layers (14–12 m).

Leaf reflectance spectra of the 14 m layer had the highest values in almost all wave bands. The bottom layer (12 m) had the lowest reflectance in near-infrared bands, while the spectra of the top two layers (sunlit leaves) depicted the lowest values in the SWIR (short wave infrared range) bands (Fig. 4.2(d)). In comparison to leaf reflectance, canopy reflectance had similar patterns but with much lower values at almost all wavelengths.

4.3.2 Model validation

As the leaf scale reflectance of MRTM was based on the PROSPECT model, it was first calibrated and validated by measured leaf reflectance data. The PROSPECT model can simulate the beech leaf reflectance accurately at most wavelengths except in the NIR domain (800–1000 nm), in which the simulated reflectance was apparently higher than the measured one (Table 4.4). RMSE, BIAS and RE of the simulated reflectance in the entire domain of wavelengths were 0.0315, 0.0174 and 11.22%, respectively. By comparison, they were 0.0512, 0.0502 and 11.06%, respectively, within the domain of NIR (Table 4.4).

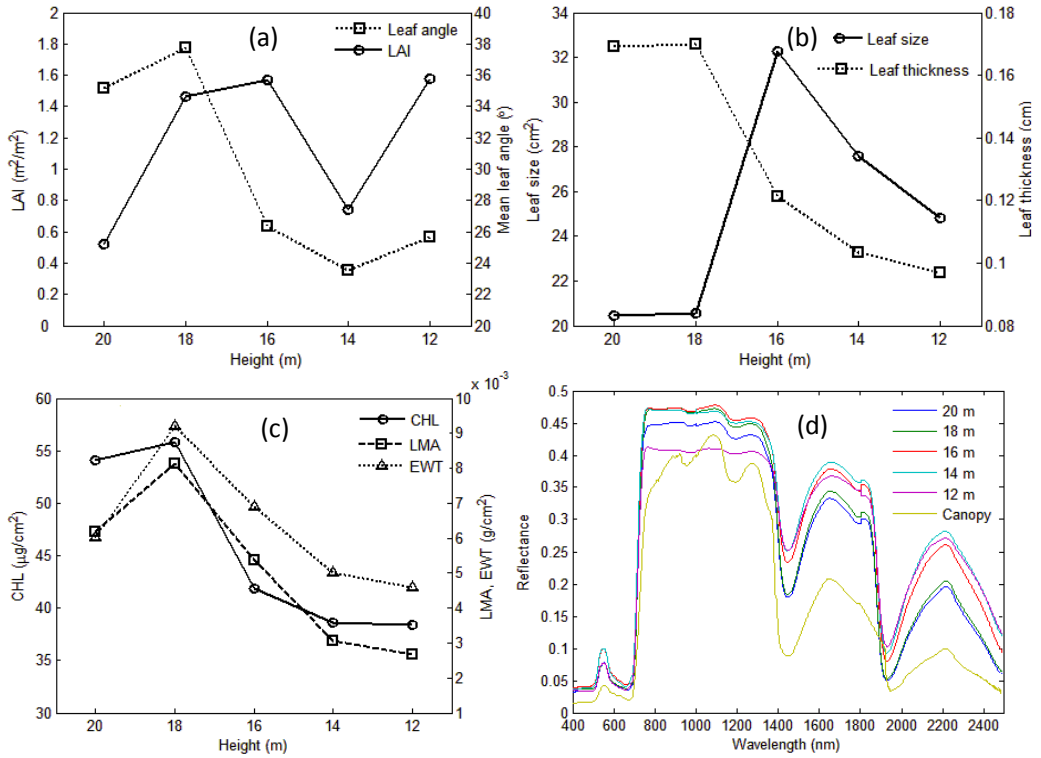

Fig. 4.2 Vertical variation of biophysical and biochemical parameters and the corresponding leaf and canopy reflectance

Validation of MRTM was carried out in two modes: the first mode grouped the canopy into only one layer (treated the canopy as being homogeneous), while the second mode separated the canopy into five layers. The results showed that simulated canopy reflectance was much higher than measured reflectance within entire wavebands with the one-layer model, where its RE reached 26.80% and 25.19% for the entire wavelength domain (400–2400 nm) and the NIR domain (800–1000 nm), respectively. However, canopy reflectance can be accurately simulated with five layer models, and the results indicated that there were obvious deviations only at 800–1000 nm. The relative error was only 10.16% for the entire wavelength domain and 10.46% in the NIR domain (800–1000 nm) (Table 4.4).

Table 4.4 Evaluation of the errors of the modeled reflectance with different models based on the field measured dataset

		400~2400 nm			800~1000 nm		
	Model	RMSE	BIAS	RE (%)	RMSE	BIAS	RE (%)
	MRTM5	0.0209	0.0084	10.16	0.0404	0.0385	10.46
	MRTM1	0.0551	0.0439	26.80	0.0973	0.0869	25.19
Canopy	PROSAIL	0.0445	0.0335	21.64	0.0776	0.0759	20.09
	ACRM	0.0314	0.0201	15.27	0.0517	0.0503	13.38
	FRT	0.0277	0.0157	13.47	0.0448	0.0432	11.60
Leaf	PROSPECT	0.0315	0.0174	11.22	0.0512	0.0502	11.06

Additionally, three widely used canopy models (PROSAIL, ACRM and FRT) were also validated using the same dataset (Fig. 4.3). The result clearly showed that MRTM in the five-layer mode gave the best simulation accuracy among all validated models.

Performances of the other three models were within those of MRTM in the five-layer mode and one-layer mode, as the RE was estimated to be 21.64%, 15.27% and 13.47% for PROSAIL, ACRM and FRT, respectively.

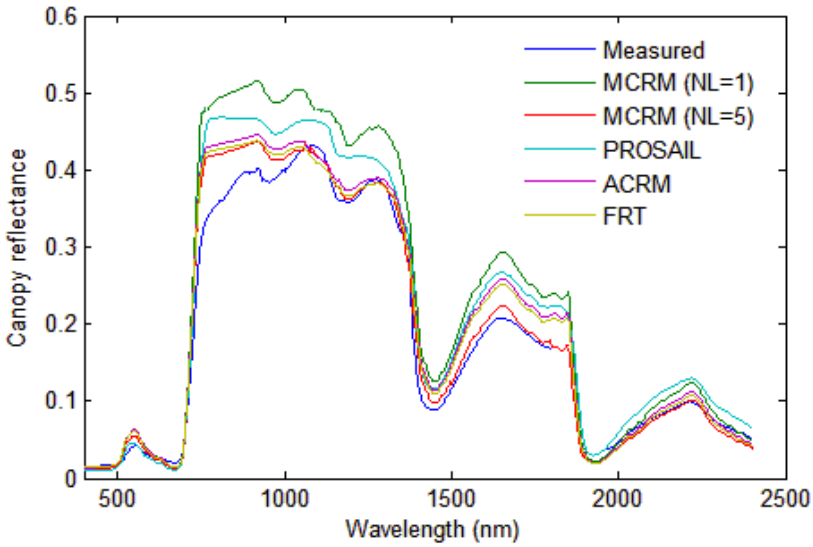

Fig. 4.3 Measured and simulated canopy reflectance using two modes (NL=1 and 5) MRTM, PROSAIL, ACRM, and FRT

4.3.3 Sensitivity analysis of canopy reflectance with biophysical and biochemical properties

The performance of MRTM was tested when the canopy was divided into different vertical layers (from one to seven layers) under three different total LAI levels (LAI = 1, 3 and 6, respectively). The simulated directional reflectance of the entire optical domain and the angular distribution of the NIR reflectance are plotted in Fig. 4.4(a)–(f). As shown in Fig. 4.4, discrepancies of simulated reflectance using different canopy layers were found mostly in the NIR and SWIR domains, especially within the domain from 800 to 1400 nm. Homogeneous canopy (NL = 1) had the highest simulated reflectance, and reflectance values decreased gradually as the number of layers increased. Meanwhile, as the number of layers increased, the difference in reflectance between neighboring layers (the n and n + 1 layer) decreased gradually. When the canopy LAI was small (e.g. LAI = 1), the difference in reflectance simulated by different layers was small (there was a minor change in simulated reflectance when the number layers was greater than three), whilst there were large discrepancies with larger LAI, where the number of the layers had to range between five and seven for the difference in simulated reflectance to be non-significant.

For angular distribution of canopy reflectance, the hot spot was sharpest in all the simulated angular distributions of NIR reflectance. This was apparent, as more shade was visible and fewer photons could escape from the canopy if the view direction did not coincide with the sun's rays. Similar to directional reflectance, the angular distribution of NIR reflectance simulated by MRTM with different numbers of canopy layers was also different, especially when the view angle was on the left side of the hot spot. And when LAI was larger, the difference was also larger (Fig. 4.4).

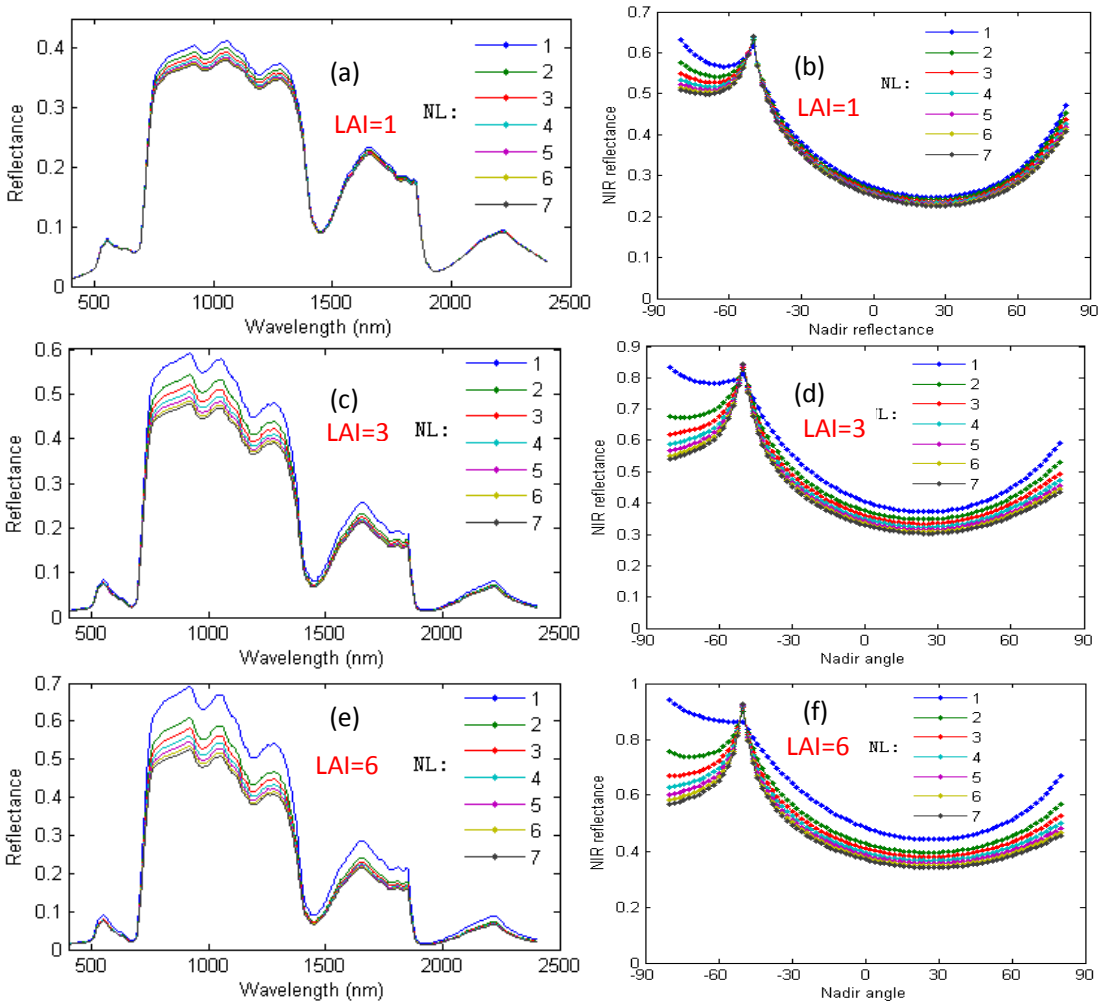

Fig. 4.4 (a)-(c) Simulated reflectance in the optical domain and (d)-(f) angular distribution at the NIR reflectance with LAI of 1, 3, 6, respectively. The canopy layers NL was varied from 1 to 7.

Fig. 4.5 shows simulated scenarios of reflectance and angular distribution with three exemplary vertical profiles of the main biophysical and biochemical parameters (LAD, CHL, EWT and LMA) within a canopy. For scenarios with three different LAD vertical profiles (termed LAD1, LAD2 and LAD3, respectively), LAD1 (the canopy top with the largest LAD) had the largest reflectance and LAD2 had the lowest reflectance, while the reflectance of LAD3 (the LAD was constant for all vertical layers) was in the middle. Reflectance discrepancies between the three LAD vertical profiles were significant in the NIR and SWIR domains, especially at 800–1400 nm. The reflectance of LAD3 was closer to the reflectance of LAD2 than that of LAD1.

For three exemplary CHL vertical profiles, averaged CHL values of the entire canopy were set to be the same (60 μg cm^{-2}). However, simulated canopy reflectance showed large differences in VIS domain. Especially for CHL2, simulated reflectance values were much higher than those of the other two CHL vertical profiles, with CHL1 having the lowest reflectance values. Similar tendencies were found for the simulated canopy reflectance for the three LMA and EWT vertical profiles, except that the largest difference in reflectance was found in 800–1400 nm domain for different LMA vertical profiles and in 1400–1900 nm domain for EWT vertical profiles.

All simulated angular distributions for different vertical profiles of LAD, CHL, LMA, and EWT exhibited similar patterns, with apparent effects of different vertical profiles. The angular distribution of reflectance at 550 nm changed tremendously between the three different vertical profiles for the case of CHL especially, followed by EWT and LMA. As a comparison, different LAD vertical profiles had the least effect on the angular distribution among the four parameters, although the effects were different for different wavebands.

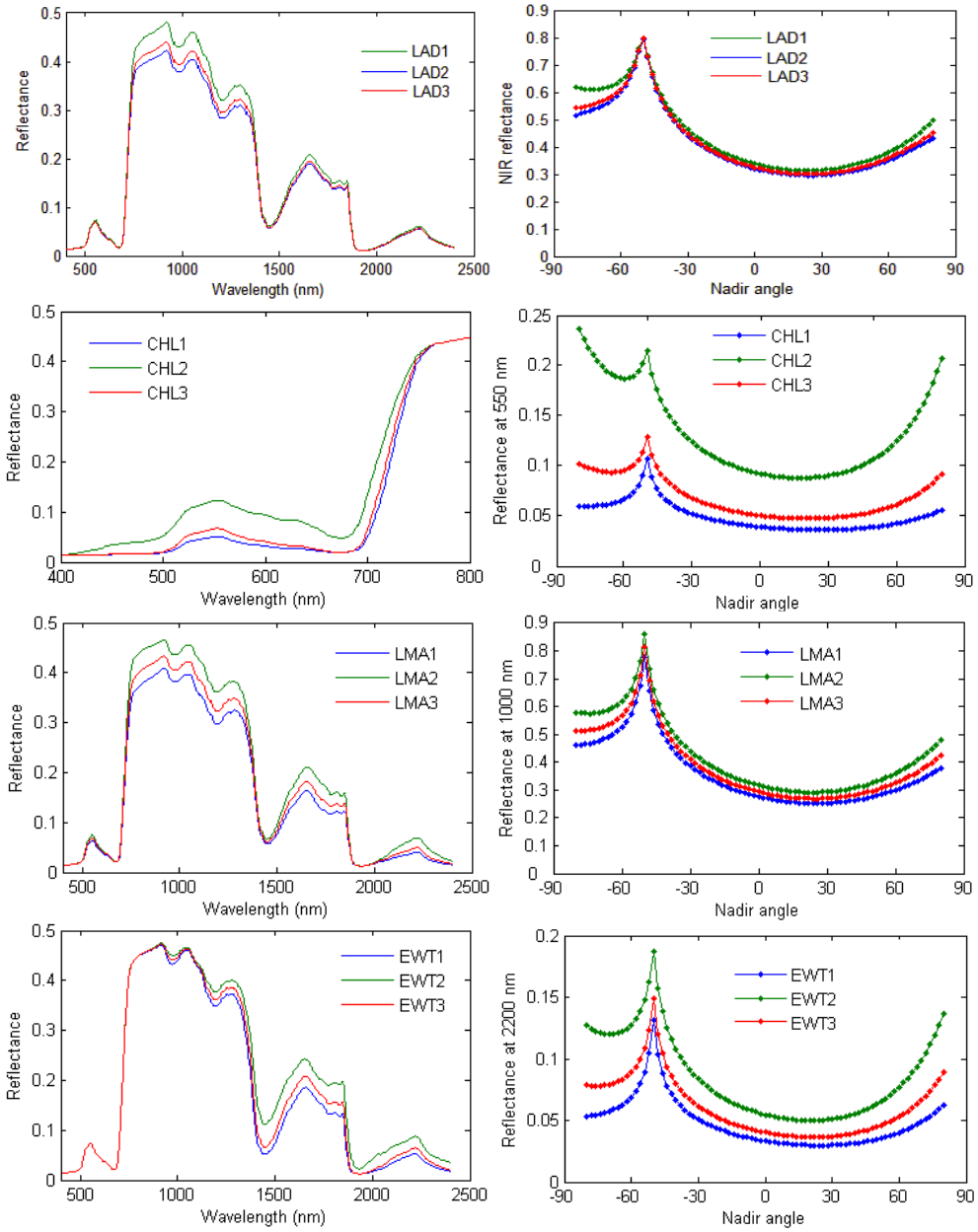

Fig. 4.5 Simulated reflectance and angular distribution with different vertical profile of biophysical and biochemical parameters (LAD, CHL, EWT, LMA) in the canopy. The model parameters LAI=3, and canopy layers NL=7.

4.4 Discussion

4.4.1 Multiple-layer canopy radiative transfer model

Field measurements indicated that apparent large vertical variations of most biophysical and biochemical properties existed, which has been well recognized and highlighted in many studies (e.g. Barton, 2000; Ciganda et al., 2008; Dwyer et al., 1992; Valentinuz and Tollenaar, 2004; Wang and Li, 2012; 2013a; 2013b). This is one of the main reasons why we developed the MRTM in order to cover the natural phenomena. On the other hand, such a model may help to effectively retrieve the vertical distribution of biophysical and biochemical parameters inversely.

MRTM rooted from ACRM or otherwise can be called a multiple-layer ACRM. However, it is more than a simple loop for accumulating reflectance from infinite n homogeneous layers, since it contains explicit descriptions of variations in both biophysical and biochemical properties within a canopy. Besides MRTM5 (five layers), three other canopy models (PROSAIL, ACRM and FRT) and MRTM1 (one layer) were also validated using the same measured dataset. The results showed that the other three models (PROSAIL, ACRM and FRT) had similar levels of estimation accuracy and performed better than MRTM1, indicating an inferior performance of the newly developed MRTM1 when using the mean values of the biophysical and biochemical parameters within a canopy for simulating canopy reflectance. Simulated canopy reflectance was generally above that of MRTM5 and field measurement data when using other canopy reflectance models (Fig. 4.5). An apparent reason was that they applied mean values of the biophysical and biochemical parameters within a canopy for simulation. MRTM5 not only performed better than MRTM1 but also performed better than the other three models, clearly indicating that large vertical variations in the biophysical and biochemical properties of vegetation had non-negligible influences on the canopy's optical properties. Therefore, the multiple-layer canopy model proposed in this study has gone further to a certain extent than the other canopy models with homogeneous canopy such as PROSAIL, ACRM and FRT.

When validated with the field measurement dataset, the canopy reflectance simulated by MRTM in the five-layer mode was found to be of the same order as measured data in the entire waveband. However, it was also apparent that simulated reflectance values in the NIR domain (800–1000 nm) were systematically above the measured reflectance, with an RE of 10.46%. Similar gaps were found in other canopy reflectance models as well (Kuusk et al., 2010; Widlowski et al., 2007). This deviation may have partially resulted from the simulated leaf reflectance of the leaf reflectance sub-model (PROSPECT), which was systematically higher than the measured data within the NIR region. The other most probable reason is that the measured spectrum shows the influence of woody material (Asner, 1998). However, none of these models have described the influence of woody material on the canopy spectrum very well, which, as pointed out by Verhoef and Bach (2007), should be addressed in the radiative transfer models. This deficiency will be enhanced in future with both spectral measurements of woody elements in situ and corresponding model simulations.

Alternatively, there are some 3-D simulation models based on true 3-D canopy structures (Cote et al., 2009; Pinty et al., 2004; Widlowski et al., 2006, 2007) available to simulate canopy reflectance, which are supposed to have greater strength in explaining the heterogeneity of the canopy. Even so, the multiple-layer model has several advantages over these 3-D models: one is that the 3-D simulation models are much more complex and require the input of many geometrical and structural parameters which are very difficult to measure and obtain, and consequently these models are ineffective for wide application. The multiple-layer model is much simpler than the 3-D models, as it only requires vertical profiles of the main biophysical and biochemical parameters within a canopy, which are generally widely monitored in ecophysiological studies. In addition, such a multiple-layer reflectance model may generally be applied not only for canopy reflectance simulation but also for effectively retrieving parameters and their vertical distributions inversely. Moreover, the MRTM proposed in this study considered not only the heterogeneity of biophysical parameters but also the heterogeneity of biochemical parameters within a canopy, an aspect that is usually lacking in most current 3-D models. As a result, MRTM obtained a simulation accuracy that was similar to that of 3-D models but with a calculation speed close to those of the SAIL and ACRM models. This improvement is crucial especially in real-time calculations and in solving inverse problems when numerous calculations by the model are necessary.

4.4.2 Effects of vertical profiles of vegetation properties on canopy reflectance

Leaf scale reflectance exhibited tremendous variations within a canopy, which corresponded to the vertical changes of biophysical and biochemical parameters. As noted from the field measurement dataset, leaf scale reflectance spectra reached the highest reflectance values in almost all wavebands. In addition, the leaves in the 14 m layer had relatively low LAD and biochemical properties (CHL, EWT and LMA) compared with other layers. The bottom layer (12 m) had the lowest reflectance values in the near-infrared bands since it had the largest LAD. The spectra of the top two layers (sunlit leaves) showed the lowest values in the SWIR bands as they had the largest LMA and EWT contents (Fig. 4.2(d)). Since canopy reflectance contains all contributions from leaves within the canopy, it was expected to be sensitive to the variations in biophysical and biochemical parameters but in a very complex way because the contributions from different layers differed from the overall reflectance.

The performance of MRTM with different numbers of layers is clearly illustrated in Fig. 4.4. The results suggest that it is essential to consider vertical changes in parameters across several layers in canopy reflectance simulation, especially with large canopy LAI, which may otherwise result in large deviations. As a rough estimation, when the total canopy LAI is small (<1), grouping the canopy into three vertical layers is sufficient; if the total LAI is larger than that, it should be set at five to seven layers.

Under the same total canopy LAI, simulated reflectance was different with different LAD vertical profiles. The results showed that simulated reflectance values were largest in the case of the vertical distribution of LAD at LAD1, which was followed by LAD3, while the lowest value was found in the case of LAD2. This is primarily because when the leaves are mostly in the upper layers (LAD1), less radiation goes

through to the lower layers, and hence less energy is absorbed, resulting in higher reflectance. The opposite reason can explain why LAD2 had the lowest reflectance value. The simulated reflectance of LAD3 was closer to the reflectance of LAD2 than that of LAD1.

For three biochemical parameters (CHL, EWT and LMA), similar tendencies of simulated canopy reflectance were obtained for three vertical profiles. The simulated reflectance values of the vertical profiles were found to follow the order (from high to low) CHL2 > CHL3 > CHL1 in the VIS bands, while EWT2 > EWT3 > EWT1 mostly in the SWIR bands, and LMA2 > LMA3 > LMA1 in both the NIR and SWIR bands. This was primarily because canopy reflectance contains more information on upper layers than lower layers, since CHL2 for leaves in the top had the lowest CHL content and hence led to the highest reflectance in the VIS bands, and the same reason applied to EWT and LMA.

Generally, vertical profiles of almost all the biophysical and biochemical properties will affect canopy directional reflectance and its angular distribution. The effect of the CHL vertical profile on canopy reflectance is in the VIS domain, while the effect of EWT is mainly in the SWIR domain, the effect of LMA is mainly in the NIR and SWIR domains, and the effect of LAD is mainly in the NIR domain. On the other hand, the same canopy reflectance curve may have resulted from different combinations of these parameters with different vertical profiles even with the same averaged values within the canopy. Fig. 4.6 presents examples of some very close reflectance curves simulated by the model with different total values and different vertical profiles of LAI, CHL, LMA or EWT parameters. This indicated that if canopy parameters are retrieved without considering the vertical variations, large errors might be presented in the results. Thus, investigating the vertical variations of the main biophysical and biochemical parameters and including such information in the canopy scale reflectance model is critical.

Application of radiative transfer models involves using these models to retrieve biophysical and biochemical parameters inversely. For the MRTM, it can be used to inversely retrieve the vertical profiles of such parameters at a scale closer to that of a real canopy. The model inversion process generally faces the well known “ill-posed” problem: when searching for the most similar simulated spectrum to an observed spectrum, a wide range of values can be retrieved, since very similar reflectance spectra can be obtained from very different combinations of input parameters (Combal et al., 2002; Li and Wang, 2011; Wang et al., 2007; Yebra and Chuvieco, 2009). Inversion of MRTM not only faces the “ill-posed” problem caused by different parameters (e.g. LMA and EWT) but may also result from the same parameter with different vertical profiles (e.g. in Fig. 4.6, different vertical variations of fixed parameters can result in similar outputs of canopy reflectance). One approach to solving the “ill-posed” problem is to use prior information obtained from in situ measurements (Combal et al., 2002). However, for those areas that lack in situ data it may be necessary to develop a new inversion algorithm for the canopy scale as in Li and Wang (2011) for leaf scale, in order to alleviate the “ill-posed” problem caused by the vertical variations of parameters. This will be explicitly addressed in future studies.

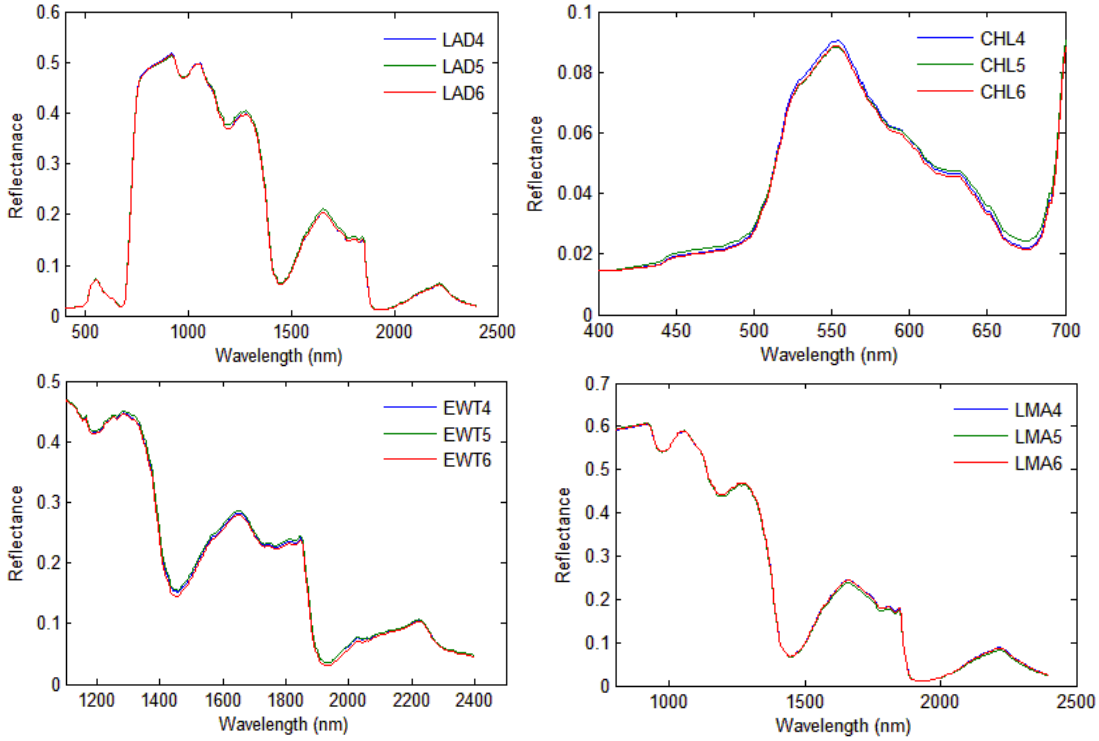

Fig. 4.6. Examples of close reflectances simulated with different total (mean) contents and vertical profiles of LAD, CHL, EWT, and LMA. Number of canopy layers NL = 5, layer depth H = 2 m. LAD4 = {0.25, 0.75, 0.75, 0.75, 0.25}, total LAI = 5.5 m^2 m^{-2}; LAD5 = {0.9, 0.5, 0.25, 0.2, 0.05}, total LAI = 3.8 m^2 m^{-2}; LAD6 = {0.5, 0.5, 0.5, 0.5, 0.5}, total LAI = 5 m^2 m^{-2}; CHL4 = {40, 60, 60, 40, 30}, mean CHL = 46 μg cm^{-2}; CHL5 = {80, 40, 20, 20, 10}, mean CHL = 34 μg cm^{-2}; CHL6 = {50, 50, 50, 50, 50}; mean CHL = 50 μg cm^{-2}; EWT4 = {0.006, 0.01, 0.007, 0.005, 0.005}, mean EWT = 0.007 g cm^{-2}; EWT5 = {0.01, 0.007, 0.004, 0.003, 0.001}, mean EWT = 0.005 g cm^{-2}; EWT6 = {0.0085, 0.0085, 0.0085, 0.0085, 0.0085}, mean EWT = 0.0085 g cm^{-2}; LMA4 = {0.005, 0.008, 0.008, 0.005, 0.004}, mean LMA = 0.006 g cm^{-2}; LMA5 = {0.01, 0.008, 0.004, 0.002, 0.001}, mean LMA = 0.005 g cm^{-2}; LMA6 = {0.007, 0.007, 0.007, 0.007, 0.007}; mean LMA = 0.007 g cm^{-2}.

4.5 Conclusion

A canopy scale radiative transfer model (MRTM) that addresses vertical heterogeneity of biophysical and biochemical parameters within the canopy has been proposed. Model simulations indicated that accounting for the multiple-layer structure of canopy is a prerequisite for canopy scale reflectance simulations. If the optical properties of plants within different layers are different, substitution of the multiple-layer canopy by a homogeneous canopy of effective optical properties may lead to significant biases in estimated directional reflectance. Validation of MRTM based on field data proved that it reproduced the measured reflectance more "truthfully" when five layers were used instead of one layer in this model and several other CR models. More field measurement datasets with long-term series, various species, and varying canopy structures with numerous vertical profiles as well as properties may be needed to validate the new model in future.

Chapter 5 Canopy scale applications: hyperspectral indices for LAI estimation

Abstract

Leaf area index (LAI) is one of the key biophysical parameters for understanding land surface photosynthesis, transpiration, and energy balance processes. Estimation of LAI from remote sensing data has been a premier method for large scale in recent years. Recent studies have revealed that the within-canopy vertical variations in LAI and biochemical properties greatly affects canopy reflectance and significantly complicates the retrieval of LAI inversely from reflectance based vegetation indices, which has never been explicitly addressed. In this study, we have used both simulated datasets (dataset I with constant vertical profiles of LAI and biochemical properties, dataset II with varied vertical profile of LAI but constant vertical biochemical properties, and dataset III with both varied vertical profiles) generated from the multiple-layer canopy radiative transfer model (MRTM) and a ground-measured dataset to identify robust spectral indices that are insensitive to such within canopy vertical variations for LAI prediction. The results clearly indicated that published indices such as normalized difference vegetation index (NDVI) had obvious discrepancies when applied to canopies with different vertical variations, while the new indices identified in this study performed much better. The best index for estimating canopy LAI under various conditions was D(920,1080), with overall RMSEs of 0.62~0.96 m^2/m^2 for all three simulated datasets and 1.22 m^2/m^2 with the field-measured dataset. This index responded mostly to the quantity of LAI but was insensitive to within-canopy variations, allowing it to aid the retrieval LAI from remote sensing data without prior information of within-canopy vertical variations of LAI and biochemical properties.

5.1 Introduction

Leaf area index (LAI) is a critical parameter for understanding biological and physical processes associated with vegetation, and a premier-required input in ecosystem productivity models (Bonan, 1993; Colombo et al., 2003; Liu et al., 1997). Generally, it is defined as one half of the total surface leaf area of the vegetation per unit area of soil (background) surfaces (Chen and Black, 1992). *In-situ* measurements of LAI can be time-consuming, expensive and often unfeasible, which leads to the striking possibility of using remote sensing data to estimate LAI (Wang et al., 2005). Recent developments in hyperspectral remote sensing and imaging spectrometry fields have allowed new ways for quick estimation of vegetation LAI.

A common approach of estimating LAI from remote sensing data has been the reliance on vegetation indices based on the relationship between field-measured LAI and spectral reflectance. As a result, a large number of vegetation indices have been established (Haboudane et al., 2004), e.g. the Normalized Difference Vegetation Index (NDVI, Thenkabail et al., 2000), Ratio Vegetation Index (RVI, Stenberg et al., 2004), Modified Simple Ratio (MSR, Chen, 1996), Modified Chlorophyll Absorption Ratio Index (MCARI, Haboudane et al., 2004), Triangular Vegetation Index (TVI, Broge

and Leblanc, 2001), Modified TVI (MTVI, Haboudane et al., 2004), Modified Soil-Adjusted Vegetation Index (MSAVI, Qi et al., 1994), and D_{LAI} (le Maire et al., 2008). These indices can be parameterized easily and have a known precision in certain studies. However, they all have apparent shortcomings since their calibration depends on particular experimental datasets. Whatever the index, its success depends preliminarily on the quality of the training dataset, the selection of the wavelengths and the availability of independent datasets for validation (le Maire et al., 2008). Various factors such as atmospheric quality, vegetation types, leaf biochemical properties, understory vegetation, and background soil reflectance, will all affect canopy scale reflectance and thus blur the generality and significance of the vegetation indices relationships with LAI, making them difficult for generalized application to large areas. Among them, some factors have been demonstrated in numerous studies already (e.g. Broge and Leblanc, 2001; Chen and Cihlar, 1996; Colombo et al., 2003; Gitelson et al., 2005), while others have yet to be addressed and studied sufficiently. These unaddressed factors include vertical variations of LAI and biochemical properties within the canopy, which presented large impacts on canopy scale reflectance as revealed in a recent study (Wang and Li, 2013a).

The main reason for the lack of studies on the effects of vertical variations of LAI and biochemical properties within canopy is due to the scarce availability of field measurements as well as lack of radiative transfer modeling that deals with such within canopy variations. In recent past, a multiple-layer canopy reflectance model (MRTM) has been developed to embrace such within canopy variations of biophysical and biochemical properties (Wang and Li, 2013a). Based on this model, the vertical variations of LAI and leaf biochemical properties have been clearly demonstrated to greatly affect canopy scale reflectance, e.g. canopy reflectance changed greatly with the same amount of total LAI but under different vertical distributions, which was also true with other biochemical components (e.g. leaf chlorophyll, equivalent water thickness, leaf mass per area). Therefore, in this study we will challenge the effect of within canopy vertical variations of LAI and biochemical components on their effectiveness, robustness and estimating accuracy of LAI with various vegetation indices.

We based the current study on three simulated datasets generated from the multiple-layer canopy reflectance model (MRTM) as well as one field-measured dataset. In this study, simulated datasets were used to identify potential robust indices for LAI, which were then validated against the field-measured dataset containing seasonal change of LAI in four sites of a typical cold-temperate mountainous landscape in Japan. Such approach of using simulated datasets from radiative transfer models is a popular and advanced way of allocating effective and general vegetation indices developed in recent years (le Marie et al., 2004; 2008; Wang and Li, 2012). Since the effect of variation in biophysical and biochemical properties on canopy reflectance are explicitly through canopy reflectance models (Asner, 1998), such approach has many advantages. They include: most canopy properties can be represented in detail (via thousands of spectra); the influence of a specific property can be decoupled from others; and the effect of a particular property on the spectra is based on physical and physiological processes. As a result, well established indices obtained through such a large simulated database may potentially be applied to a wide range of spectra. However, it is worth noting that the accuracy of the approach relies on the capacity of applied radiative models to correctly simulate canopy reflectance

under various conditions. Thus, it is essential to validate such indices with experimental measurements.

The objective of this chapter is to develop a potentially general and robust vegetation index that is insensitive to within canopy vertical variations of LAI and biochemical components for estimating LAI. We described the multiple-layer canopy radiative transfer model (MRTM) simply at first for generating simulated datasets as well as experimental protocols for field measurements. Then, we validated reported spectral indices from precious studies and proposed the method of designing and determination of new types of indices. The newly identified indices were then validated with simulated and measured datasets.

5.2 Material and methods

5.2.1 Simulated datasets

Three simulated datasets have been generated via the multiple-layer model MRTM using the 5 vertical-layer mode, as previous studies revealed that 5-layer mode can cover large LAI for accurate reflectance simulation (Wang and Li, 2012a). A detailed description of this model can be referred to Wang and Li (2012a). Among the three datasets, dataset I was generated with the model when both LAI and biochemical properties distributions were treated identically along canopy vertical profile, while dataset II was generated from simulations with various vertical profiles of LAI but with constant vertical distribution of biochemical properties along the canopy. For comparison, dataset III was generated with considerations of vertical changes of LAI and biochemical properties along the canopy. Parameter settings for generating these datasets are presented in Table 5.1, where reflected spectra were simulated for every combination of these parameters within the input ranges. To ensure that representative results are obtained, a uniform distribution was set for each varying parameter, so that a reflectance spectrum obtained with extreme parameter values had the same weight as other spectra on the indices' calibration procedure. However, some parameters have been treated as constants (see Table 5.1 legend). In order to reproduce the observed radiometric noise of real measured reflectance in the simulations, a random noise was added to each spectrum of both databases (leaf and canopy). This step is important for eliminating noise sensitive indices and indices with artificially close wavelengths (le Maire et al., 2004). An additive random Gaussian noise with a standard deviation of 3% of reflectance amplitude has been applied on all wavelengths of each reflectance spectrum of the simulated datasets in this study.

5.2.2 Field-measured dataset

The field measured dataset has been compiled from synchronous measurements of leaf biophysical and biochemical parameters, as well as leaf and canopy reflectance in the Naeba site. Detail description of the measured dataset can see chapter 1.3.3. The sampling number, corresponding means and the range of the measurements in the dataset are listed in Table 5.1. The measurements on contents of pigments, leaf water,

leaf dry matter, leaf thickness, leaf angle, and leaf size were used (1) as reference for determine the ranges of these parameters for simulated datasets and (2) to prove the big vertical variation exist within canopy. The canopy reflectance measurement was used to calculate spectral indices for estimating LAI, and LAI measurement was used to evaluate the estimating accuracy.

Table 5.1 Main Characteristics of the measured dataset and parameters used to build the three simulated datasets (other parameters are constant in the model: Canopy layers=5; mean leaf angle=60˚; leaf size=40 cm2; view nadir angle=0˚; Ratio of refraction indices of leaf wax and air=0.9).

Dataset		Measured	Simulated I	Simulated II	Simulated III
Number of samples		83	9800	102900	1190700
Vertical layers		5	5	5	5
Spectroradiometer		ASD FieldSpec	MRTM	MRTM	MRTM
CHL ($\mu g/cm^2$)	Mean	41.40	60	60	60
	Min	13.94	10	10	10
	Max	69.10	110	110	110
	Vertical variation	32% vertical variation	Vertical constant	Vertical constant	Various vertical profiles
LMA (g/cm^2)	Mean	0.007	0.011	0.011	0.011
	Min	0.002	0.002	0.002	0.002
	Max	0.012	0.02	0.02	0.02
	Vertical variation	38%	Vertical constant	Vertical constant	Various vertical profiles
EWT (g/cm^2)	Mean	0.008	0.014	0.014	0.014
	Min	0.002	0.004	0.004	0.004
	Max	0.016	0.024	0.024	0.024
	Vertical variation	36% vertical variation	Vertical constant	Vertical constant	Various vertical profiles
N_{stuc}	Mean	-	1.7	1.7	1.7
	Min	-	1.1	1.1	1.1
	Max	-	2.3	2.3	2.3
	Vertical variation	-	Vertical constant	Vertical constant	Various vertical profiles
LAI (m^2/m^2)	Mean	2.84	4	4	4
	Min	0.60	0.3	0.3	0.3
	Max	5.03	7	7	7
	Vertical variation	42% vertical variation	Vertical constant	Various vertical profiles	Various vertical profiles

5.2.3 Published indices for estimating LAI

A wide range of vegetation indices has been reported to estimate vegetation LAI where most of them are based on ratios or normalized ratios. In this study, eight reported indices from a literature review were selected and validated with our simulated and experimental datasets. The selected indices are listed in Table 5.2. For each index, an exponential regression is fitted between index values and LAI to be predicted.

Table 5.2 Published spectral indices for retrieval LAI

Spectral index	Acronym	Formula	Reference
Normalized difference vegetation index	NDVI	$\frac{R_{800} - R_{680}}{R_{800} + R_{680}}$	Thenkabail et al., 2000
Ratio vegetation index	RVI	R_{800}/R_{680}	Stenberg et al., 2004
Modified Simple ratio	MSR	$(\frac{R_{800}}{R_{680}} - 1)/\sqrt{\frac{R_{800}}{R_{680}} + 1}$	Chen, 1996
Modified soil-adjusted vegetation index	MSAVI	$\frac{1}{2}\left[(2R_{800} + 1) - \sqrt{(2R_{800} + 1)^2 - 8(R_{800} - R_{670})}\right]$	Qi et al., 1994
Modified Chlorophyll absorption ratio index	MCARI	$1.2[2.5(R_{800} - R_{670}) - 1.3(R_{800} + R_{550})]$	Haboudane et al., 2004
Triangular vegetation index	TVI	$0.5[120(R_{750} - R_{550}) - 200(R_{670} + R_{550})]$	Broge and Leblanc, 2001
Modified TVI	MTVI	$1.2[1.2(R_{800} - R_{550}) - 2.5(R_{670} + R_{550})]$	Haboudane et al., 2004
D type LAI index	D_{LAI}	$R_{1725} - R_{970}$	le Maire et al., 2008

5.2.4 New indices

Four common types of indices based on spectrum reflectance have been designed for this study, ranging from very simple (R) to more sophisticate ones (ND) as given below:

$$R(\lambda 1) = R_{\lambda 1}$$
$$D(\lambda 1, \lambda 2) = R_{\lambda 1} - R_{\lambda 2}$$
$$SR(\lambda 1, \lambda 2) = R_{\lambda 1}/R_{\lambda 2}$$
$$ND(\lambda 1, \lambda 2) = (R_{\lambda 1} - R_{\lambda 2})/(R_{\lambda 1} + R_{\lambda 2})$$

Where R is reflectance, D is the difference of reflectance, SR is the simple ratio of reflectance, ND is the normalized difference of reflectance, and λ_1 and λ_2 are wavelengths.

The determination of specific wavelengths (λ_1, λ_2) of the four indices is performed by examining all possible combinations of wavelengths (λ_1, λ_2) from 400 ~ 2500 nm. For each combination, index values are calculated for each spectrum of datasets. An exponential regression is fit between index values and LAI to be predicted. The root mean square error (RMSE) used in this study is commonly applied to compare indices with different wavebands. For a given type of index, the best combination of wavelengths should have the lowest RMSE.

Further revelation of the sensitivity of each identified index to spectral bands was carried out by constructing a 2-D graphical representation of RMSE for indices using two reflectance values in two wavelengths ($R_{\lambda 1}$ and $R_{\lambda 2}$). The RMSE calculated for each index is represented by a two dimensional contour plot with axes λ_1 and λ_2. This representation has several advantages, one being that the absolute minimum be seen directly, and also that the extent of the local minimum area can be easily evaluated. In addition, all local low RMSE zones are visible, with their respective RMSE values. Other studies have also applied such representations where the R-squared of the fitted

relationship is used instead of the RMSE (Hansen and Schjoerring, 2003). RMSE is specifically fitted within our purpose because it shows the precision of the index directly, and it is the best statistic to evaluate the error associated with the index model (le Maire et al., 2008).

Summarily, the determination of best indices consisted of four steps: (1) determination of the best wavelength for a given type of index, (2) determination of the index vs. LAI regression curve, (3) validation of each index using the field-measured dataset, and (4) trade-off results of simulated and measured datasets before final outputting the best index for estimating LAI.

5.2.5 Evaluation of spectral indices

About 30% of the total spectra randomly selected from each dataset were used to determine the best new spectral indices as described in 2.4, and the other 70% were used to evaluate these spectral indices on LAI estimating. The root mean square error (RMSE) and bias (BIAS) were chosen to evaluate the performance of each spectral index.

To find the spectral index that insensitive to vertical variation of LAI and biochemical properties within canopy is the ultimate purpose of this study. In order to evaluate the effects of these vertical variations on reflectance and corresponding indices, nine different scenarios of reflectance and corresponding new spectral indices and typical published index NDVI with three exemplary vertical profiles (LAI, CHL, EWT, and LMA) were examined. Three types of vertical profiles (termed as vertical profile I, II, and III, respectively, hereafter), which were constantly distributed within canopy (Profile I), or increased from top to bottom of the canopy (Profile II), or decreased from top to bottom (Profile III) were included for simulations. The detailed settings for all nine simulated scenarios (S1~S9) are listed below. S1 was a part of simulated dataset I, S1~S3 were contained in simulated dataset II, and S1~S9 were all contained in simulated dataset III.

S1: LAI with vertical profile I; CHL, EWT, and LMA all with vertical profile I;
S2: LAI with vertical profile II; CHL, EWT, and LMA all with vertical profile I;
S3: LAI with vertical profile III; CHL, EWT, and LMA all with vertical profile I;
S4: LAI with vertical profile I; CHL, EWT, and LMA all with vertical profile II;
S5: LAI with vertical profile I; CHL, EWT, and LMA all with vertical profile III;
S6: LAI with vertical profile II; CHL, EWT, and LMA all with vertical profile II;
S7: LAI with vertical profile II; CHL, EWT, and LMA all with vertical profile III;
S8: LAI with vertical profile III; CHL, EWT, and LMA all with vertical profile II;
S9: LAI with vertical profile III; CHL, EWT, and LMA all with vertical profile III.

5.3 Results

5.3.1 Published indices

Eight reported indices were examined with both simulated and field measured datasets in this chapter (Table 5.3). Results based on simulated datasets revealed that the Triangular Vegetation Index (TVI) and modified TVI (MTVI) had the worst performance among the eight indices, both with RMSEs of 1.82~1.84 m^2/m^2 and BIASs of 1.55~1.57 m^2/m^2 for all three simulated datasets. The Normalized Difference Vegetation Index (NDVI), Ratio Vegetation Index (RVI), Modified Simple Ratio (MSR), and Modified Chlorophyll Absorption Ratio Index (MCARI) performed similarly, with RMSEs in the range of 1.53~1.63 m^2/m^2 and BIASs of 1.27~1.38 m^2/m^2 for all three simulated datasets. The Modified Soil-adjusted Vegetation Index (MSAVI) performed better than the above six indices, with RMSEs of 1.20~1.24 m^2/m^2 and BIASs of 1.06~1.09 m^2/m^2 for the three simulated datasets. The best index among the eight indices was found to be D_{LAI}, a D type index devised by le Maire et al. (2008). The RMSEs of D_{LAI} were 0.80, 0.94 and 1.09 m^2/m^2 and BIASs were 0.66, 0.69 and 0.72 m^2/m^2 for the simulated datasets (I, II, and III), respectively. When the eight indices were validated against the measured dataset, they all had similar performance (with RMSEs of 1.42~1.47 and BIASs of 1.00~1.07 m^2/m^2) except the D_{LAI} index (with an RMSE of 1.36 and BIASs of 0.87 m^2/m^2).

Table 5.3 Results of the eight published vegetation indices calibrated to the three simulated datasets and measured dataset.

Index type	Regression $y=e^{a+bx}$		Simulated dataset						Measured dataset	
			I		II		III			
	a	b	RMSE	BIAS	RMSE	BIAS	RMSE	BIAS	RMSE	BIAS
NDVI	2.06	0.12	1.61	1.37	1.62	1.37	1.63	1.38	1.42	1.00
RVI	-4.40	10.16	1.59	1.33	1.59	1.33	1.61	1.35	1.47	1.07
MSR	1.04	0.86	1.57	1.31	1.58	1.32	1.59	1.33	1.45	1.05
MSAVI	-3.56	3.44	1.20	1.06	1.22	1.07	1.24	1.09	1.45	1.03
MCARI	1.63	6.70	1.53	1.27	1.54	1.28	1.56	1.30	1.46	1.05
TVI	3.59	0.10	1.82	1.56	1.82	1.56	1.84	1.57	1.47	1.06
MTVI	3.65	3.03	1.82	1.55	1.82	1.55	1.83	1.56	1.47	1.07
D_{LAI}	-0.88	-25.59	0.80	0.66	0.94	0.69	1.09	0.72	1.36	0.87

Table 5.4 Results of the four types of spectral indices calibrated to the simulated dataset and measured dataset.

Index type	λ1 (nm)	λ2 (nm)	Regression $y=e^{a+bx}$		Simulated dataset						Measured dataset	
					I		II		III			
			a	b	RMSE	BIAS	RMSE	BIAS	RMSE	BIAS	RMSE	BIAS
R	940		-1.21	5.45	1.56	1.14	1.63	1.16	1.86	1.20	1.49	1.11
D	920	1080	1.05	53.24	0.62	0.42	0.85	0.47	0.96	0.55	1.22	1.01
SR	900	1080	-19.32	20.68	0.75	0.54	0.87	0.58	1.01	0.63	1.29	1.04
ND	900	1080	1.37	40.27	0.76	0.55	0.86	0.58	1.02	0.63	1.28	1.03

5.3.2 New types of indices

Four types of indices for deriving canopy LAI were examined (Table 5.4). For each type of index, the index of wavelength combination with the least RMSE among all the three simulated datasets and for the field-based dataset was identified (Table 5.4). The results revealed that all the identified best indices had the wavelength combinations (λ1 and λ2) within the 900~1100 nm domain. Based on the results of RMSE (Table 5.4), the best among all indices for estimating LAI was found to be D(920,1080), a D type index (reflectance difference between two wavelengths). It had an RMSE of 0.62, 0.85, 0.96, and 1.22 m^2/m^2, and a BIAS of 0.42, 0.47, 0.55, and 1.01 m^2/m^2 for simulated datasets I, II, III and the field measured dataset, respectively. In fact, it was the most robust index for LAI prediction and was the only one that was efficient for both simulated and field measured datasets. This was surprising, since most former studies applied the ND type of indices, especially the NDVI ($ND_{800, 680}$).

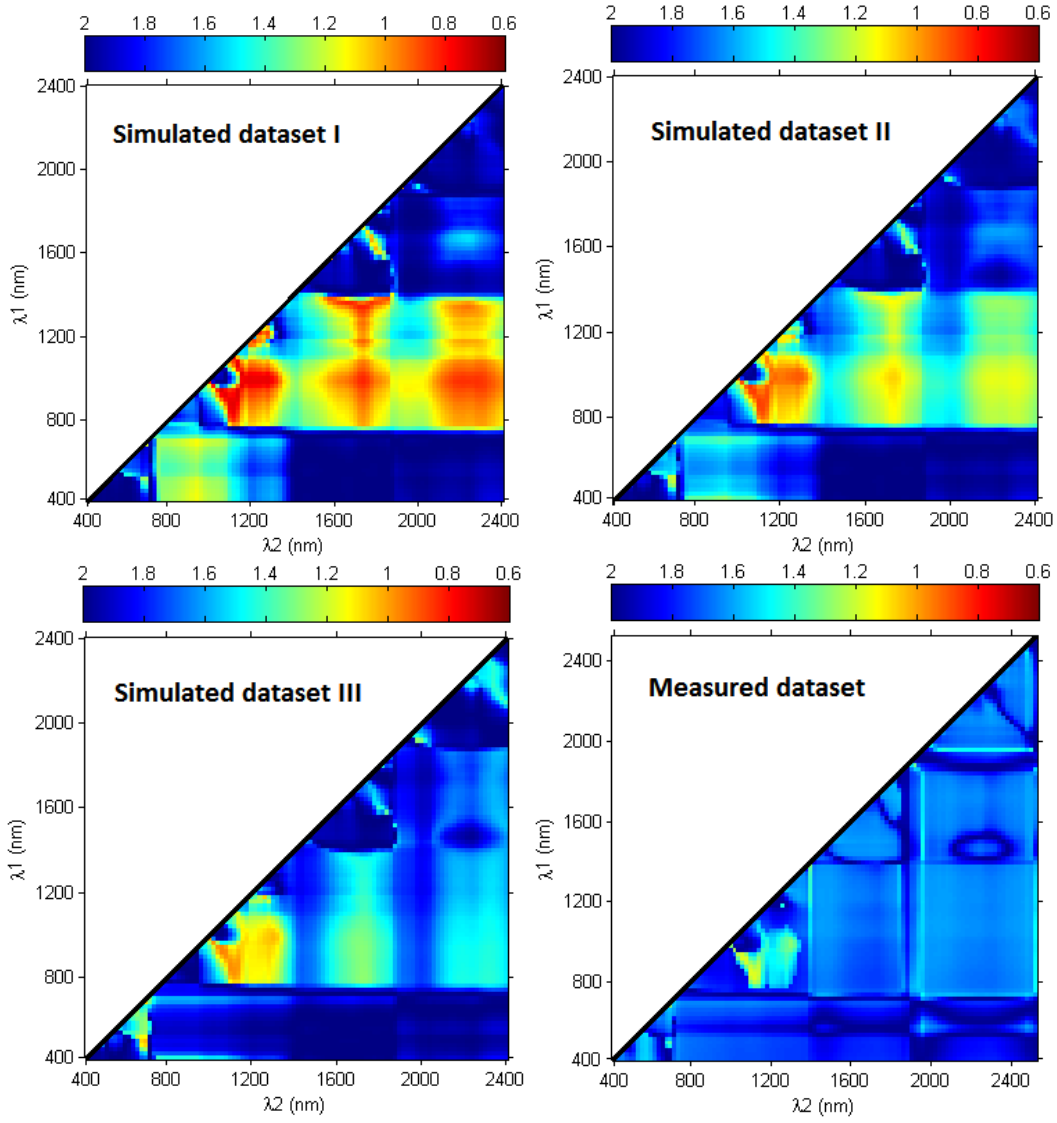

Fig. 5.1 Matrices representing the RMSE of leaf area index (LAI) prediction with D type indices, calculations are done on the three simulated datasets and the measured dataset.

RMSE matrices were calculated for D type indices for all three simulated datasets and measured dataset (Fig. 5.1). Both RMSE matrices of MRTM simulated and measured datasets showed similar patterns. D type indices had a minimum zone of RMSE with λ_1 centered in [900nm, 1000 nm] and λ_2 within [1000nm, 1100 nm] for all three simulated datasets and field measured dataset. The difference between the four datasets laid in that the minimum RMSE zone of the simulated dataset I had the largest area with the smallest RMSE values. As a comparison, the measured dataset had the smallest area of minimum RMSE zone and with larger RMSE values. In addition, the simulated dataset I had two additional minimum RMSE zones, in which one had λ_1 centered in [900nm, 1300 nm] and λ_2 in [1700nm 1800 nm] while the other had λ_1 centered in [900nm, 1300 nm] and λ_2 in [2200nm, 2400 nm], respectively. However, these two minimum zones largely vanished in simulated dataset II and III, and even disappeared in the measured dataset. On the contrary, RMSE metrics of NDVI revealed that this type of indices (i.e. $ND_{800, 680}$) did not appear as efficient for both simulated and measured datasets.

Field measured and set LAI values for reflectance simulations were regressed against the D (920, 1080) index (Fig. 5.2). Although most points were distributed near the regression line, the regression coefficients apparently differed among the simulated and measured datasets since the values from measured dataset were usually located above those of the simulated datasets. As noted, the index performed better with simulated datasets than with field measured data but remained statistically significant (Fig.5. 2).

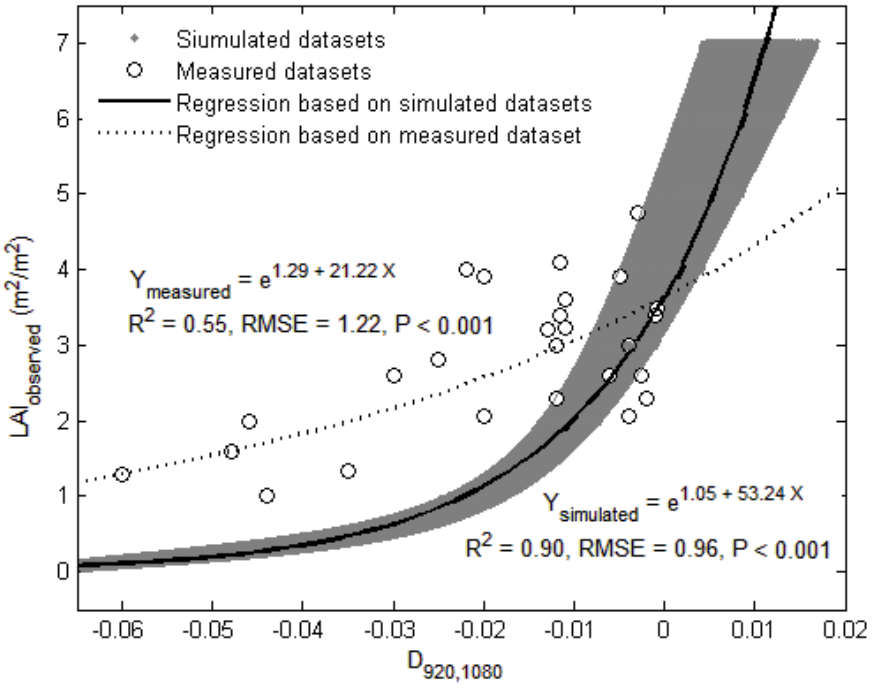

Fig. 5.2 Best LAI index calibrated to canopy in situ measurements.

The normalized difference (ND) type and simple ratio (SR) type of indices performed similarly both for simulated and field measured datasets with two selected wavelengths of 900 nm and 1080 nm. Their RMSEs were nearly 10% larger than those of the best D type index (Table 5.4). The reflectance (R) type of index had only a single wavelength and was the simplest type among all index types examined. The

best R type index, R_{940}, performed rather poorly compared with other types of indices examined which had the RMSE nearly twice as large as that of the best D type of index.

5.3.3 Effects of vertical variations on spectral indices

In order to show the effects of vertical variations of LAI and biochemical properties within canopy on reflectance and corresponding indices, nine different scenarios of reflectance and corresponding new spectral indices and typical published index NDVI with three exemplary vertical profiles (LAI, CHL, EWT, and LMA) were examined. As shown in Fig. 5.3, the reflectance spectra of S1~S9 had big difference in the entire wavelength domain (400~2400 nm) even though the mean values of three biochemical properties and bulk amount of LAI were all kept same for all nine scenarios. Results confirmed that the difference of the new spectral indices derived in this study D(920,1080), SR(920,1080) and ND(920,1080) among the nine simulated scenarios were small (difference among 0.98~1.02), while the variation of the R-type index R(940) and the typical published index NDVI(=ND(680,800)) among all scenarios were much more apparent. This result was consistent with the accuracy of LAI estimation by these spectral indices as shown in Table 5.3 and 5.4.

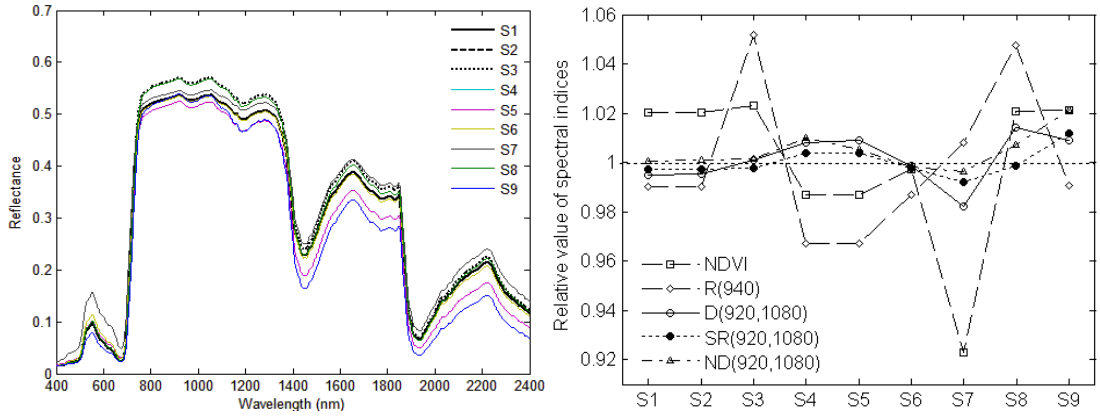

Figure 5.3 Nine simulated reflectance samples (above) and their corresponding D(920,1080) and NDVI values (below). The model parameters LAI=3 m2/m2, mean CHL=60 μg/cm2, mean LMA=0.025 g/cm2, mean EWT=0.025 g/cm2, and canopy layers NL=5. The nine samples contained different vertical profiles of LAI and biochemical properties as shown in section 2.5.

5.4 Discussion

5.4.1 Effects of vertical variations of LAI and biochemical properties for LAI estimation from vegetation indices

Vertical profiles of both biophysical and biochemical properties are part of the main heterogeneities within a vegetation canopy that have been well recognized and highlighted in many studies (Barton, 2000; Ciganda et al., 2008; Dwyer et al., 1992; Valentinuz and Tollenaar, 2004). Generally, vertical distribution of the target components is a major factor controlling canopy reflectance (Wang and Li, 2013a). As

vertical variations of LAI and biochemical properties will impact both canopy reflectance and vegetation indices largely, thus will affect the LAI prediction from spectral indices in return. Unfortunately, this dilemma has not been fully addressed yet. In this study, we used three synthetic datasets generated from the MRTM model with different treatments of vertical changes of LAI and biochemical properties. The results clearly indicated that the accuracy of LAI prediction was in the series of dataset I > II > III for all the four types of indices (Table 5.4), suggesting that vertical variations of different properties within canopy will greatly affect the retrieval of LAI via vegetation indices. Although NDVI probably is the most popular index used for LAI estimation, the D(920,1080) index developed in this study performed best when compared with the NDVI index, indicating the conservative behavior of the new index to the vertical variations within canopy.

Fig. 5.1 clearly shows that dataset I has three obvious big minimum zones of RMSE for LAI estimation. All the three areas are big and have very red color (corresponding to small RMSE values). For dataset II, the RMSE matrix had similar pattern with that of dataset I, but the three corresponding zones became smaller and the color became more yellowish (RMSE values become larger), especially for the second and third minimum zones. For dataset III, the color of second and third minimum zones became cyan, with almost no red and yellow colors within these two zones; and the first zone became more yellowish than those of dataset I and II. These results indicated that there are more proper wavelengths that can be selected for the D type indices for LAI estimation if no vertical variations of LAI and other properties within a canopy. However, when considering vertical variations of LAI and biochemical properties within canopies, some wavelengths were dismissed for LAI estimation. le Maire et al. (2008) used the PROSAIL model to create a synthetic dataset for finding the best indices for LAI prediction, but without considering the canopy vertical variations. Their results also proved that the D-type indices was the best among some other indices (R, SR, ND, mSR, and mND), and the selected wavelengths (λ_1 and λ_2) were 970 and 1750 nm. These wavelengths were just in the center of the second minimum zone of our study. However, when we considered the vertical variations of canopies, this area did not perform as well as of that for dataset I.

5.4.2 Reported indices vs. newly proposed indices for LAI estimation

Researchers have commonly used empirical relationships between hyperspectral indices and leaf area index (LAI). Numerous published indices have been designed to detect LAI because of the critical role of LAI in ecosystem functions. As reviewed by Haboudane et al. (2004), dozens of indices ranging from simple ratios and normalized difference types have been designed to estimate LAI. As summarized by le Maire et al. (2008), the D-type is insensitive to additive changes of the reflectance, and the simple ratio (SR) and normalized difference (ND) types are insensitive to proportional effects. However, our results demonstrated that the above indices perform less well than the newly identified indices with our datasets. The best indices identified in this study, except the R and D type of indices, all had a normalized RMSE of lower than 50%; the results were comparable with those of le Maire et al. (2008), even though the datasets contained canopy vertical variations in this study.

Furthermore, the results showed that the efficiency of the index was improved when

additive effects was considered, since D-type indices gave better results than R, SR, and ND-type indices. This result may declare that the vertical variations within canopy showed more likely additive effects than proportional effects. Even though most of the time ND type indices are used, especially the NDVI (=ND800,680), the NDVI zone did not turn out to be efficient for both simulated and field measured datasets as shown in this study. Hence, when applying NDVI data for estimating LAI, more caution along with full calibration and validation are needed before application, especially for the canopy with large vertical variations.

As noted, the selected wavelengths were similar for the D, SR, and ND-type indices, and their performances based on RMSE values were comparable (RMSE for SR and ND-type indices is almost the same, while D-type indices is about 10% smaller than SR and ND-type indices). The best indices for LAI estimation identified in this study, all used wavelengths within the 900~1100 domain, indicating the close relationship between reflectance information of these wavebands and LAI quantity, as reported by le Maire et al. (2008). The wavelengths we found are generally consistent with the findings of le Maire et al. (2008), who indicated these selected wavelengths correspond to a region of high scattering effects inside the canopy and had high correlation with LAI.

Although vegetation indices with the specific wavelengths were determined via synthetic databases, it is necessary to calibrate and validate with real field measurements. Deviations from simulation-based regressions may be due to either errors in the MRTM model and biases in the inputs for simulated databases, or from both. Generally, the real field measurements at canopy scale may not be broad enough to represent the ranges as in synthetic databases, or the simulation database may be too broad compared to measurements, which will also attribute to biases.

In general, estimation discrepancies were larger for higher values of LAI than smaller values of LAI. These results again confirmed that predicting high values of LAI from vegetation indices remains a problem, even with this type of index, as its saturation appeared for cases of LAI greater than 3 – 4. This is a well known problem, as shown in previous studies (Anderson et al., 2004; Birky, 2001; Fassnacht et al., 1997; Qi et al., 2000; Soudani et al., 2006; Wang et al., 2005).

5.4.3 Simulated dataset *vs.* measured dataset

A large dataset for calibration is essential to obtain general indices (Wang and Li, 2012). A simulated dataset generated from a mechanistic reflectance model like MRTM can represent a vast range of canopy reflectance spectra, which may provide an important resource for identifying general indices. Furthermore, as claimed by le Maire et al. (2008), the use of a simulated dataset can reduce problems of covariance that often occur with field-measured datasets where some of the measured characteristics may have significant covariance, such as LAI and LMA at different phenological stages, which decreases the generic application of such empirically based indices. However, using simulated datasets alone is not enough for identifying practical and general indices, as pointed out by Wang and Li (2012). The underlying hypothesis for applying simulated datasets is that the reflectance model can accurately simulate the actual reflectance spectra. However, for most cases this criterion cannot

be cleared. Concerning the model, the MRTM model has proven to be efficient in the finding of indices (see RMSE matrices). However, it is possible that the relatively simple MRTM model does not accurately simulate the absolute value of the reflectance of a tree canopy because canopies not only have vertical heterogeneity but also horizontal heterogeneity, even with high values of LAI. Zarco-Tejada et al. (2001) have shown that there was practically no shadow effect when pigment sensitive indices rather than entire canopy reflectance spectra were simulated with models for closed canopies of deciduous stands with LAI greater than 3. For LAI < 3, some particular effects of clumping and shadows are included in other radiative transfer models (Gastellu-Etchegorry et al., 1996; Huemmrich, 2000) that may be used instead of MRTM to generate another database.

In addition, it may be difficult to identify an index with general applicability when many combinations of wavebands for a given type of index produce similar RMSEs, as was the case with the D type of index for LAI estimation in simulated dataset I (Fig. 5.1). Thus, a simulated dataset under certain conditions will not be sufficient for identifying an index with general applicability. The database used for identifying an index should contain various simulated datasets under various conditions as well as various *in situ* measured datasets with different conditions, such as vertical and horizontal variations within canopy, more types of soils, understory information, and variation of other parameters like leaf angle or sun and view angles. To identify a robust index for general applicability, a large number of simulated and measured datasets should be used for comprehensive calibration and validation, even though field-measured and field-based data sets are always confined to a given species, growth stages, and region, because of cost limitations.

5.5 Conclusion

To obtain generic and widely applicable hyperspectral indices for leaf area index prediction with vertical heterogeneous canopy, we examined four types of indices using every possible combination of wavelength based on three simulated datasets generated by the multiple-layer radiative transfer model (MRTM) and a field *in situ* measured dataset. The results indicated that certain indices can be generally used to estimate leaf area index and still remain resistant to canopy vertical variations. The best index identified in this study is D (920, 1080), which performed well for all datasets, with an overall RMSE of 0.62~0.96 m^2/m^2 for all three simulated datasets and with an RMSE of 1.22 m^2/m^2 when validated against the field measured dataset. Since consistent performance prevailed with different vertical variations of LAI and biochemical properties within canopy, we infer that the newly identified indices will have general applicability, especially for vegetation canopies, which have large LAI and biochemical vertical heterogeneities.

Chapter 6 Synthesis—Estimating biochemical and biophysical parameters with hyperspectral remote sensing

6.1 Introduction

Accurate quantitative estimation of vegetation biochemical and biophysical characteristics is necessary for a large variety of agricultural, ecological, and meteorological applications (Asner, 1998). Remote sensing, because of its global coverage, repetitiveness, and non-destructive and relatively cheap characterization of land surface, has been recognized as a reliable method and a practical means of estimating various biochemical and biophysical vegetation variables (Cohen et al., 2003). In general, current remote sensing approaches for estimating vegetation biochemical and biophysical parameters include physically based models (such as radiative transfer models) and statistical (such as spectral indcies) (Skidmore, 2002); each having advantages and disadvantages (Kimes et al., 2000; Liang, 2004). Both models (physical / statistical) have been used widely for estimating biochemical and biophysical parameters in agricultural and forestry environments. Nevertheless, the estimation of vegetation characteristics for structurally different vegetations and vertical heterogeneous canopies with different vegetation communities using either of the approaches has not been widely addressed in the literature.

The main objective of this study are (1) to investigate the potential of inversely leaf scale radiative transfer models for estimating biochemical properties for both broadleaves of typical temperate deciduous species and assimilating branches of typical desert species; (2) to find several efficient and robust hyperspectral indices for estimating leaf biochemical parameters which insensitive to various species, various phenological stages, different sites, and various leaf anatomies; (3) to develop a multiple-layer canopy radiative transfer model which considers the vertical heterogeneity of biochemical and biophysical parameters within the canopy; (4) to identify a potentially general and robust spectral index for estimating LAI that insensitive to within canopy vertical variations of LAI and biochemical components. The study consists of two scales of investigation: leaf scale (6.2) and canopy scale (6.3). Two different sites (Naeba site in Japan and Desert site in China) were used as study sites for field measurements.

6.2 Leaf scale

To date, much of the present researches linking vegetation parameters such as leaf chlorophyll to spectral data has focused on single plant species (or structurally similar plant types). Hence, the leaf scale study was designed to further investigate the relationship between spectral data and the biochemical parameters (CHL, EWT and LMA), involving plant species widely different in terms of leaf structure (broadleaves of typical temperate deciduous vegetations and assimilate branches of typical desert vegetation), various phenological stages and various locations. The utility of hyperspectral remote sensing in predicting biochemical parameters was then investigated by the means of radiative transfer models inversion (section 6.2.1) and spectral indices (section 6.2.2).

6.2.1 Estimating of biochemical parameters from radiative transfer models inversion

Many studies have investigated the radiative transfer model inversion for estimating leaf biochemical variables (such as CHL, EWT and LMA). However, most of these studies were for broadleaves and several for needles at the same leaf develop stages and the same locations, no attempt to investigate the assimilate branches of desert vegetations, and few studies have collected data set from different leaf develop stages and different locations. The leaf scale study was designed to test the common leaf radiative transfer models PROSPECT and LIBERTY on both broadleaves of typical temperate deciduous vegetations and assimilate branches of typical desert vegetation for retrieval biochemical parameters. The results indicated that:

(1) Retrieval of biochemical parameters using model inversion generally faces "ill-posed" problems, which dramatically decreases the estimation accuracy of an inverse model. This problem can be much improved by designed new model inversion algorithm and make the model inversion obtaining a better estimating accuracy. However, the new model inversion algorithm cannot solve the problem thoroughly.

(2) The models need calibration using the local *in situ* measurements before inversely the models to retrieval biochemical parameters, otherwise big errors may appear. This process was especially needed for the desert vegetation, as the original LIBERTY and PROSPECT exhibited tangible error for simulating leaf reflectance of the desert vegetation. However, the calibration will cause this approach being less general and make it hard to be used widely, especially in the area with absent of *in situ* measured data. The reason of the models without calibration performing lower estimating accuracy may some factors that affect the leaf spectra but have not been considered in the models, such as the physiological process in the leaves, which need further investigate.

(3) Both LIBERTY and PROSPECT are applicable for estimation leaf biochemical parameters inversely for all datasets collected from both temperate deciduous and desert forests after careful calibration. For field-measured datasets of typical temperate deciduous forests, the inversed PROSECT estimates of biochemical parameters recorded an RMSE of 8.11 $\mu g/cm^2$, 0.0012 g/cm^2 and 0.0008 g/cm^2 for leaf chlorophyll (CHL), leaf water (EWT) and leaf mass content (LMA). For typical desert vegetation, the inversed LIBERTY estimates of CHL, EWT and LMA recorded RMSE of 3.43 $\mu g/cm^2$, 0.0012 g/cm^2 and 0.0008 g/cm^2, and the RMSE of 34.76 mg/m^2, 0.0012 g/cm^2 and 0.0010 g/cm^2 for the inversed PROSPECT.

6.2.2 Estimating of biochemical parameters from hyperspectral indices

Many studies have investigated the relationships between spectral indices and leaf biochemical parameters (such as CHL, EWT and LMA). However, the conclusions drawn are contradictory, even for similar vegetation types. For this reason, we used a new approach to identify the spectral indices for estimating leaf biochemical parameters based on both a simulated data set (produced with the calibrated leaf reflectance model PROSPECT) and with data sets from measurement of field-collected leaves. The results indicated that:

(1) The spectral indices approach requires extensive field survey to collect sufficient field data, however, this is very difficult to exploit in practice. Hence, using a simulated data set generated from a mechanistic reflectance model like PROSPECT which can represent a vast range of leaf reflectance spectra to identify general spectral indices for estimating biochemical parameters is the best method in present. However, the spectral indices indentified from simulated data set should be calibrated and validated using field measured data sets. The results from simulated data set and field measured data set are not always consistent, thus the best efficient spectral indices should be trade-off between simulated and measured data sets. Simulated data should be used with measured data to identify indices that are supported by physiological or physical mechanisms and that have wide application.

(2) The Double Deference index (DDn) performed the best among other types of indices (such as ND and SR, which are the common spectral indices types in previous studies) for all the three parameters (CHL, EWT and LMA). The best indices identified in this study are DDn(715, 185) for leaf CHL, DDn(1530, 525) for EWT, and DDn(1235, 25) for LMA. These indices performed well, with an overall RMSE of 6.87 μg cm^{-2} for CHL, 0.0011 g cm^{-2} for EWT, and 0.0015 g cm^{-2} for LMA. Moreover, they performed consistently well with different field-based data sets. The regressions (biochemical parameter values regressed against spectral values), however, differed somewhat among the data sets, indicating the need for a further calibration before the indices can be applied to other sites.

(3) When applying the best indices indentified from datasets of temperate deciduous forests to a typical desert forest, all the indices for CHL, EWT and LMA performed failure, with very high estimating error (RMSE of 12.58 μg cm^{-2} for CHL, 0.0032 g cm^{-2} for EWT and 0.0036 g cm^{-2} for LMA). One of the potential reason is that these indices were indentified based on the PROSPECT model (calibrated for temperate deciduous forests data sets), but this calibrated version did not suit for the desert forest, thus these indices performed failure when using the data set from the desert forest. To indentify the best spectral indices for the desert forest should use the simulated data set from PROSPECT model which calibrated using the field measured data set from desert forest. Thus, how to identify generic and robust spectral indices which suit to all vegetation types (e.g. both temperate deciduous and desert vegetations) is still a challenge and need further investigate.

6.3 Canopy scale

Vertical heterogeneous canopies present a challenge for remote sensing applications because the reflectance is often a mixture of different vertical layers materials. Therefore, more investigation is required to assess the capability of remote sensing models when it comes to natural vertical heterogeneous canopies with a combination of different vertical layers in varying proportions. Canopy spectral measurements were made in the field using a field spectroradiometer (ASD FR, USA), along with concomitant in situ measurements of LAI and leaf biochemical properties of each layer within the canopy. The spectral reflectance of vertical heterogeneous canopy was simulated by developing a multiple-layer radiative transfer model (section 6.3.1) and the utility of hyperspectral remote sensing in predicting canopy characteristics

such as LAI in a vertical heterogeneous canopy by means of spectral indices derivate from the multiple-layer canopy radiative transfer model simulated data sets was investigated (section 6.3.2).

6.3.1 Develop a multiple-layer radiative transfer model for vertical heterogeneous canopies

Vertical profiles of both biophysical and biochemical properties are one of the main sources of heterogeneity within a vegetation canopy, which has been well recognized and highlighted in many studies (Barton, 2000; Ciganda et al., 2008; Dwyer et al., 1992; Valentinuz and Tollenaar, 2004). Generally, vertical distribution of the target components is a major factor controlling canopy reflectance. Using homogeneous canopy reflectance models for calculating directional reflectance from a vertical heterogeneous canopy by taking average values of biophysical and biochemical properties within the canopy may lead to systematic errors. Hence, accurate modeling of canopy reflectance requires taking this factor into consideration. With this in mind, a computationally efficient model, the multiple-layer canopy radiative transfer model (MRTM), has been developed with the focus on the effect of canopy vertical heterogeneity on canopy reflectance. The results indicated that:

(1) MRTM considered the canopy to multiple layers (e.g. 5 vertical layers), the idea of mathematical modeling of MRTM is coupling the homogeneous canopy models (considering the canopy to a single layer) with the adding method (which is to deduce the reflectance and transmittance of the combined layer by calculating the successive reflectances and transmittances between these two layers, and the desired optical layer is achieved by repeating the adding method). As the field measurements showed that apparent large vertical variations of most biophysical and biochemical properties existed. The MRTM can cover such natural phenomena, and such a model may help to effectively retrieve the vertical distribution of biophysical and biochemical parameters inversely.

(2) MRTM with 5 layers not only performed better than MRTM with 1 layer but also performed better than the other three models (PROSAIL, ACRM and FRT), clearly indicating that large vertical variations in the biophysical and biochemical properties of vegetation had non-negligible influences on the canopy's optical properties. Therefore, the multiple-layer canopy model proposed in this study has gone further to a certain extent than the other canopy models with homogeneous canopy such as PROSAIL, ACRM and FRT.

(3) Results of sensitivity analysis and scenario simulation of MRTM showed that vertical profiles of almost all the biophysical and biochemical properties will affect canopy directional reflectance and its angular distribution. The effect of the CHL vertical profile on canopy reflectance is in the VIS domain, while the effect of EWT is mainly in the SWIR domain, the effect of LMA is mainly in the NIR and SWIR domains, and the effect of LAD is mainly in the NIR domain. On the other hand, the same canopy reflectance curve may have resulted from different combinations of these parameters with different vertical profiles even with the same averaged values within the canopy. This indicated that if canopy parameters are retrieved without considering the vertical variations, large errors might be presented in the results. Thus, investigating the vertical variations of the main biophysical and biochemical

parameters and including such information in the canopy scale reflectance model is critical.

6.3.2 Develop a new spectral index for estimating LAI in vertical heterogeneous canopies

The estimation of canopy characteristics such as LAI using hyperspectral remote sensing, for vertical heterogeneous canopies has not, to our knowledge, been addressed by researchers yet. Therefore, the effectiveness of hyperspectral remote sensing in estimating LAI in a vertical heterogeneous canopy using spectral indices approach was examined. Similar to the approach of identifying the best indices for leaf biochemical parameters, the best spectral indices for estimating LAI also used simulated data sets based on the multiple-layer radiative transfer model (MRTM) and validated with field measure data set. The results indicated that:

(1) The within-canopy vertical variations in LAI and biochemical properties significantly complicates the retrieval of LAI inversely from reflectance based vegetation indices which has not been addressed in previous studies and been proved in this study. The accuracy of LAI prediction was in the series of simulated dataset I > II > III (see Table 5.4) for all the four types of indices, suggesting that vertical variations of different properties within canopy will greatly affect the retrieval of LAI via vegetation indices. Thus, it is critical to identify a new spectral index for estimating LAI that insensitive to the vertical heterogeneous within the canopy.

(2) The MRTM model has proven to be efficient in the finding of indices that insensitive to the vertical heterogeneous within the canopy. The best index for estimating canopy LAI under various conditions was D(920,1080), with overall RMSEs of 0.62~0.96 m^2/m^2 for all three simulated datasets and 1.22 m^2/m^2 with the field-measured dataset. This index responded mostly to the quantity of LAI but was insensitive to within-canopy variations, allowing it to aid the retrieval LAI from remote sensing data without prior information of within-canopy vertical variations of LAI and biochemical properties.

(3) The index D(920,1080) for estimating LAI performed much worse when applying in a typical desert forest (with RMSE if 1.57 m^2/m^2) than in temperate deciduous forests. One of the potential reasons is that the MRTM can suit to temperate deciduous forests very well but not suit to the desert vegetation canopies, as the desert vegetation canopy has very low LAI value and the soil information has a large proportion in the canopy spectra. To indentify an efficient spectral index for estimating LAI for desert vegetations need first improved and calibrated the MRTM with field measured data set from desert forests, which need further investigate.

The intention was to investigate the potential of hyperspectral remote sensing for estimating biochemical and biophysical vegetation characteristics such as leaf chlorophyll, leaf water, leaf mass content and canopy leaf area index (LAI) with focus on physical and statistical models (radiative transfer model and spectral indices). We have examined the performance of both physical and statistical models for predicting biochemical and biophysical vegetation properties from leaf to canopy scale in two typical vegetation types (temperate deciduous and desert forests). We have shown in this thesis that the information contained in hyperspectral data can accomplish these

tasks. To summarize, the study not only contributes to the field of information extraction from hyperspectral measurements but also enhances our understanding of vegetation biochemical and biophysical characteristics estimation. A number of achievements have been registered in exploiting spectral information for the retrieval of vegetation parameters using radiative transfer models and spectral indices approaches. These concern the successful implementation of radiative transfer models inversion (with extensive validation) and the derivation of new vegetation indices, which involved the development of a new model inversion algorithm, a new canopy multiple-layer model, and a new spectral indices developed method based on both simulated and field measured data sets.

6.4 Future studies

An apparent direction in the future is to extend the methods used and developed in this study to hyperspectral space-borne sensors such as MERIS, MODIS and HYPERION for the prediction and mapping of vegetation biochemical and biophysical characteristics of large areas.

Research such as studying vegetation through the use of remote sensing and biophysical modeling is usually confronted with the problem of unknown input parameters. On the other hand, statistical modeling (such as spectral indices) requires extensive field survey to collect sufficient field data. In an operational project, however, a compromise can be made that includes achieving the research aim and meeting the constraints of time and data availability.

The research presented here illustrates some of the possibilities for estimating biochemical parameters (such as chlorophyll, water and dry mass content) at leaf scale and biophysical parameter (such as LAI) at canopy scale in two different types of forests (temperate deciduous and desert forests). However, the applications of the developed methods to other vegetation types and larger scales not considered in this study needs to be evaluated using different data sets. In this way scale and senor effects as well as phenological influences and physiological effects can be studied. For this, proper ground sampling measurements for obtaining biochemical and biophysical variables are required.

Furthermore, a practical extension of the present work would be on the use of information obtained from statistical models to parameterize the physical models. This information may help in choosing the initial parameter values for model inversion and may probably improve the regularization of the model inversion, thus overcoming the ill-posed problem. However, the possibility of integrating statistical models with physical models needs to be further explored. A more accurate estimation of the biochemical and biophysical parameters for a variety of vegetation types can be expected from such an integrated approach, which may meet the requirements of ecological and technology-enhanced decision making processes and policies.

Acknowledgements

Gratitude is owed to many individuals who have helped me in one way or another over the past three years, often without knowing they were doing so.

My deepest appreciation goes to my supervisor, Prof. Wang Quan, for his confidence, advice, encouragement, commitment and unsparing support during the period of my study. He taught me how to be an independent scientist by letting me make my own choices at decisive points along the way. And I am grateful for the many inspiring scientific discussions we shared. It was easy for me to communicate with him because of his friendly and sincere attitude. This work would not have been possible without the invaluable contribution and help I received from him. Further I would like to express my gratitude to Prof. Suzuki Yoshimi, Prof. Casareto B.E., Imamura-san, Masumto-san, and all the other professors, staffs and students in the "Environmental Leadership Program, Shizuoka University (ELSU)". Without the financial support of the ELSU program, I would not have the chance to be here doing this research.

Special thank all members of Institute of Silviculture, Shizuoka University for their helps on field works, lab analysis, discussions and let me feel very comfortable and easy to live in Japan. Special thanks to Prof. Kakubari, Prof. Mizunaga, Prof. Naramoto, Mochizuki-san, and all the other students.

I would like to thank my good friends in Japan, Dr. Zheng Chaolei, Liu Gang, Lu Shuang, Cao Zhengxing, and others. They always give me happy time when out of work.

Finally, it would have been impossible without the devout support of my entire family. The love and practical support I got and continue to enjoy from my wife Huang Xiaoli have always given me reason to strive for higher heights. It would difficult to ever understand and even to find words to describe the sacrifices my beloved child; Li Xingyue has had to endure in my absence.

Last but not least, to my farther Li Songlin, I say thank you for your presence, support and encouragement.

List of Figures

List of Tables

References

Aber, J. D., Federer, C. A., 1992. A generalized, lumped-parameter model of photosynthesis, evaporation and net primary productino in temperate and boreal forest ecosystems. Oecologia 92, 463-474.

Allen WA, Gausman HW, Richardson AJ, Cardenas R. 1971. Water and air changes in grapefruit, corn, and cotton leaves with maturation. Agronomy Journal 63 : 392–394.

Anderson, M.C., Neale, C.M.U., Li, F., Norman, J.M., Kustas, W.P., Jayanthi, H., Chavez, J., 2004. Upscaling ground observations of vegetation water content, canopy height, and leaf area index during SMEX02 using aircraft and Landsat imagery. Remote Sensing of Environment, 92, 447−464.

Arnon, D.I., 1949. Copper enzymes in isolated chloroplasts. Polyphenoloxidase in Beta vulgaris. Plant Physiology 24, 1–15.

Ashton, P. M. S., Berlyn, G. P., 1994. A comparison of leaf physiology and anatomy of Quercus (setion Erythrobalanus-Fagaceae) species in several shade plants. Am. J. Bot. 81, 589-597.

Asner, G.P., 1998. Biophysical and Biochemical Sources of Variability in Canopy Reflectance. Remote Sensing of Environment, 64, 234-253.

Ataberger, C., 1995. Accuracy of multitemporal LAI estimates in winter wheat using analytical (PROSPECT+SAIL) and semi-empirical reflectance models. In: Guyot, G. (Eds.), Proc. Photosynthesis and Remote Sensing, EARSeL colloquium, Montpellier, 28-30 August 1995, pp. 423-428.

Atzberger, C., 1997. Esimates of winter wheat production through remote sensing and crop growth modeling. VWF Verlag, Berlin, Germany.

Atzberger, C., 2004. Object-based retrieval of biophysical canopy variables using artificial neural nets and radiative transfer models. Remote Sensing of Environment, 93, 53-67.

Bacour, C., Jacquemoud, S., Tourbier, Y., Dechambre, M., Frangi, J.P., 2002. Design and analysis of numerical experiments to compare four canopy reflectance models. Remote Sensing of Environment, 79, 72-83.

Baret F. and Fourty T., 1997. Estimation of leaf water content and specific leaf weight from reflectance and transmittance measurements, Agronomie, 17, 455−464,

Baret, F. and Guyot, G., 1991. Potentials and limits of vegetation indices for LAI and APAR assessment. Remote Sensing of Environment 35, 161−173.

Baret, F., 1991. Vegetation canopy reflectance: Factors of variation and application for agriculture. In: Hunt D. (eds.), Physical measurements and signatures in remote sensing, France: Courchevel, pp. 145−167.

Barton, C.V.M., 2000. A theoretical analysis of the influence of heterogeneity in chlorophyll distribution on leaf reflectance. Tree Physiology 21, 789–795.

Birky, A.K., 2001. NDVI and a simple model of deciduous forest seasonal dynamics. Ecological Modelling, 143, 43−58.

Blackburn, G. A., 1998. Quantifying chlorophylls and carotenoids at leaf and canopy scales: an evaluation of some hyperspectral approaches. Remote Sens. Environ.

66, 273-285.
Blackburn, G.A., 2007. Hyperspectral remote sensing of plant pigments. Journal of Experimental Botany 58, 855-867.
Bonan, G.B., 1993. Importance of leaf area index and forest type when estimating photosynthesis in boreal forests. Remote Sensing of Environment, 43, 303–314.
Bowyer P, Danson FM. 2004. Sensitivity of remotely sensed spectral reflectance to variation in live fuel moisture content. Remote Sensing of Environment 92 : 297–308.
Broge, N.H., and Leblanc, E., 2001. Comparing prediction power and stability of broadband and hyperspectral vegetation indices for estimation of green leaf area index and canopy chlorophyll density. Remote Sensing of Environment, 76, 156-172.
Broge, N.H., Mortensen, J.V., 2002. Deriving green crop area index and canopy chlorophyll density of winter wheat from spectral reflectance data. Remote Sensing of Environment 81, 45–57.
Ceccato P, Flasse S, Tarantola S, Jacquemoud S, Grégoire JM. 2001. Detecting vegetation leaf water content using reflectance in the optical domain. Remote Sensing of Environment 77 : 22−33.
Chen, J.M. and Cihlar, J., 1996. Retrieving leaf area index of boreal conifer forests using Landsat TM images. Remote Sensing of Environment, 55, 153–162.
Chen, J.M., 1996. Evaluation of vegetation indices and modified simple ratio for boreal applications. Canadian Journal of Remote Sensing, 22, 229–242.
Chen, J.M., and Black, T.A., 1992. Defining leaf area index for non-flat leaves. Plant, Cell and Environment, 15, 421–429.
Cho, M.A., 2007. Hyperspectral remote sensing of biochemical and biophysical parameters: the derivative red-edge “double-peak feature”: a nuisance or an opportunity? Wageningen University.
Ciganda, V., Gitelson, A., Schepers, J., 2008. Vertical profile and temporal variation of chlorophyll in maize canopy: Quantitative “crop vigor” indicator by means of reflectance-based techniques. Agronomy Journal 100, 1409–1417.
Cohen, W.B., Maiersperger, T.K., Grower, S.T., Turner, D.P., 2003. An improved strategy for regression of biophysical variables and Landsat ETM+ data. Remote Sensing of Environment, 84, 561-571.
Colombo, R., Bellingeri, D., Fasolini, D., Marino, C. M., 2003. Retrieval of leaf area index in different vegetation types using high resolution satellite data. Remote Sensing of Environment 86, 120–131.
Colombo, R., Meroni, M., Marchesi, A., Busetto, L., Rossini, M., Giardino, C., Panigada, C., 2008. Estimation of leaf and canopy water content in popular plantations by means of hyperspectral indices and inverse modeling. Remote Sens. Environ. 112, 1820-1834.
Combal, B., Baret, F., Weiss, M., Trubuil, A., Macé, D., Pragnère, A., Knyazikhin, Y., Wang, L., 2002. Retrieval of canopy biophysical variables from bidirectional reflectance using prior information to solve the ill-posed inverse problem. Remote Sensing of Environment 84, 1−15.
Coops, N.C., Stone, C., 2005. A comparison of field-based and modelled reflectance spectra from damaged Pinus radiata foliage. Australian Journal of Botany 53, 417–429.

Cote, J.F., Widlowski, J.L., Fournier, R.A., Verstraete, M.M., 2009. The structural and radiative consistency of three-dimensional tree reconstruction from terrestrial lidar. Remote Sensing of Environment 113, 1067-1081.

Curran, P.J., 1994. Imaging spectrometry. Progress in Physical Geography, 182, 247-266.

Curran, P.J., Dungan, J.l., Peterson, D.L., 2001. Estimating the foliar biochemical concentration of leaves with reflectance spectrometry: testing the Kokaly and Clark methodologies. Remote Sensing of Environment 76, 349-359.

Danson FM, Bowyer P. 2004. Estimating live fuel moisture content from remotelysensed reflectance. Remote Sensing of Environment 92 : 309−321.

Datt, B., 1999. Visible/near infrared reflectance and chlorophyll content Eucalyptus leaves. Int. J. Remote Sens. 20, 2741-2759.

Daughtry, C.S.T., Ranson, K.J., Biehl, L.L., 1989. A new technique to measure the spectral properties of conifer needles. Remote Sensing of Environment 27 (1), 81-91.

Dawson, T.P., Curran, P.J., Plummer, S.E., 1998. LIBERTY - Modeling the Effects of Leaf Biochemical Concentration on Reflectance Spectra. Remote Sensing of Environment 65, 50-60.

Demarez, V., 1999. Seasonal variation of leaf chlorophyll content of a termperate forest. Inversion of the PROSPECT model. International Journal of Remote Sensing 20 (5), 879−894.

Dwyer, L.M., Stewart, D.W., Hamilton, R.I., Houwing, L., 1992. Ear position and vertical distribution of leaf area in corn. Agronomy Journal, 84, 430–438.

Elvidge, C.D. and Chen, Z., 1995. Comparison of broad-band and narrow-band red and near-infrared vegetation indices. Remote Sensing of Environment 54, 38-48.

Fang, H. and Liang, S., 2005. A hybrid inversion method for mapping leaf are index from MODIS data: experiments and application to broadleaf and needleaf canopies. Remote Sensing of Environment 94, 405-424.

Fassnacht, K.S., Gower, S.T., MacKenzie, M.D., Nordheim, E.V., Lillesand, T.M., 1997. Estimating the leaf area index of north central Wisconsin forest using the Landsat Thematic Mapper. Remote Sensing of Environment, 61, 229–245.

Feret, J.B., François, C., Asner, G.P., Gitelson, A.A., Martin, R. E., Bidel, L., Ustin, S., le Maire, G., Jacquemoud, S., 2008. PROSPECT-4 and 5: Advances in the leaf optical properties model separating photosynthetic pigments. Remote Sens. Environ. 112, 3030–3043.

Ferwerda, J.G., Skidomre, A.K., Mutanga, O., 2005. Nitrogen detection with hyperspectral normalized ratio indices across multiple plant canopies. International Journal of Remote Sensing, 26, 4083-4095.

Filella I., Penuelas J., 1994. The red edge position and shape as indicators of plant chlorophyll content, biomass and hydric status. International Journal of Remote Sensing, 15, 1459-1470.

Gamon, J.A., Qiu, H., 1999. Ecological applications of remote sensing at multiple scales. In: F. I. Pugnaire, F. Valladares (Eds.) Handbook of functional plant ecology, pp. 805-846. New York: Marcel Dekker.

Gamon, J.A., Penuelas, J., Field, C.B., 1992. A narrow-band spectral index that tracks diurnal changes in photosynthetic efficiency. Remote Sensing of Environment,

41, 35-44.
Gamon, J.A., Rahman, A. F., Dungan, J. L., Schildhauer, M., Huemmrich, K. F., 2006. Spectral Network (SpecNet) – What is it and why do we need it? Remote Sens. Environ. 103, 227-235.
Gamon, J.A., Surfus, J. S., 1999. Assessing leaf pigment content and activity with a reflectometer. New Phytol. 143, 105-117.
Ganapol, B.D., Johnson, L.F., Hammer, P.D., Hlavka, C.A., Peterson, D.L., 1998. LEAFMOD: A new within-leaf radiative transfer model. Remote Sensing of Environment 63, 182–193.
Gao, B.C., 1996. NDWI, a normalized difference water index for remote sensing of vegetation liquid water from space. Remote Sens. Environ. 58, 257-266.
Gastellu-Etchegorry, J.P., Demarez, V., Pinel, V., Zagolski, F., 1996. Modeling radiative transfer in heterogeneous 3-d vegetation canopies. Remote sensing of environment, 76, 1−15.
Gitelson, A. A., Viña, A., Ciganda, V., Rundquist, D. C., Arkebauer, T. J., 2005. Remote estimation of canopy chlorophyll content in crops. Geophysical Research Letters 32, L08403, doi:10.1029/2005GL022688.
Gitelson, A., Merzlyak, M., 1996. Signature analysis of leaf reflectance spectra: Algorithm development for remote sensing of chlorophyll. J. Plant Physiol. 148, 495-500.
Gitelson, A., Merzlyak, M., 1997. Remote Estimation of Chlorophyll Content in higher Plant Leaves. Int. J. Remote Sensing, 18, 291-298.
Gobron, N., Pinty, B., Verstraete, M.M., Govaerts, Y., 1997. A semidiscrete model for the scattering of light by vegetation. Journal of Geophysical Research-Atmospheres 102, 9431–9446.
Gone, P., Pu, R., Miller, J.R., 1992. Correlating leaf area index of ponderosa pine with hyperspectral CASI data. Canadian Journal of Remote Sensing, 18, 275-282.
Haboudane, D., Miller, J.R., Pattey, E., Zarco-Tejada, P.J., Strachan, I.B., 2004. Hyperspectral vegetation indices and novel algorithms for predicting green LAI of crop canopies: Modeling and validation in the context of precision agriculture. Remote Sensing of Environment 90, 337−352.
Hansen, P.M., and Schjoerring, J.K., 2003. Reflectance measurement of canopy biomass and nitrogen status in wheat crops using normalized difference vegetation indices and partial least squares regression. Remote Sensing of Environment, 86, 542−553.
Hardisky MA, Klemas V, Smart RM. 1983. The influence of soil salinity, growth form, and leaf moisture on the spectral reflectance of Spartina alterniflora canopies. Photogrammetric Engineering and Remote Sensing 49 : 77–83.
Hinzman, L.D., Bauer, M.E., Daughtry, C.S.T., 1986. Effects of nitrogen fertilization on growth and reflectance characteristics of winter wheat. Remote Sensing of Environment, 19, 47-61.
Hosgood, B., Jacquemoud, S., Andreoli, G., Verdebout, J., Pedrini, G., and Schmuck, G.,1994. Leaf Optical Properties Experiment 93 (LOPEX93. Ispra (Italy) European Commission – Joint Research Centre EUR 16095 EN, pp. 20 (http://www-gvm.jrc.it/stars/lopex.htm).
Houborg, R., Anderson, M., Daughtry, C., 2009. Utility of an image-based canopy reflectance modeling tool for remote estimation of LAI and leaf chlorophyll

content at the field scale. Remote Sensing of Environment 113, 259 – 274.
Houborg, R., Soegaard, H., Boegh, E., 2007. Combining vegetation index and model inversion methods for the extraction of key vegetation biophysical parameters using Terra and Aqua MODIS reflectance data. Remote Sensing of Environment 106, 39−58.
Huemmrich, K.F., 2000. BOREAS TE-18 GeoSail Canopy Reflectance Model.
Hunt Jr ER, Rock BN. 1989. Detection of changes in leaf water content using near– and middle–infrared reflectance. Remote Sensing of Environment 30 : 43–54.
Jacquemoud S, Bacour C, Poilve´ H, Frangi J–P. 2000. Comparison of four radiative transfer models to simulate plant canopies reflectance — direct and inverse mode. Remote Sensing of Environment 74 : 471–481
Jacquemoud S, Baret F. 1990. PROSPECT: a model of leaf optical properties spectra. Remote Sensing of Environment 34 : 74–91.
Jacquemoud S, Ustin S L, Verdebout J, Schmuck G, Andreoli G, Hosgood B. 1996. Estimating leaf biochemistry using the PROSPECT leaf optical properties model. Remote Sensing of Environment 56 : 194−202.
Jacquemoud S, Verdebout J, Schmück G, Andreoli G, Hosgood B. 1995. Investigation of leaf biochemistry by statistics, Remote Sensing of Environment 54, 180-188.
Jacquemoud, S., Verhoef, W., Baret, F., Bacour, C., Zarco-Tejada, P.J., Asner, G.P., François, C., Ustin, S.L., 2009. PROSPECT + SAIL Models: a review of use for vegetation characterization. Remote Sensing of Environment 113, S56-S66.
Kakubari, Y., 1977. Distribution of primary productivity along the altitudinal gradient. JIBP Synthesis 16, 201-212.
Kimes, D. S., Knyazikhin, Y., Privette, J. L., Abuelgasim, A. A., Gao, F., 2000. Inversion methods for physically-based models. Remote Sens. Rev. 18, 381−439.
Kims, D.S., Nelson, R.F., Manry, M.T., Fung, A.K., 1998. Attributes of neural networks for extracting continuous vegetation variables from optical and radar measurements. International Journal of Remote Sensing, 19, 2639-2662.
Kobayashi, S., Rokugawa, S., Yamagata, Y., Oguma, H., 2001. A Study on predicting the spectral character of larch needles: A study on LIBERTY model. Proceedings of the Japanese Conference on Remote Sensing 30, 23–24.
Kuusk, A., 1991. The hot spot effect in plant canopy reflectance, in Photon-Vegetation Interactions. In: Myneni, R. and Ross, J. (eds.), Springer, New York, pp. 139-159.
Kuusk, A., 1994. A multispectral canopy reflectance model. Remote Sensing of Environment 50, 75–82.
Kuusk, A., 1995. A Markov chain model of canopy reflectance. Agricultural and Forest Meteorology 76, 221–36.
Kuusk, A., 2001. A two-layer canopy reflectance model. Journal of Quantitative Spectroscopy and Radiative Transfer, 71, 1−9.
Kuusk, A., Nilson, T., 2000. A directional multispectral forest reflectance model, Remote Sensing of Environment 72, 244– 252.
Kuusk, A., Nilson, T., 2009. Forest Reflectance and Transmittance. FRT User Guide. Version 08.2009. Tartu Observatory Available on-line at http://www.aai.ee/bgf/frt/ frt.html.
Kuusk, A., Nilson, T., Kuusk, J., Lang, M., 2010. Reflectance spectra of RAMI forest stands in Estonia: Simulations and measurements. Remote Sensing of

Environment 114, 2962–2969.
le Maire G, François C, Dufrêne E. 2004. Towards universal deciduous broad leaf chlorophyll indices using PROSPECT simulated dataset and hyperspectral reflectance measurements. Remote Sensing of Environment 89 : 1−28.
le Maire G, François C, Soudani K, Berveiller D, Pontailler JY, Bréda N, Genet H, Davi H, Dufrêne E. 2008. Calibration and validation of hyperspectral indices for the estimation of broadleaved forest leaf chlorophyll content, leaf mass per area, leaf area index and leaf canopy biomass. Remote Sensing of Environment 112 : 3846–3864.
Lee, K.S., Cohen, W.B., Kennedy, R.E., Maiersperger, T.K., Gower, S.T., 2004. Hyperspectral versus multispectral data for estimating leaf area index in four different biomes. Remote Sensing of Environment, 91, 508-520.
Li, P., Wang, Q., 2011. Retrieval of Leaf Biochemical Parameters Using PROSPECT Inversion: A New Approach for Alleviating Ill-posed Problems. IEEE Transactions on Geoscience and Remote Sensing, 49 (7), 2499–2506.
Liang, S., 2004. Quantitative Remote Sensing of Land Surface. Wiley Praxis Series in Remote Sensing, Wilev & Sons, Hoboken etc.
Liangrocapart, S., Petrou, M., 2002. A two-layer model of the bidirectional reflectance of homogeneous vegetation canopies. Remote Sensing of Environment 80, 17–35.
Liu, J., Chen, J.M., Cihlar, J., Park, W.M., 1997. A process- based boreal ecosystem productivity simulator using remote sensing inputs. Remote Sensing of Environment, 62, 158–175.
Liu, Q., Weng, F., 2006. Advanced Doubling–Adding Method for Radiative Transfer in Planetary Atmospheres. Journal of Atmospheric Sciences 63, 3459–3465.
Ludwig, J. A., Tongway, D. J., Freudenberger, D., Noble, J., Hodgkinson, K., 1997. Landscape ecology function and management: Principles from Australia's ranglands. Collingwood, Australia: CSIRO Publications.
Malenovsky, Z., Albrechtova, J., Lhotakova, Z., Zurita-Milla, R., Clevers, G.P.W., Schaepman, M.E., 2006. Applicability of PROSPECT model for Norway spruce needles. International Journal of Remote Sensing 27 (24), 5315−5340.
Mcmurtrey, J.E., Chappelle, E.W., Kim, M.S., Meisinger, J.J, Crop, L.A., 1994. Distinguishing nitrogen fertilization levels in field corn (Zea maus L.) with actively induced fluorescence and passive reflectance measurements. Remote Sensing of Environment, 47, 36-44.
Melamed, M.T., 1963. Optical properties of powders. Part I. Optical absorption coefficients and the absolute value of the diffuse reflectance. Journal of Applied Physics 34, 560-570.
Melillo, J. A., Aber, J. D., Muratore, J. F., 1982. Nitrogen and lignin control of hardwood leaf litter decomposition dynamics. Ecology 63, 621-626.
Meroni, M. Colombo, R., Panigada, C., 2004. Inversion of a radiative transfer model with hyperspectral observations for LAI mapping in poplar plantations. Remote Sensing of Environment, 92, 195-206.
Moorthy, I., Miller, J.R., Noland, T.L., 2008. Estimating chlorophyll concentration in conifer needles with hyperspectral data: An assessment at the needle and canopy level. Remote Sensing of Environment 112 (6), 2824-2838.
Moorthy, I., Miller, J.R., Zarco-Tejada, P.J., Noland, T.L., 2004. Needle chlorophyll

content estimation: a comparative study of PROSPECT and LIBERTY. International Geoscience and Remote Sensing Symposium, IGARSS'03, ISBN 0-7803-7929-2 - 0-7803-7930-6, pp. 1676-1678.

Mutanga, O., Skidmore,A.K., 2004. Narrow band vegetation indices overcome the saturation problem in biomass estimation. International Journal of Remote Sensing, 25, 3999-4014.

Mutanga, O., Skidmore, A.K., Kumar, L., Ferwerda, J., 2005. Estimating tropical pasture quality at canopy level using band depth analysis with continuum remocal in the visible domain. International Journal of Remote Sensing, 26, 1093-1108.

Myneni, R.B., Asrar, G., Hall, F.G., 1992. A three-dimensional radiative transfer method for optical remote sensing of vegetated land surfaces. Remote Sensing of Environment 41, 105–121.

Nelson, N., Yocum, C. F., 2006. Structure of function of photosystem I and II. Ann. Rev. Plant Biol. 57, 521-565.

Newnham G.J. and Burt T., 2001. Validation of a leaf reflectance and transmittance model for three agricultural crop species, In IEEE Geoscience and Remote Sensing Symposium (IGARSS'01), Vol. 7, pp. 2976-2978.

Nilson, T., Kuusk, A., 1989. A reflectance model for the homogeneous plant canopy and its inversion. Remote Sensing of Environment 27, 157-167.

Ourcival, J. M., Joffre, R., Rambal, S., 1999. Exploring the relationships between reflectance adn anatomical and biochemical properties in Quercus ilex leaves. New Phytol. 143, 351-364.

Peñuelas J, Filella I, Biel C, Serrano L, Save R. 1993. The reflectance at the 950–970 nm region as an indicator of plant water status. International Journal of Remote Sensing 14 : 1887–1905.

Peñuelas J, Piñol J. Ogaya R, Filella I. 1997. Estimation of plant water concentration by the reflectance Water Index WI (R900/R970). International Journal of Remote Sensing 18 : 2869–2875.

Peterson, D. L., Hubbard, G. S., 1992. Scientific issues and potential remote-sensing requirements for plant biochemical content. J. Imaging Sci. Techn. 36, 446-456.

Peterson, D.L., Aber, J.D., Matson, P.L., Card, D.H., Swanberg, N., Wessman, C.A., Spanner, M., 1988. Remote sensing of forest canopy and leaf biochemical contents. Remote Sensing of Environment, 24, 85-108.

Pinty, B., Gobron, N., Widlowski, J.L., Gerstl, S.A.W., Verstraete, M.M., Antunes, M. et al., 2001. Radiation transfer model intercomparison (RAMI) exercise. Journal of Geophysical Research 106, 11937−11956.

Pinty, B., Widlowski, JL., Tabermer, M., Gobron, N., Verstraete, M.M., Disney, M. et al., 2004. Radiation Transfer Model Intercomparison (RAMI) exercise: Results from the second phase. Journal of Geophysical Research 109, doi: 10.1029 / 2003JD004252.

Price, J.C., 1990. On the information content of soil reflectance spectra. Remote Sensing of Environment, 33, 113–121.

Pu, R., Gong, P., Biging, G.S., 2003. Simple calibration of AVIRIS data and LAI mapping of forest plantation in southern Argentina. International Journal of Remote Sensing, 24, 4699-4714.

Pyankov, V.I., Black, Jr. C.C., Artyusheva, E.G., Voznesenskaya, E.V., Kuu, M.S.B.,

Edwards, G.E., 1999. Features of photosynthesis in Haloxylon species of Chenopodiaceae that are dominant plants in Central Asia desert. Plant and Cell Physiology 40, 125–134.

Qi, J., Chehbouni, A., Huete, A. R., Kerr, Y. H., Sorooshian, S., 1994. A modified soil adjusted vegetation index. Remote Sensing of Environment, 48, 119–126.

Qi, J., Kerr, Y.H., Moran, M.S., Weltz, M., Huete, A.R., Sorooshian, S., Bryant, R., 2000. Leaf area index estimates using remotely sensed data and BRDF models in a semiarid region. Remote Sensing of Environment, 73(1), 18−30.

Riaño, D., Vaughan, P., Chuvieco, E., Zarco-Tejada, P. J., Ustin, S. L., 2005. Estimation of fuel moisture content by inversion of radiative transfermodels to simulate equivalent water thickness and dry matter content: analysis at leaf and canopy level. IEEE T. Geosci. Remote 43, 819−826.

Roberts, D. A., Gardner, M., Church, R., Ustin, S. L., Scheer, G., Green, R. O., 1998. Mapping chaparral in the Santa Monica Mountains using multiple endmember spectral mixture models. Remote Sens. Environ. 65, 267-279.

Saltelli A., Chan K. and Scott M., 2000. Sensitivity analysis, Chichester: John Wiley.

Schlerf, M., Atzberger, C., 2006. Inversion of a forest reflectance model to estimate structural vegetation attributes using hyperspectral remote sensing data. Remote Sensing of Environment, 100, 281-294.

Schlerf, M., Atzberger, C., Hill, J., 2005. Remote sensing of forest biophysical variables using HyMap imaging spectrometer data. Remote Sensing of Environment, 95, 177-194.

Seelig HD, Hoehn A, Stodieck LS, Klaus DM, Adams III WW, Emery WJ. 2008 Relations of remote sensing leaf water indices to leaf water thickness in cowpea, bean, and sugarbeet plants. Remote Sensing of Environment 112 : 445–455.

Sims, D. A., Gamon, J. A., 2002. Relationships between leaf pigment content and spectral reflectance across a wide range of species, leaf structures and developmental stages. Remote Sens. Environ. 81, 337– 354.

Sims, D. A., Luo, H., Hstings, S., Oechel, W.C., Rahman, A.F., Gamon, J.A., 2006. Parallel adjustments in vegetation greenness and ecosystem CO2 exchange in response to drought in a Southern Calinfornia chaparral ecosystem. Remote Sens. Environ. 103, 289-303.

Skidmore, A.K., 2002. Taxonomy of environmental models in the spatial sciences. In: Environmental modelling with GIS and remote sensing. A. Skidmore (ed.). London etc. : Taylor & Francis, 2002. ISBN 0-415-24170-7 pp. 8-24.

Sobol I.M., 1993. Sensitivity estimates for nonlinear mathematical models, Mathematical Modeling and Computational Experiment, 1, 407-414.

Sobolev, V.V., 1956. Radiative transfer in the atmospheres of stars and planets. Moscow: The State Publishing Company of Technical and Theoretical Literature, pp. 391.

Soudani, K., Francois, C., le Maire, G., Le Dantec, V., Dufrene, E., 2006. Comparative analysis of IKONOS, SPOT, and ETM+ data for leaf area index estimation in temperate coniferous and deciduous forest stands. Remote Sensing of Environment, 102, 161−175.

Stenberg, P., Rautiainen, M., Manninen, T., Voipio, P., Smolander, H., 2004. Reduced simple ratio better than NDVI for estimating LAI in Finnish pine and spruce stands. Silva Fennica, 38, 3–14.

Stimson, H. C., Breshears, D. D., Ustin S. L., Kefauver, S. C., 2005. Spectral sensing of foliar water conditions in two co-occurring conifer species: Pinus edulis and Juniperus monosperma. Remote Sens. Environ. 96, 108-118.

Thenkabail, P. S., Enclona, E. A., Ashton, M. S., van Der Meer, B., 2004. Accuracy assessments of hyperspectral waveband performance for vegetation analysis applications. Remote Sens. Environ. 91, 354-376.

Thenkabail, P.S., Smith, R.B., De Pauw, E., 2000. Hyperspectral Vegetation Indices and their relationships with agricultural crop characteristics. Remote Sensing of Environment, 71, 158-182.

Ustin S.L., Smith M.O., Jacquemoud S., Verstraete M.M., Govaerts Y.M., 1999. Geobotany: Vegetation mapping for earth sciences, in Rmote Sensing of the Earth Sciences: Manual of Remote Sensing, A.N. Rencz (Ed.), John Wiley & Sons (New York), Vol. 3, pp. 189-248.

Ustin, S.L., Gitelson, A.A., Jacquemoud, S., Schaepman, M., Asner, G. P., Gamon, J. A., Zarco-Tejada, P., 2009. Retrieval of foliar information about plant pigment systems from high resolution spectroscopy. Remote Sens. Environ. 113, S67-S77.

Valentinuz, O.R., and Tollenaar, M., 2004. Vertical profile of leaf senescence during the grain-filling period in older and newer maize hybrids. Crop Science, 44, 827–834.

Verdebout J., Jacquemoud S. and Schmuck G., Optical properties of leaves: modelling and experimental studies, In J., & J. (Eds.) Imaging Spectrometry-a Tool for Environmental Observations, J. Hill and J. Mgier Ed. ECSC, EEC, EAEC, Brussels and Luxembourg 1994, pp. 169-191.

Verhoef, W., 1984. Light scattering by leaf layers with application to canopy reflectance modeling: the SAIL model. Remote Sensing of Environment 16, 125–141.

Verhoef, W., 1985. Earth observation modeling based on layer scattering matrices. In: Remote sensing of environment, 17, 165-178.

Verhoef, W., 2002. Improved modelling of multiple scattering in leaf canopies: The model SAIL++, in Proceedings of the First Symposium on Recent Advances in Quantitative Remote Sensing, Torrent, Spain, September 2002, edited by A. Sobrino, pp. 11 – 20, Serv. de Publ. Univ. de Valencia, Valencia, Spain.

Verhoef, W., Bach, H., 2007. Coupled soil - leaf - canopy and atmosphere radiative transfer modeling to simulate hyperspectral multi - angular surface reflectance and TOA radiance data. Remote Sensing of Environment 109(2), 166-182.

Verstraete, M.M., Pinty, B., Dickinson, R.E., 1990. A physical model of the bidirectional reflectance of vegetation canopies. I. Theory. Journal of Geophysical Research 95, 11755-11765.

Vittorio, A.V., Di, 2009. Enhancing a leaf radiative transfer model to estimate concentrations and in vivo specific absorption coefficients of total carotenoids and chlorophylls a and b from single-needle reflectance and transmittance. Remote Sensing of Environment 113 (9), 1948–1966.

Vogelman, J. E., Rock, B. N., Moss, D. M.,1993. Red edge spectral measurements from sugar maple leaves. Int. J. Remote Sens. 14, 1563-1575.

Wang, Q., Adiku, S., Tenhunen, J. Granier, A., 2005. On the relationship of NDVI with leaf area index in a deciduous forest site. Remote Sensing of Environment, 94, 244-255.

Wang, Q. Li, P., 2011. Identification of robust hyperspectral indices on forest leaf water content using PROSPECT simulated dataset and field reflectance measurements. Hydrological Processes, DOI: 10.1002/hyp.8221.

Wang, Q., Li, P., 2012. Hyperspectral indices for estimating leaf biochemical properties in temperate deciduous forests: Comparison of simulated and measured reflectance data sets. Ecological Indicators, 14, 56-65.

Wang, Q., Li, P., 2013a. Canopy vertical heterogeneity plays a critical role on reflectance simulation. Agricultural and Forest Meteorology, revised.

Wang, Q., Li, P., 2013b. Developing and validating novel hyperspectral indices for leaf area index estimation: Effect of canopy vertical heterogeneity. Ecological Indicators, 32, 123–130.

Wang, Y.F., Li, W.X., Nashed, Z., Zhao, F., Yang, H., Guan, Y. and Zhang, H., 2007. Regularized kernel-based BRDF model inversion method for ill-posed land surface parameter retrieval, Remote Sensing of Environment, 111, 36-50.

Weiss, M., Baret, F., 1999. Evaluation of canopy biophysical variable retrieval performances from the accumulation of large swath satellite data. Remote Sens. Environ. 70, 293−306.

Widlowski, J.-L., Pinty, B., Lavergne, T., Verstraete, M.M., Gobron, N., 2006. Horizontal radiation transport in 3-D forest canopies at multiple spatial resolutions: Simulated impact on canopy absorption, Remote Sensing of Environment 103, 379– 397.

Widlowski, J.L., Taberner, M., Pinty, B., Bruniquel-Pinel, V., Disney, M., Fernandes, R., Gastellu-Etchegorry, J. P., Gobron, N, Kuusk, A., Lavergne, T., Leblanc, S., Lewis, P.E. , Martin, E., Mottus, M., North, P.R.J., Qin, W., Robustelli, M., Rochdi, N., Ruiloba, R., Soler, C., Thompson, R., Verhoef, W., Verstraete, M.M., Xie, D., 2007. The third RAdiation transfer Model Intercomparison (RAMI) exercise: Documenting progress in canopy reflectance modelling. Journal of Geophysical Research 112, doi:10.1029/2006JD007821.

Williams, P.C., 1987. Variables affecting near-infrared reflectance spectroscopic analysis. In Near-infrared Technology in the Agricultural and Food Industries, Williams P.C. and Norris K.H. Ed. St. Paul (MN) American Association of Cereal Chemists, pp. 143−167.

Wu, Z.Y., 1995. Vegetation of China. Academic Press, Beijing, pp. 1382. (in Chinese).

Xu, H., Li, Y., Xu, G., Zou, T., 2007. Ecophysiological response and morphological adjustment of two Central Asian desert shrubs towards variation in summer precipitation. Plant, Cell & Environment 30 (4), 399-409.

Yebra M, Chuvieco E, Riaño D. 2008. Estimation of live fuel moisture content from MODIS images for fire risk assessment. Agricultural and Forest Meteorology 148 : 523−536.

Yebra M. and Chuvieco E., 2009. Linking ecological information and radiative transfer models to estimate fuel moisture content in the Mediterranean region of Spain: Solving the ill-posed inverse problem, Remote Sensing of Environment, 113, 2403-2411.

Zarco-Tejada PJ, Rueda CA, Ustin SL. 2003. Water content estimation in vegetation with MODIS reflectance data and model inversion methods. Remote Sensing of Environment 85 : 109−124.

Zarco-Tejada PJ, Ustin SL. 2001. Modeling canopy water content for carbon estimates

from MODIS data at land EOS validation sites. Proceedings of the IEEE 2001 International Geoscience and Remote Sensing Symposium, IGARSS'01. Sydney, Australia. DOI: 10.1109/IGARSS.2001.976152.

Zarco-Tejada, P., Miller, J., Harron, J., Hu, B., Noland, T., Goel, N., 2004. Needle chlorophyll estimation through model inversion using hyperspectral data for boreal conifer forest canopies. Remote Sensing of Environment 89, 189−199.

Zarco-Tejada, P.J., Miller, J.R., Noland, T.L., Mohammed, G.H., Sampson, P.H., 2001. Scaling-up and model inversion methods with narrow-band optical indices for chlorophyll content estimation in closed forest canopies with hyperspectral data. IEEE Transactions on Geoscience and Remote Sensing, 39, 1491–1507.

Zarco-Tejada, P. J., Miller, J. R., Mohammed, G. H., Noland, T. L., Sampson, P. H., 2002. Vegetation stress detection through chlorophyll a+b estimation and fluorescence effects on hyperspectral imagery. Journal of Environmental Quality, 31 (5), 1433–1441.

Zhang, Y., Chen, J.M., Miller, J.R., Noland, T.L., 2008. Retrieving chlorophyll content in conifer needles from hyperspectral measurements. Canadian Journal of Remote Sensing 34 (3), 296-310.

Zhang, Y., Chen, J.M., Thomas, S.C., 2007. Retrieving seasonal variation in chlorophyll content of overstory and understory sugar maple leaves from leaf-level hyperspectral data. Canadian Journal of Remote Sensing 33 (5), 406-415.

Author's publications

(1) **Li, P.**, Wang, Q., Retrieval of chlorophyll for assimilating branches of a typical desert plant through inversed radiative transfer models. ***International Journal of Remote Sensing***, 34, 2402-2416, 2013.

(2) Wang, Q., **Li, P.**, Canopy vertical heterogeneity plays a critical role on reflectance simulation. ***Agricultural and Forest Meteorology***, 169, 111-121, 2013.

(3) **Li, P.**, Wang, Q., Endo, T., Zhao, X., Kakubari, Y., Soil organic carbon stock is closely related to aboveground vegetation properties in cold-temperate mountainous forests. ***Geoderma***, 154, 407-415, 2010.

(4) **Li, P.**, Wang, Q.， Retrieval of biochemicals for assimilating branches of Haloxylon ammodendron through inversed radiative transfer models. Proceedings of the 123th Annual Meeting of the Japanese Forest Society at Utsunomiya, Japan, 2012/3/26-2012/3/29, 2012/3/26.

(5) **Li, P.**, Wang, Q.， Calibration and simulation of leaf scale reflectance and its inversion applications in typical arid ecosystems. Shizuoka University International Symposium 2011, "Initiatives for crossing boundaries within science and technology", 2011/11/28-2011/11/29, 2011/11/28.

Summary

Accurate quantitative estimation of vegetation biochemical and biophysical characteristics is necessary for a large variety of agriculture, ecological, and meteorological applications. Remote sensing, because of its global coverage, repetitiveness, and non-destructive and relatively cheap characterization of land surface, has been recognized as a reliable method and a practical means of estimating various biophysical and biochemical vegetation variables. The advent of hyperspectral remote sensing has offered possibilities for measuring specific vegetation variables that were difficult to measure using conventional multi-spectral sensors.

Utilizing hyperspectral measurements, we examined the performance of radiative transfer models inversion techniques versus spectral indices approaches for predicting biochemical and biophysical vegetation properties such as chlorophyll, leaf water, leaf mass content and leaf area index (LAI) from leaf to canopy scale in two typical vegetation types (temperate deciduous and desert forests). It was concluded that, at leaf scale, for transfer model inversion approaches, retrieval of biochemical parameters generally faces "ill-posed" problems, which dramatically decreases the estimation accuracy of an inverse model, and this problem can be much improved by designed new model inversion algorithm and make the model inversion obtaining a better estimating accuracy. The models need calibration using the local *in situ* measurements before inversely the models to retrieval biochemical parameters, especially for the desert vegetation. After careful calibration, both LIBERTY and PROSPECT are applicable for estimation leaf biochemical parameters inversely for all datasets collected from both temperate deciduous and desert forests. For spectral indices approaches, using a simulated data set generated from a mechanistic reflectance model like PROSPECT which can represent a vast range of leaf reflectance spectra to identify general spectral indices for estimating biochemical parameters is the best method in present. However, the spectral indices indentified from simulated dataset should be calibrated and validated using field measured datasets. The results from simulated dataset and field measured dataset are not always consistent, so the best efficient spectral indices should be trade-off between simulated and measured data sets.

At canopy scale, vertical profiles of both biophysical and biochemical properties are one of the main sources of heterogeneity within a vegetation canopy, and these vertical variations are the major factors controlling canopy reflectance. Using homogeneous canopy reflectance models for calculating reflectance from a vertical heterogeneous canopy may lead to systematic errors. Hence, a computationally efficient model, the multiple-layer canopy radiative transfer model (MRTM), has been developed with the focus on the effect of canopy vertical heterogeneity on canopy reflectance. The results of validation with field measured datasets indicated that the MRTM performed better than the other homogeneous canopy models. The MRTM may help to effectively retrieve the vertical distribution of biophysical and biochemical parameters inversely. In addition, the estimation of canopy characteristics such as LAI using hyperspectral remote sensing, for vertical heterogeneous canopies has not been addressed by researchers yet. Therefore, the effectiveness of hyperspectral remote sensing in estimating LAI in a vertical

heterogeneous canopy using spectral indices approach was examined in this study. The results indicated that the within-canopy vertical variations in LAI and biochemical properties significantly complicate the retrieval of LAI inversely from published spectral indices. Thus, it is critical to identify a new spectral index for estimating LAI that insensitive to the vertical heterogeneous within the canopy. The method of finding the best spectral indices for estimating LAI is using simulated datasets based on the multiple-layer radiative transfer model (MRTM) and validating with field measure dataset. The MRTM model has proven to be efficient in the finding of indices that insensitive to the vertical heterogeneous within the canopy. The best index for estimating canopy LAI under various conditions was D(920,1080). This index responded mostly to the quantity of LAI but was insensitive to within-canopy variations, allowing it to aid the retrieval LAI from remote sensing data without prior information of within-canopy vertical variations of LAI and biochemical properties.

In summary, the study contributes to the field of information extraction from hyperspectral measurements and enhances our understanding of vegetation biochemical and biophysical characteristics estimation. Several achievements have been registered in exploiting spectral information for the retrieval of vegetation parameters using physical (radiative transfer models) and statistical (spectral indices) approaches. These concern the successful implementation of radiative transfer models inversion (with extensive validation) and the derivation of new vegetation indices, which involved the development of a new model inversion algorithm, a new canopy multiple-layer model, and a new spectral indices developed method based on both simulated and field measured datasets. The future of hyperspectral remote sensing could hinge on enhancing the link between statistical and physically based approaches.